PALEOSEISMOLOGY OF THE MERCUR FAULT AND SEGMENTATION OF THE OQUIRRH - EAST GREAT SALT LAKE FAULT ZONE, UTAH

Submitted to:

U.S. Geological Survey

National Earthquake Hazards Reduction Program
Award No. 98HQGR1036

Program Elements I and II

Submitted by:

URS CORPORATION
(*FORMERLY URS GREINER WOODWARD CLYDE*)

Principal Investigator: Susan S. Olig
Assisted By: Andrew E. Gorton, Bill D. Black, and Steven L. Forman

January 25, 2001

Research supported by the U.S. Geological Survey (USGS) Department of the Interior, under USGS award number 98HQGR1036. The views and conclusions contained in this document are those of the authors and should not be interpreted as necessarily representing the official policies, either expressed or implied, of the U.S. Government.

Project No. 51-F0SK9707.00

PALEOSEISMOLOGY OF THE MERCUR FAULT AND SEGMENTATION OF THE OQUIRRH - EAST GREAT SALT LAKE FAULT ZONE, UTAH

Submitted to:

U.S. Geological Survey

National Earthquake Hazards Reduction Program
Award No. 98HQGR1036

Program Elements I and II

Submitted by:

URS CORPORATION
(FORMERLY URS GREINER WOODWARD CLYDE)

Principal Investigator: Susan S. Olig
Assisted By: Andrew E. Gorton, Bill D. Black, and Steven L. Forman

January 25, 2001

Research supported by the U.S. Geological Survey (USGS) Department of the Interior, under USGS award number 98HQGR1036. The views and conclusions contained in this document are those of the authors and should not be interpreted as necessarily representing the official policies, either expressed or implied, of the U.S. Government.

Project No. 51-F0SK9707.00

TABLE OF CONTENTS

Acknowledgements **A-1**

Abstract **A-2**

Section 1 Introduction **1-1**

1.1 Purpose and Scope 1-1
1.2 Geologic Setting 1-2
1.3 Previous Work 1-3

Section 2 Results of Trench Investigations - Mercur Canyon Site **2-1**

2.1 Surficial Geology 2-1
2.2 Trench Exposures 2-2
2.2.1 West Trench 2-3
2.2.2 Central Trench 2-8
2.2.3 East Trench 2-9

Section 3 Summary of Paleoseismic Parameters and Discussion **3-1**

3.1 Earthquake Timing and Recurrence 3-1
3.1.1 Summary of Event Chronology 3-1
3.1.2 Recurrence Intervals 3-2
3.2 Displacements and Slip Rates 3-3
3.3 Paleomagnitude Estimates 3-4
3.4 Implications for Fault Segmentation and Evolution 3-7
3.4.1 Fault Segmentation 3-7
3.4.2 Fault Evolution 3-10

Section 4 References **4-1**

List of Figures

1 Map of the Oquirrh-East Great Salt Lake Fault Zone and Selected nearby Faults

2 Surficial Geology and Trench Locations on the South Oquirrh Mountains Fault

3 Aerial Photograph with Surficial Geology of the Mercur Canyon Trench Site

4 Topographic Fault Scarp Profiles for the Mercur Canyon Trench Site

5 Annotated Photograph of Main Fault Zone, Mercur Canyon, West Trench, South Wall

6 Mercur Canyon West Trench Log

7 Reconstruction of Mercur Canyon West Trench Log

8 Photograph of Mercur Canyon Central Trench, South Wall

9 Mercur Canyon East Trench Log

10 Summary Diagram of Surface-Faulting Events at the Mercur Canyon Site

List of Tables

1 Radiocarbon and Luminescence Ages for Mercur Canyon Trenches

2 Paleomagnitude Estimates for Surface-Faulting Earthquakes on the South Oquirrh Mountains Fault

3 Ages of Surface-Faulting Events Along Sections of the Oquirrh-East Great Salt Lake Fault Zone

List of Appendixes

Appendix A Lithologic Unit Descriptions

Appendix B Soil Profile Descriptions

Appendix C Paleo Research Laboratories Report on Radiocarbon Sample Pretreatment

Appendix D Beta Analytic Inc. Report on Radiocarbon Dating Analyses

Appendix E Associated Publications

This study was funded by the National Earthquake Hazard Reduction Program Grant No. 98HQGR1036 in cooperation with the Utah Geological Survey and with support for report preparation from the URS Professional Development Fund. Mining claim owners, Mr. Wesley Webb, and Mr. and Mrs. Robert Davis graciously granted access and permission to conduct this study. Alice Stephenson coordinated our BLM permit application with assistance from Laird Naylor and Lori Hunsaker. Kathy Puseman of Paleo Research Laboratories painstakingly picked through bulk soil samples to miraculously find the best suitable organics for radiocarbon dating. Our work benefited from helpful discussions with Ben Everitt, Ted Barnhard, Ann Mattson, Bill Lund, Dean Ostenaa, and Ron Bruhn. We thank Ann, Ted, and Ron for generously sharing unpublished data, and Ben and Ron for loaning aerial photographs. We also thank Gregg McDonald for assistance with logging and backfilling trenches and Gary Christiansen for coordinating UGS participation. Fumiko Goss, Melinda Lee, Rachel Griener, and Deborah Fournier assisted with report preparation. Finally, we thank Ivan Wong for his tireless interest and support.

A series of *en echelon* down-to-the west normal faults bound the western flank of the southern Oquirrh Mountains and comprise the South Oquirrh Mountains fault (SOMF). These include the Mercur, West Eagle Hill, Soldier Canyon and Lakes of Kilarney faults, extending a total length of 25 km. Although these faults pose an earthquake threat to Salt Lake City, Provo, and the nation's chemical weapon cryofracture plant and storage facility at the Deseret Chemical Depot, very little is known about their paleoseismicity, and what is known remains controversial. Therefore, to better understand the Quaternary behavior and earthquake potential of the SOMF, we conducted a detailed paleoseismic trench investigation of the Mercur fault, the longest fault with the best geomorphic expression.

Our mapping, scarp profiling, trenching and geochronology (radiocarbon and luminescence ages) of the SOMF provide insights into late Quaternary paleoseismicity, indicating a basinward migration of faulting and possible coseismic rupture with the Oquirrh fault to the north. Both the SOMF and the Oquirrh fault are part of the Oquirrh-East Great Salt Lake fault zone, a north-striking, west-dipping, range-bounding, 205-km-long normal fault that lies 22 to 55 km west of the Wasatch fault in the eastern Basin and Range. Trenches across three traces of the Mercur fault reveal paleoseismic evidence for 5 to 7 surface-faulting earthquakes that occurred since 92 ± 14 ka (2-sigma errors), offsetting an alluvial fan with 9.25 to 11.1 m of net vertical tectonic displacement. Four of these events occurred on the westernmost (basinward) trace since 75 ± 10 ka, including the youngest event that occurred shortly after 4110 ± 60 ^{14}C yr BP and before 1510 ± 60 ^{14}C yr BP. This is much younger than previous published estimates for the Mercur fault, but is consistent with recent mid-Holocene cosmogenic ages for a northern bedrock scarp of the Lakes of Kilarney fault along the northern part of the SOMF. The average recurrence interval between the past 5 to 7 events is 12,000 to 25,000 years, but some intervals vary from less than a few thousand years to over tens of thousands of years. Vertical displacements per event average 1.3 to 2.2 m, much larger than expected for a 25-km long rupture (total SOMF length). Slip rate estimates for individual seismic cycles vary between 0.03 to 1.9 mm/yr due to large uncertainties. However, the average vertical slip rate for the past 4 to 6 complete seismic cycles is 0.09 to 0.14 mm/yr across the entire Mercur fault, which is similar to slip rates for the Oquirrh fault to the north. Overall, the overlapping ages for the youngest event, the large displacements per event for both faults, the similar late Quaternary slip rates, and along-strike displacement patterns for the SOMF all suggest coseismic rupture of the SOMF and Oquirrh fault. Paleomagnitude estimates for such a 52-km long rupture range from M_w 7.1 to 7.3, much larger than previous estimates of M_w 6.5 that were based on the Mercur fault length alone. Larger magnitude events have important implications for seismic hazards in nearby Salt Lake City and the Deseret Chemical Depot where chemical weapons are stored and destroyed. These results are already being used in a microzonation study of Salt Lake Valley (NEHRP Award No. 98HQGR1038) and several other seismic hazard evaluations of dams and pipelines throughout the Wasatch Front.

The Mercur fault is part of a series of en echelon down-to-the west normal faults that lie along the west side of the southern Oquirrh Mountains in central Utah. We collectively refer to these faults, which extend from Soldier Canyon south to Fivemile Pass, as the South Oquirrh Mountains fault (SOMF) after Wu and Bruhn (1994). The SOMF is one of several generally north-striking, west-dipping, range-bounding Quaternary normal faults that extend along the western portion of the Wasatch Front urban corridor (Figure 1), where over 80% of Utah's 2.4 million people live. Despite the many paleoseismic investigations that have been conducted along the Wasatch Front, the paleoseismic behavior of the SOMF is poorly understood and controversial. Prior to this study, late Quaternary slip rates, recurrence intervals and paleomagnitudes were unknown. Additionally, issues regarding rupture segmentation and the timing of most recent faulting were unresolved. This is significant because not only do large earthquakes on the SOMF pose a potential threat to the metropolitan areas of Salt Lake City and Provo, but traces of the Mercur fault lie less than 1 km west of the Deseret Chemical Depot (formerly the Tooele Army Depot-South Area), where the nation's chemical weapons storage facility and cryofracture plant are located. Thus, a better understanding of the SOMF is vital for evaluating and mitigating seismic hazards in the region.

1.1 PURPOSE AND SCOPE

This trenching study builds on our previous mapping study of the SOMF (Olig *et al.,* 1999a, 1999b), focusing on the Mercur fault because it appears to be the most recently active and geomorphically prominent portion of the SOMF (Figure 2). The Mercur fault comprises 17 km of the total along-strike length of 25 km for the SOMF. The other faults of the SOMF include the West Eagle Hill, Lakes of Killarney, and Soldier Canyon faults. The latter two faults are primarily evident as faults in bedrock or bedrock-alluvial fault contacts (Gilully, 1932; Wu and Bruhn, 1994). Mapping and profiling of fault scarps on alluvial surfaces along the Mercur and West Eagle Hill faults indicates repeated late Quaternary offsets occurred on both these faults, but scarps overall are higher, more prominent and appear younger on the Mercur fault (Olig *et al.,* 199a, 1999b). The purpose of this study was to develop a better understanding of the late Quaternary paleoseismicity of the Mercur fault through a detailed trench investigation. Our study included: (1) interpretation of black and white stereo aerial photographs of the trench site at different scales (1:46,000-scale 1987 NAPP, ≈1:36,000-scale 1974 and ≈1:24,000-scale 1959 SCS, and ≈1:62,000-scale 1953 AMS photographs); (2) detailed mapping of the surficial geology at the trench site; (3) topographic profiling of fault scarps; and (4) excavation, interpretation and logging of trench exposures; (5) description of soil profiles and lithologic units; and, (6) radiocarbon and luminescence analyses of samples to determine numerical ages.

We excavated three trenches, one each across the western, central, and eastern fault traces north of Mercur Creek (Figure 2). We logged two of the three trenches at a ≈1:20 scale on a planimetric grid. Measurements were made from a level-line to the nearest centimeter. We did not log the trench across the central fault trace because bioturbation obliterated or obscured much of the stratigraphic, pedologic, and structural relations exposed in this trench, precluding a detailed interpretation of the paleoseismic record for the central fault trace. However, mapping and scarp profiling still provide some general paleoseismic constraints on this extremely short (<2 km long), and small fault, which only accounts for about 10% of the late Quaternary slip across the entire zone at this latitude.

1.2 GEOLOGIC SETTING

The SOMF lies within the central portion of the Intermountain Seismic Belt (ISB), a north-south trending zone of shallow, diffuse intraplate seismicity that extends from Montana, through central Utah, to northern Arizona (Smith and Sbar 1974; Smith and Arabasz, 1991). Although diffuse seismicity has occurred in the area of the SOMF, no historical earthquakes have been directly attributed to the fault, a pattern typical of seismic activity in the region (Arabasz *et al.*, 1992).

The SOMF also lies 40 to 45 km west of the Wasatch fault zone, the most active Quaternary fault in Utah. The Wasatch fault zone forms the eastern boundary of the Basin & Range Province, which is characterized by late Cenozoic east-west extension on numerous, generally north-striking, range-bounding normal faults (Zoback, 1983; Hecker, 1993), such as the SOMF. Major west-dipping, range-bounding Quaternary faults that generally lie along strike with the SOMF include: the East Great Salt Lake and the Oquirrh fault zones to the north; and the Topliff Hills fault zone and faults along the East Tintic Mountains to the south (Figure 1). Because these faults have a similar sense of displacement and form a north-south-trending, albeit somewhat discontinuous, zone of faults through central Utah, they could be considered individual segments of a large fault zone that extends for 205 kilometers from Rozel Bay in Great Salt Lake south to Furner Pass (Figure 1). In their probabilistic seismic hazard evaluations of the area, both Youngs *et al.* (1987) and Wong *et al.* (1995) combined these faults into one zone that is likely segmented.

There are also north-northwest striking Quaternary faults west of the SOMF (Figure 1) within Rush Valley. These include the St. John Station fault zone (Barnhard and Dodge, 1988) or the Mid Valley Horst of Everitt and Kaliser (1980) that is within Rush Valley, and the Clover fault zone (Barnhard and Dodge, 1988) or Onaquai east marginal fault of Everitt and Kaliser (1980) that lies along the western margin of Rush Valley, at the base of the Onaquai Mountains. Most of the scarps of the St. John Station fault zone cut the Tertiary Salt Lake Formation but appear to predate Lake Bonneville deposits, except a series of west-facing scarps that lie about 9½ km west of the northern end of the Mercur fault (Everitt and Kaliser, 1980). East-facing scarps of the Clover fault zone are formed on pre-Bonneville alluvium and are probably late Pleistocene or younger (Barnhard and Dodge, 1988). They lie about 18 km west of the southern half of the Mercur fault. The seismogenic relation of the St. John Station and Clover fault zones to the SOMF is unknown, but their close proximity within Rush Valley suggests there is at least a structural relation between the faults.

The Quaternary stratigraphic and geomorphic framework of the area is critical to mapping scarps of the SOMF and better understanding its most recent behavior. Late Quaternary sedimentation along the western base of the southern Oquirrh Mountains has been dominated by alluvial-fan sediments shed from the mountains and deposition of lacustrine sediments in Rush Valley (Solomon *et al.*, 1992). Unfortunately, very little is known about periods of fan deposition along the southern Oquirrh Mountains, but they likely are strongly influenced by climate with higher deposition rates during pluvial periods.

Rush Valley lies within the Bonneville basin, which was repeatedly inundated by paleolakes during the late Quaternary. The age of associated lacustrine deposits and features can often be used to constrain the timing of faulting events (e.g., Machette *et al.*, 1992; Olig *et al.*, 1994). However, of the three most-recent deep-lake cycles, only the Bonneville cycle was apparently

high enough to spill over into Rush Valley (Scott *et al.*, 1983; Currey and Oviatt, 1985; Machette *et al.,* 1992), which generally lies above an elevation of 1512 m. Thus, geologic deposits of the older Cutler Dam or Little Valley lake cycles have not been encountered in Rush Valley.

Lacustrine sediments of Lake Bonneville dominate the surficial geology in central Rush Valley. They form a generally thin mantle over older alluvial deposits and are in turn locally buried by post-lake alluvium, colluvium and eolian deposits. Lake Bonneville reached its highstand, forming the Bonneville Shoreline about 15,000 ^{14}C yr BP (Oviatt *et al.*, 1992) and intermittently overflowed its basin until about 14,500 ^{14}C yr BP. The lake level then catastrophically dropped about 100 meters to the Provo shoreline during the Bonneville flood. Subsequently, Lake Bonneville was not high enough to extend into Rush Valley, so Rush Lake became isolated from Lake Bonneville and is still separated from the modern Great Salt Lake today.

1.3 PREVIOUS WORK

Although the SOMF was first identified in the nineteenth century, its paleoseismic behavior and relation to adjacent faults remains controversial. Gilbert (1890) discovered young normal faults along the west flank of the southern half of the Oquirrh Mountains and interpreted fault scarps near Ophir Canyon to be post-Lake Bonneville and part of the Oquirrh fault, which bounds the northern half of the Oquirrh Mountains from Tooele northward (Everitt and Kaliser, 1980; Barnhard and Dodge, 1988; Solomon, 1996). Atwood (1916) disagreed, believing that the southern end of the range was not faulted. However, through careful mapping of the Stockton and Fairfield 15-minute Quadrangles, Gilully (1928, 1932) provided conclusive evidence of young normal faults along the west flank of the southern Oquirrh Mountains that produced the modern basin-mountain topography of Rush Valley. He cited fault exposures, stratigraphic offsets, structural relief and topographic relief as evidence for a zone of *en echelon* faults, extending from one-mile southeast of Mercur Canyon to just north of Soldier Canyon. He estimated a cumulative throw of 915 to 1524 m down to the west across a "Basin and Range Fault System" that consisted of five principal faults: (1) an unnamed fault south of Mercur Canyon at the range front (this is the northern part of the West Eagle Hill fault); (2) the West Mercur fault (referred to here as just the Mercur fault), almost continuously exposed from Ophir Canyon to West Mercur; (3) the Lakes of Killarney fault, extending from one mile south of Soldier Creek to south of Silverado Canyon; (4) an unnamed bedrock-alluvial fault contact north of Dry Canyon (which we include with the Lakes of Kilarney fault in our mapping); and, (5) the Soldier Canyon fault that extends from two miles north to two miles south of Soldier Canyon.

Gilully (1932) mapped the West Eagle Hill fault as concealed beneath alluvium, extending along the base of the range from one drainage south of Mercur Canyon to two drainages north of McFait Canyon. He inferred the total throw to be 30 to 61 m down to the west based on an exposure in a shaft, on the downthrown side of the fault, of a black carbonaceous shale that is likely the Long Trail Shale member of the Great Blue Limestone and is not exposed anywhere in the footwall section to the east. Gilully (1928, 1932) identified the Mercur fault as a range front fault extending from Mercur Canyon to just north of Ophir Canyon. He described a fault scarp trending N30°W that was nearly continuous except at Silverado Canyon. He noted that the fault was exposed in several prospect pits and shafts as a breccia zone separating alluvium from limestone. Drag-folding in the alluvium indicated normal movement down to the west and fault dips ranged from 40° to 60° west. He cited the presence of faulted alluvium exposed in the

footwall of one shaft as evidence for repeated movement "on a fault whose scarp had been partly buried by alluvium."

Cook and Berg (1961) identified a 60-mile long continuous gravity gradient of 10 milligals per mile that bounds the west side of the southern Oquirrh, East Tintic and Boulter Mountains. They attributed the gradient to a range-front fault, the Oquirrh-Boulter-Tintic fault zone. Everitt and Kaliser (1980) followed this nomenclature in their geologic mapping of Rush Valley, referring to faults extending from Ophir Canyon to near Fivemile Pass as the northern Oquirrh-Boulter-Tintic fault zone. Although they included the Lakes of Killarney and Soldier Canyon faults after Gilully (1932), they did not include the West Eagle Hill fault on their 1:50,000-scale maps. They also mapped surficial deposits and fault scarps on alluvium of the Mercur fault, extending it much farther south than Gilully's mapping, to the latitude of Fivemile Pass. They identified three main age categories of deposits along the scarps: (1) QToa, older (pre-Lake Bonneville) alluvium; (2) Qb, Lake Bonneville deposits; and (3) Qya, younger (post-Lake Bonneville) alluvium. Their mapping shows QToa deposits as faulted, whereas Qya deposits are not faulted. Along most of its length, traces of the Mercur fault lie well above the Bonneville Shoreline and associated Qb deposits, except for the western most fault trace at its southern end, where scarps extend down to elevations below 5,200 feet. Here, at a site roughly 4-1/2 km west of Fivemile Pass, Everitt and Kaliser (1980) excavated a trench across a small west-facing scarp that lies just below the Bonneville shoreline. Their trench exposed a west-dipping north-south striking main fault and a 12-m-wide graben. They interpreted the Lake Bonneville deposits exposed in the trench to be faulted based on the presence of shear fabric (B.L. Everitt, personal communication, 1995) and warping of contacts.

In contrast, Barnhard and Dodge (1988) interpreted the youngest movement on the Mercur fault to have occurred prior to formation of the Bonneville shoreline ($\geq$ 15,000 ^{14}C yr BP) based on: analysis of the morphology of 11 fault scarp profiles, reinterpretation of Everitt and Kaliser's (1980) trench log, and excavation of a shallow trench located south of Everitt and Kaliser's, where they observed that post-Bonneville alluvium was unfaulted. However, the age of the alluvium was unconstrained and could be very young. Similar to Everitt and Kaliser (1980), neither Bucknam (1977) nor Barnhard and Dodge (1988) included the West Eagle Hill fault on their maps of fault scarps in unconsolidated deposits. However, Barhard and Dodge (1988) did map fault scarps in alluvium of the Mercur fault, extending for 15 km from just north of Ophir Canyon south to Fivemile Pass, similar to Everitt and Kaliser's (1980) mapping. In keeping with these studies, Hecker (1993) did not include the West Eagle Hill fault, either separately or as part of the Mercur fault, on her Quaternary fault map of Utah. However, in their investigation of the SOMF, Wu and Bruhn (1994) mapped discontinuous late Quaternary fault scarps in alluvium, extending from Mercur to Sunshine Canyons at the foot of the range. They named these scarps the West Eagle Hill fault. Primarily based on geomorphic map relations, they interpreted the youngest faulted alluvium (their unit Qf_2) to have been deposited early in the Bonneville lake cycle. From this, and their analysis of fault scarp profiles across the West Eagle Hill, Lakes of Killarney, and Mercur faults, Wu and Bruhn (1994) suggested that the youngest faulting anywhere on the SOMF occurred prior to formation of the Bonneville shoreline.

Most recently, cosmogenic ^{14}C ages determined for a bedrock scarp of the northern Lakes of Kilarney fault suggest a mid-Holocene surface rupture occurred around 4,400 $\pm$ 1,200 cal yr BP (Handwerger *et al.,* 1999), possibly contemporaneous with the most-recent event on the Oquirrh fault to the north (Olig *et al.*, 1994; 1996). This raises questions about segmentation of the

Oquirrh-East Great Salt Lake Fault zone. If a mid-Holocene event occurred on the SOMF and it ruptured with the Oquirrh fault, the rupture would have been over 52 km long and capable of producing a M_w 7.1 earthquake versus an expected M_w of 6.7 for a 25-km –long rupture of the SOMF alone. These are important seismic hazard issues for Desert Chemical Depot, and the Salt Lake and Provo metropolitan areas, which are located roughly 20 km east of the faults.

2.1 SURFICIAL GEOLOGY

The Mercur Canyon trench site is located roughly 30 km south of Tooele, near the intersection of Highway 73 and Mercur Canyon Road. It lies near the along-strike midpoint of the Mercur fault, just north of the northern end of the West Eagle Hill fault (Figure 2), where Wu and Bruhn (1994) estimate cumulative displacements are between 1800 and 1900 m. This is about 75 to 80% of their maximum estimate of cumulative displacement along the entire SOMF, which is about 2400 m and occurs about 4 km to the north near Lewiston Peak.

At Mercur Canyon, the Mercur fault is geomorphically expressed as a complex pattern of northwest trending fault scarps on a late Pleistocene alluvial fan (af2 on Figure 3). These scarps are dominantly west-facing and form three principal traces, with the westernmost scarp being the highest and most prominent. Offset on scarps along the central fault trace dies out less than 0.8 km to the south, whereas the western and eastern fault traces continue southward to the southern end of the Mercur fault near the Old Pony Express Road (Figure 2). To the north, the three faults appear to merge, forming a single bedrock-alluvial fault contact north of West Dip Gulch (Figure 2).

In our previous mapping along the SOMF, (Olig *et al.,* 1999a), we distinguished six different relative ages of stream and fan alluvium (units af1 through a6/af6, oldest to youngest, respectively), and two different intermediate age terrace deposits (units t3 and t4) (Figure 2). At the Mercur Canyon site, a large late Pleistocene alluvial fan (unit af2) is partially inset into an older, higher fan (unit af1) preserved near the mouth of the canyon (Figure 2). The af2 fan surface is in turn dissected and locally incised by younger stream and fan alluvium (units a5-6, af5-6 and af6), most notably along Mercur Creek (Figure 3) where the modern channel has incised between 15 and 20 m below the af2 surface in the footwall of the Mercur fault. Along the south side of Mercur Creek, a small terrace remnant (t4) is locally preserved at elevations between 3 and 7 m above the modern drainage (Figure 3). Scarps of the Mercur fault clearly offset the af2 and t4 surfaces but appear to be buried by the younger a5-6/af6 alluvium.

Relative age constraints (including geomorphic position, cross-cutting relations, pedogenic development and surface morphologies) suggest that af2 and t4 surfaces are likely late Pleistocene and the a5-6/af6 alluvium is latest Pleistocene to Holocene (Olig *et al.,* 1999a). Elevations at the Mercur Canyon trench site range between 1686 and 1738 meters (5530 and 5700 feet), well above the Bonneville shoreline of Lake Bonneville. However, approximately 2 km southwest of the trench site, the Bonneville shoreline is clearly cut into af2 deposits whereas af5-6 deposits appear to partially bury the shoreline (Figure 2). Thus, the af5-6 alluvium is likely younger than 15,000 ^{14}C yr BP and af2 alluvium is older. This interpretation is also consistent with relative soil development on the deposits. Soil profiles on af2 surfaces along the SOMF are characterized by thick (average is 50 cm) stage III to IV K horizons and carbonate rind thicknesses that average 4.2 ($\pm$ 2.7) mm on clasts. $^{10}Be/^{26}Al$ cosmogenic ages for limestone boulders on the af2 surface at Mercur Canyon suggest a minimum age of 75 $\pm$ 5 ka (Mattson and Bruhn, 2000). In comparison, soils on af5-6 surfaces are characterized by weakly developed Bk horizons (stage I to I+ morphologies) and thin (< 1mm) discontinuous rinds on clasts (Olig *et al.,* 1999a).

Topographic profiles measured across scarps of the three principal traces at the trench site are shown on Figure 4. Measured net vertical tectonic displacements (NVTD, as defined by Swan *et*

al., 1980) are 6.25 m for the western fault, 1.0 m for the central fault and 2.5 m for the eastern fault (see Section 3.2 for further discussion of displacements). The western scarp is the highest, most prominent and continuous scarp, with a maximum slope angle of 23° and a triple bevel. The western scarp crest and base are relatively distinctive and there is no surficial evidence for antithetic faulting in the aerial photographs. However, a high-resolution seismic profile across the western scarp suggests that a buried (?) antithetic fault lies about 35 m west of the main fault (A. Mattson, Univ. of Utah, written comm., 1-09-01). Although underlying older fan sediments (af1?) appear offset it is not clear whether af2 deposits are offset or not. North of the trench on the western scarp, the western fault branches into two to four subparallel traces, whereas south of the trench the fault scarp is dissected by two small ephemeral drainages before it intersects the Mercur Creek drainage (Figure 3). The central fault has the smallest and most subdued scarp, with a maximum slope angle of only 8° and a single bevel. This scarp is relatively distinct on aerial photographs, but it is more subtle on the ground, as it is very dissected, discontinuous and has a broad crest. No scarps associated with the central trace are visible on the t4 terrace south of Mercur Creek, and although some scattered small scarps are present on af2 deposits further to the south, (Figure 3), offsets decrease to the south and die out within a couple of kilometers. The eastern scarp is intermediate in height and geomorphic prominence between the western and central scarps, showing a maximum slope angle of 8° and a double bevel. A small, short, east-facing antithetic fault is associated with the eastern fault, forming a 60-m-wide graben (Figure 3). Although the eastern fault does continue to the south with a distinct scarp on both the t4 and af2 surfaces, the antithetic fault scarp is not evident south of Mercur Creek drainage on either the t4 or af2 surfaces (Figure 3).

2.2 TRENCH EXPOSURES

We excavated three trenches north of Mercur Creek, at the Mercur Canyon site, one across each fault trace (Figure 3). We chose to trench scarps north of Mercur Creek over those south of Mercur Creek for several reasons: (1) displacement on the West Eagle Hill fault, to the east, picks up and increases south of Mercur Creek, coincident with where displacements decrease on the Mercur fault (Olig *et al.* 1999a); (2) scarps are geometrically simpler and better preserved to the north being more continuous and less dissected by small drainages; and (3) there is better access overall to scarps on the north. The West Trench was about 44 m long and as deep as 5 m near the main fault. The Central Trench was about 28 m long and up to 2½ m deep. The East Trench was about 62 m long and as deep as 2¾ m. All trenches were excavated with a trackmounted excavator using a 4-foot (1.2 m) wide bucket. Walls were scraped and cleaned to remove bucket smear. The West and East Trenches were logged at a scale of 1 inch = 0.5 meters (≈1:20 scale) on a planimetric grid. For reasons previously discussed, we did not log the Central Trench. In the trenches that we logged, we strung level lines and marked stations at one-meter intervals to provide reference lines. Locations of samples, and key fault, stratagraphic and pedologic contacts were marked with nails and/or spray paint, and measured relative to the level line to the nearest centimeter. Total errors of measured points on the logs are estimated to be less than 5 cm. Original trench logs were then reduced (≈50%) and simplified during drafting, the latter primarily by reducing detail in clast fabrics and using generalized patterns for some units. We note that we did not log the easternmost portions of both the East and West Trenches as alluvial fan sediments were undeformed; however, we did examine and trace contacts

throughout these portions to look for any evidence of faulting, tilting, warping, fracturing or other signs of deformation.

We collected samples for radiocarbon and luminescence analyses to provide numerical age constraints for faulting events (Table 1). During sampling, care was taken to try and avoid bioturbated areas, including insect and animal burrows and large roots. Organic samples collected for radiocarbon analysis were hand-picked from the trench wall with a clean soils knife, stored in zip-loc bags, prepared by Paleo Research Laboratories (Appendix C) and analyzed by Beta Analytic Inc. (Appendix D). Paleo Research Laboratories washed bulk samples, and identified and sorted organic fragments for potential dating (Appendix C). Only charcoal was dated, samples were small (<0.01 g), and required analysis using an accelerator mass spectrometer (AMS). We report both ^{14}C ages, with 1 σ errors, and calendar calibrated ages with 2 σ errors as calculated by Beta using calibration data in *Radiocarbon* (v. 40, no. 3, 1998), and methods by Talma and Vogel, *Radiocarbon*, v. 35, no. 2, p. 317-322, 1993: A Simplified Approach to Calibrating C14 Dates (Appendix D).

Application of thermoluminescence dating in paleoseismic studies of normal faults was pioneered along the Wasatch Front (e.g., Forman *et al.*, 1988, 1991). Thermoluminescence is the release of light when mineral grains are heated above 150°C and sediments acquire thermoluminescence from background radiation. Thermoluminescence in sediments increases steadily with time and age estimates are made by determining the ratio of the equivalent dose (proportional to the luminescence signal accumulated since burial) to the dose rate (or background radiation at the sample site) (see Forman *et al.*, 1999, for further discussion).

The recent development of using infrared stimulated luminescence (IRSL), which measures luminescence of the infrared portion of the light spectrum, has some significant advantages for paleoseismic applications (Spooner *et al.*, 1990; Forman, 1999). Samples for IRSL analysis for this study were collected by first scraping the trench wall back 20 cm, driving a brass or PVC sampling tube into the wall, extracting the tube and capping its ends. In the laboratory, samples were extracted, the ends shaved and discarded, and IRSL analyses were completed on the 4-11 micron polymineral fraction of the sample. The resultant blue emission is isolated by 5-58 and GG-400 Corning filters and measured by a standard photomultiplier tube. The total bleach method was used with the residual level defined by 1 hour sunlight exposure. An exponential or linear fit were used to model the additive dose response with the interpolation to the residual level <20% of the highest applied beta dose. The equivalent dose was calculated for 3 to 90 seconds after initial exposure to infrared excitation (880 ± 80 nm). The precision of analysis is very good, with dispersion in additive dose response usually ≤10%. Dose rate estimate was calculated from alpha counting to determine U and Th content (assuming secular equilibrium) and elemental analysis to provide for ^{40}K component. Moisture content of 10 ± 3% was assumed in the final age calculation. Errors of 1 σ are reported for all IRSL ages. However, 2 σ errors are used in calculating paleoseismic parameters such as recurrence intervals and slip rates.

2.2.1 West Trench

The West Trench extended from the crest of the main scarp to over 15 m downslope of the scarp base. The trench exposed a main west-dipping normal fault, located about halfway up the scarp, with a series of smaller normal and reverse faults, that overall offset older alluvial fan deposits (af2 or Unit 1) down to the west (Figures 5 and 6). A series of stacked colluvial wedge and

eolian deposits locally overlie the fan deposits in the hanging wall adjacent to the main fault. Structural, stratigraphic and pedologic relations exposed in the trench, discussed in detail below, provide evidence for four surface-faulting events that occurred since the alluvial fan surface stabilized. We refer to these as events W_w (oldest) through Z_w (youngest).

2.2.1.1 Stratigraphy

We logged eight stratigraphic units in the West Trench; abbreviated descriptions are shown on Figure 6 and detailed descriptions are provided in Appendix A. Units generally decrease in age sequentially (i.e., Unit 1 is oldest and Unit 7a is youngest), with Unit 5b – 7b being the undifferentiated downslope correlative deposit to Units 5a through 7a. Some of these units include buried soils and the tops of these catenas are designated S_1 through S_5 on Figure 6, with S_1 being the soil to initially form on the alluvial fan surface and S_5 being the modern soil. Soils are generally stripped in the footwall and catenas generally converge downslope to form cumulative profiles in the hanging wall. Detailed soil profile descriptions for two locations (Figure 6) are provided in Appendix B.

Unit 1 includes older fan alluvium exposed in both the footwall and hanging wall and is comprised of interbedded debris-flow and stream channel deposits that dip gently (3° to 5°) southwest, parallel to the present surface, outside of the zone of deformation (Figure 6). The top of Unit 1 includes a buried soil, S_1, which consists of a variably stripped K horizon (stage III morphlogy) in the footwall and a Btk horizon that is extensively overprinted by the overlying S_2 soil profile in the hanging wall. Interbeds range from sandy silts with gravels (e.g., bed above marker horizon 1c) to sandy, cobbley gravels with boulders (e.g., bed below marker horizon 1a) (Figure 6). The interbeds provide distinctive markers to distinguish stratigraphic truncations at the main fault, and measure vertical separations on smaller faults. In regard to the latter, a coarser subunit with boulders, below marker horizon 1a (Figure 6), could be traced throughout the hanging wall. However, this subunit could not be distinguished in the footwall (including the 18-m-long portion exposed east of st. 0 m and not shown on Figure 6), and thus, was apparently eroded away subsequent to faulting. Significant erosion of Unit 1 in the footwall is also indicated by: (1) stripping of the S_1 soil, particularly close to the main fault; and, (2) the angular discordance between the steeper slope of the scarp face (maximum slope of 23°) and the gentler dip of fan interbeds (3° to 5°). Unit 1 (and S_1) is backtilted 5° to 6° toward the main fault in the hanging wall between st. 10 and 16 to 18 m. In contrast, it is warped (and faulted) up to the east between st. 10 and 6 m, adjacent to the main fault in the hanging wall, and it is warped down to the west, between st. 4 and 6 m, adjacent to the main fault in the footwall.

Unit 2 locally overlies Unit 1 (and S_1) in the hanging wall between st. 9 and 22 m. It pinches out to the east, and becomes indistinguishable from overlying Units 4 and 5b-7b to the west (Figure 6). We interpret this faintly laminated but somewhat bioturbated pinkish tan sandy silt to be a loess deposit, locally filling swales on the original fan surface. The buried S_2 soil that is developed on Unit 2 and overprints the buried S_1 soil on Unit 1 varies laterally, with carbonate morphology generally increasing in stage from II to IV downslope, where it converges with overlying soil profiles near st. 16 m (Figure 6). However, it also appears to be affected by partial dissolution and stripping near some faults between st. 6 and 9 m. IRSL ages for two samples (MCWT2-L1 and MCWT2-L2) collected from the A_v horizon of the buried soil S_2 on Unit 2 (Figure 6) are 68.7 ± 5.2 and 80.7± 6.3 ka, respectively. (Table 1). These ages nearly overlap

within 1 σ errors and are consistent with the cosmogenic ages (minimum of 75 ± 5 ka) for the af2 fan surface (Mattson and Bruhn, 2000).

Unit 3 locally overlies Units 1 and 2 between st. 7½ and 13½ m in the hanging wall (Figure 6). This very poorly-sorted, matrix-supported, heterogeneous, wedge-shaped sediment package varies from gravels with cobbles and boulders in a sandy silt matrix to a sandy silt with gravel. It tapers westward, interfingering and becoming indistinguishable with the overlying Unit 4 as it pinches out. It thins to the east and appears to be truncated and eroded where it has been faulted and warped up between st. 7 and 9 m. However, the contact with the overlying Unit 5a is inferred primarily based on color and textural differences in the matrices of the two units, and it becomes less distinct and more difficult to identify as Unit 3 becomes more bouldery east of st. 8 m (Figure 6). Based on its stratigraphic characteristics, shape and location, we interpret Unit 3 to be colluvium derived from a fault scarp that exposed Unit 1 (and possibly Unit 2) in its free face. The associated surface faulting event, Event W_w, was the oldest event exposed in the West Trench.

Unit 4 locally overlies Units 3 and 2 between st. 9 and 18 m in the hanging wall (Figure 6). This mottled sandy silt generally fines downslope, contains intraclasts and has a weakly developed buried soil, S_3, with a stage I+ Bk horizon. Similar to Unit 3, Unit 4 also appears to have been truncated by erosion to the east. In contrast, to the west, Unit 4 becomes extensively bioturbated and west of st. 18 m it finally becomes indistinguishable from overlying and underlying units as buried soils converge. Based on its stratigraphic characteristics, we interpret Unit 4 to be a mix of eolian and reworked eolian deposits washed downslope to the base of a fault scarp. IRSL ages for two samples (MCWT4-L3 and MCWT4-L4) collected from Unit 4 (Figure 6) Are 37.0 ± 3.0 and 46.7 ± 3.8 ka, respectively (Table 1). These ages overlap within 2 σ errors and are consistent with stratigraphic and pedologic relations.

Unit 5a is a wedge-shaped deposit that locally overlies Units 3 and 4 between st. 6 and 12½ m in the hanging wall (Figure 6). Unit 5a is similar to Unit 3 in texture, composition and sorting, but generally contains more gravel, has a coarser, sandier matrix, and includes a large intraclast or block of Unit 1 near st. 9 m (Figure 6). Similar to Unit 3, we interpret Unit 5a to be fault-scarp colluvium that likely was derived from reworked deposits of Units 1, 3 and 4 subsequent to the antepenultimate surface-faulting event, Event X_w.

Unit 6a locally overlies Units 5a and 4 between st. 5 and 13 m in the hanging wall (Figure 6). This wedge-shaped, poorly-sorted, matrix-supported, brown, gravelly sandy silt with cobbles generally fines downslope and is intensely bioturbated west of st. 12½ m. The upper portion is somewhat stratified with clasts generally showing a slope-parallel fabric that slightly steepens toward the main fault. It includes a thick, well-developed buried soil, S_4, with a Btk horizon that varies laterally but generally has prominent subangular peds and a stage I to II carbonate morphology (Appendix B). Based on its shape, location and stratigraphic characteristics, we interpret Unit 6a to be a thick package of colluvium derived from a relatively large fault scarp created during the penultimate surface-faulting event, Event Y_w. Near the base of unit 6a, immediately adjacent to the main fault, the loose u-shaped fabric of several large clasts is suggestive of a "heal" or broad fissure that often forms at the bottom of a large free-face. This has been subsequently faulted in the most-recent faulting event, Event Z_w. AMS analysis of charcoal (sample MCWT6-1RC on Figure 6) collected from a small remnant of A horizon at the top of Unit 6a on S_4 yielded a ^{14}C age of 4110 ± 60 yr BP, and a calendar calibrated age of 4430 to 4830 cal yr BP (Table 1; Appendix D).

Unit 7a is a gray-brown, cobbley, sandy, silty gravel that lies at the top of the colluvial stack between st. 4 and 15 m in the hanging wall (Figure 6). This poorly-sorted, elongated wedge-shaped deposit contains blocks of Unit 6a immediately downslope of the main fault, and includes the modern soil, S_5, at the top of the trench (Figure 6). It generally fines downslope and varies from clast-supported at the base near the main fault to matrix-supported away from the fault. We interpret Unit 7a to be the colluvial wedge deposit for the most recent surface faulting event (Event Z_w). It shows classic fault-scarp colluvial stratigraphy (e.g., Nelson, 1992), with a coarser, clast-supported, very poorly-sorted debris facies filling a 90-cm-wide depression adjacent to the buried free-face of the main fault (Figure 6). Overlying this is the poorly-sorted, but somewhat stratified, slopewash facies that extends 8 m downslope (Figure 6). AMS analysis of charcoal collected from the debris facies (sample MCWT7-1RC on Figure 6) yielded a ^{14}C age of 1510 ± 60 yr BP and a calendar calibrated age of 1295 to 1530 cal yr BP (with 2 σ error) (Table 1; Appendix D). Thus, radiocarbon ages for Units 6a and 7a are stratigraphically consistent.

2.2.1.2 Structure

Structures exposed in the West Trench included the main, west-dipping normal fault between st. 4 and 6 m, and several smaller normal and reverse faults that form a 4-m-wide zone in the hanging wall, immediately adjacent to the main fault (Figure 6). Additionally, beds are: (1) locally drag-folded down to the west in the footwall adjacent to the main fault; (2) backtilted overall 5° to 6° toward the main fault in the hanging wall east of st. 18 m; and, (3) locally warped down to the west in a faulted monocline between st. 5½ and 9 m (Figure 6).

The main fault overall strikes N20° to 25° W and dips 76°-82° W, but includes several sub-vertical to east-dipping splays. Below Unit 7a, the main fault is characterized by well-developed shear fabric in a gray gravelly shear zone that varies from a few centimeters to over 80 cm wide. Along the eastern boundary of Unit 7a, but below the modern soil, the main fault is characterized by a buried and eroded fault scarp free-face (above vertical st. + ½ m on Figure 6). The main fault clearly cuts all units exposed in the West Trench, except Unit 7a, and displaces them down to the west. Additionally, four associated splay faults appear to terminate at the base of Unit 7a.

The zone of faults cutting the monocline between st. 5½ and 9 m include reverse and normal faults that dominantly dip steeply to the east and overall displace beds down to the west. They were identified based on offsets of contacts and variably-developed shear fabric of gravel clasts. Some of the faults appear to terminate at the base of Unit 7a, whereas some appear to die-out below this (Figure 6). Individual fault offsets are small (stratigraphic separations <40 cm), but cumulatively the zone displaces the Unit 1a marker horizon about 2.3 m down to the west (Figure 6). Estimates of displacements per event on the structures exposed in the West Trench are discussed in the following section.

2.2.1.3 Trench Log Reconstruction and Event Summary

Figure 7 shows our step-wise reconstruction of the West Trench log. This interpretation of the sequence of events is developed by progressively removing deformation (faulting and folding) associated with each surface faulting event. It assumes 2-D-strain along the section with no volume loss. We pinned the footwall and constrained the total net throw of marker horizon 1a to

be equivalent to 6.25 to 7.1 m (see Section 3.2 for discussion – Figure 7 shows 6.25 m), the total estimated NVTD based on the scarp profile and stratigraphic and pedologic relations exposed in the trench. Offsets per event on the main fault are estimated from relative colluvial wedge thicknesses, and units (and subunits) likely exposed in the free-face subsequent to each surface-faulting event. Thus, the net offsets per event are crude, but probably provide a reasonable indication of the relative size of individual events and this comparison is important for evaluating whether fault behavior is characteristic or not (see for example Schwartz and Coppersmith, 1984). Additionally, although this reconstruction is non-unique in many respects, it does help test the plausibility and internal consistency of our interpretation of the paleoseismic history of the western fault trace. A summary discussion of the structural, stratigraphic, and pedologic evidence for each surface-faulting event, the associated estimates of net vertical displacements per event, and the timing of events follows.

Event Z_w – Compelling structural, stratigraphic and pedologic evidence for this youngest surface-faulting (Unit 7a) event includes: (1) a buried free-face at the top of the main fault; (2) a colluvial wedge deposit adjacent to the free-face, with both debris and slopewash facies that bury an underlying soil (S_4); (3) multiple fault terminations at the top of this buried soil; and, (4) backtilting of the buried soil (Figure 6). Soon, if not immediately after, the surface ruptured during Event Z_w, blocks of the S_4 soil apparently toppled off of the free-face into the large fissure or "heal" created at the base of scarp. We estimate the paleo-free-face height to have been about 1.3 m, including the heal. Restoring the S_4 paleosurface, we estimate about 1 (± ¼) m of net vertical displacement for Event Z_w. This includes 85 cm of vertical slip on the main fault and the net remainder across four secondary faults. These secondary faults show both reverse and normal slip with individual offsets ranging from negligible to as much as 27 cm of dip slip. Event Z_w occurred shortly after 4430 to 4830 cal yr BP (based on the radiocarbon age of the top of S_4) and sometime before 1295 to 1530 cal yr BP (based on the radiocarbon age of the debris facies of Unit 7a). Stratigraphic and pedologic relations suggest the former is a close maximum-limiting age, whereas the latter may be a distant minimum-limited age for Event Z_w.

Event Y_w – Strong evidence for the penultimate event includes: (1) a 2.0 to 2.2 m thick colluvial wedge deposit adjacent to the main fault (Unit 6a); (2) termination of a small reverse fault at the top of Unit 5a near st. 7.5. m; (3) apparent differential offsets between the top and base of Unit 6a on secondary faults between st. 5½ and 7 m; and (4) apparent backtilting of the top of Unit 5a suggested by differential slopes between the tops of Unit 5a and Unit 6a. The coarse, poorly-sorted, matrix-supported, loose, jumbled character of Unit 6a near its base adjacent to the main fault is typical of the debris facies of fault-scarp derived colluvium. In contrast, further up section and downslope, Unit 6a is matrix-supported and clasts show a distinct slope-parallel fabric and stratification that steepens toward the fault. We interpret this portion of Unit 6a to be the slopewash facies of the penultimate event colluvial wedge. However, disruption by bioturbation and subsequent deformation during the youngest faulting event has generally obscured the contact between the two facies. Regardless, the apparent preservation of the heal of the debris facies overlying the termination of a nearly ½- m wide shear-zone (at about vertical st. -1½ m on Figure 6) also supports our interpretation of Unit 6a as the penultimate event colluvial wedge.

Based on the thickness of Unit 6a, and restoring offsets on the base of Unit 6a (including the ≈ 4 cm of down-to-the-west warping and slip on the reverse fault at st. 7½ m), we estimate at least 2 to 2¼ m of net vertical slip for Event Y_w. Numerical age constraints on the timing of Event Y_w

are poor; <42 ka and > 4.4 ka, but soils also provide some relative constraints. Based on the well-developed Btk horizon of S_4 on Unit 6a, Event Y_w likely occurred many (tens of?) thousands of years before 4.4 ka. In comparison, based on the lack of apparent soil development on the underlying Unit 5a, much less time passed between deposition of Unit 5a and the occurrence of Event Y_w than between deposition of Unit 6a and the occurrence of Event Z_w.

Event X_w – Evidence for this, the antepenultimate event, is strong, despite the somewhat anomalous character of the associated deformation, including down-to-the-west warping and reverse faulting. The evidence for Event X_w includes: (1) differential warping and down-to-the-west faulting of the base of Unit 5a (and the underlying soils S_1 – S_3 and Units 1 through 4) compared to the top of Unit 5a (Figure 7); and, (2) the lithology (including blocks of Unit 1), texture, shape, location and other stratigraphic characteristics of Unit 5a indicate it is colluvium shed from a scarp created by the deformation associated with Event X_w. Although Unit 5a was apparently not deposited at the base of a "typical" normal fault-scarp, it still shows many of the typical characteristics of colluvial wedges associated with normal fault scarps (e.g., Nelson, 1992) as the processes influencing deposition were likely very similar. One difference is that the tapered shape of Unit 5a is more elongated to the east and there is apparently no associated buried free-face (inferred or otherwise), although it is noteworthy that the maximum thickness of Unit 5a is immediately downslope of the maximum zone of downwarping of underlying units between st. 7 and 8 m (Figures 6 and 7). Stratigraphic relations suggest that subsequent to Event X_w, Unit 3 and possibly Unit 4 were eroded away east of st. 7½ m. This is supported by the apparent partial stripping of the top of Unit 1 and the S_1 – S_2 soil in this same area (Figure 6). What is difficult to decipher is how thick and how far east Unit 3 originally extended, and if slip occurred on the main fault during Event X_w (Figure 7). Based on the thinning of Unit 5a to the east, we infer little, if any, slip occurred on the main fault during Event X_w, but this is poorly constrained. Indeed, net slip for Event X_w is the most difficult to estimate and although our preferred estimate is about 1¾ m, it could have ranged between 1 and 2 m, depending on the amount of sip on the main fault and how the warping deformation is removed (Figure 7). Event X_w occurred sometime before Event Y_w and after, most likely shortly after, 42 ± 8 ka (the average of luminescence ages of the underlying Unit 4, 2 σ error).

Event W_w – Evidence for the oldest event in the West Trench, Event W_w, includes an associated colluvial wedge deposit (Unit 3) that buried the alluvial fan surface (S_1 – S_2 soil) and an inferred free-face along the main fault (Figure 7). However, because Unit 3 was apparently eroded away between st. 5 and 7½ m after Event X_w (Figures 6 and 7), the original geometry of Unit 3 is poorly constrained. The geometry we show in our reconstruction (Figure 7) is based on the amount of vertical slip remaining on marker horizon 1a (the top of the bouldery bed in Unit 1), which is about 1½ m. This geometry places the bouldery bed in Unit 1 near the top of the free-face of Event W_w, which is consistent with the bouldery nature of Unit 3 (and Unit 5 that includes material reworked from Units 3 and 1). However, given all of the uncertainties, slip could have ranged between 1 and 2¼ m. Event W_w occurred shortly after 75 ± 10 ka (based on the average of luminescence ages for the underlying A_v horizon on Unit 2, 2 σ error), and well before 42 ± 8 ka.

2.2.2 Central Trench

The Central Trench was oriented N64°E and extended for about 28m from a couple meters east of the central scarp crest (Figure 3). The south wall and selected portions of the north wall were

cleaned, inspected and photographed. The Central Trench exposed older alluvial fan deposits (af2 in Figure 3 and correlative to Unit 1 in the West and East Trenches) overlain by an extensively bioturbated loess (a tan, sandy silt with gravel) that varied in thickness from 0 m (upslope) to over 1 m (downslope). Near the location of the maximum slope on the scarp was a subvertical, 1- to 3-m-wide zone of bioturbation that obscured nearly all alluvial fan stratigraphy and may have originally been the fault zone that formed the central fault scarp (Figure 8). This zone was present on both the north and south walls. Alluvial fan deposits in the Central Trench were markedly coarser than in the West and East Trenches, and included more heterogeneous channel and debris-flow deposits that varied laterally over short distances, precluding definitive stratigraphic correlations of beds across the burrowed zone.

In Figure 8, Andrew Gorton is pointing to the base of a debris flow deposit with boulders in a tan, silty-gravel matrix that may be correlative across the burrowed zone. If it is does correlate across the burrowed zone, the debris flow is offset about 1 m down to the west, consistent with the amount of NVTD measured across the central scarp. Although the modern soil and underlying buried K horizon appear to drape the slope, suggesting that much of the soil development predated any faulting that may have been present, relations were ambiguous due to the extensive bioturbation.

In summary, the paleoseismic record exposed in the Central Trench was ambiguous, but stratigraphic and pedologic relations were suggestive of about a meter of offset that may have occurred in an older event. This is consistent with geomorphic relations along the central scarp where 1 m of NVTD on the af2 surface appears to predate the t_4 terrace along Mercur Creek (Figure 3). It is also consistent with the morphology of the central scarp, which is broad, low-angle, degraded, discontinuous, and shows a single bevel.

2.2.3 East Trench

The eastern scarp is very broad, and we excavated the East Trench from several meters upslope of the crest to about 62 m downslope across the wide graben (Figure 3). We did not log the eastern 20 m of the East Trench as there was no evidence of any deformation (faulting, folding or fracturing of any marker horizons) in this portion. The trench exposed a main east-dipping fault and several smaller east-dipping to subvertical faults that overall offset older alluvial fan deposits (Unit 1) down to the west 2.5 ± 0.5 m (Figure 9). The fan deposits were well-stratified, providing good marker horizons to identify faults and folding (e.g., 1a, 1b, and 1c on Figure 9). Locally overlying the fan deposits on the downthrown side of some faults were fine-grained, wedge-shaped packages of colluvum and loess deposits (Unites 2, 2a, and 2b). Unfortunately, on both the north and south walls, large krotovina obscured some of the key cross-cutting relations near some faults (e.g., near st. 14 to 15 m and st. 37 to 38 m). Regardless of all the uncertainties, differential offsets and cross-cutting relations exposed in the trench indicate two separate faulting events occurred on the eastern fault. We refer to the older faulting event as Event V_E, and the younger one as Event W_E. The stratigraphic, pedologic, and structural evidence for these events is described in the following sections.

2.2.3.1 Stratigraphy

We logged three stratigraphic units (1 through 3) in the East Trench (brief descriptions are on Figure 9 and detailed descriptions are in Appendix A). Similar to the West Trench, units

decrease in age sequentially. The East Trench also exposed two buried soils (S_1 and S_2), in addition to the modern soil, S_3 (Figure 9). The two buried soils can be tentatively distinguished from each other on the downthrown portions adjacent to some faults (e.g., between st. 15 and 24 m), but more typically S_1 and S_2 are indistinguishable, forming a cumulative profile that is characterize by a thick K horizon. A soil profile description (SP3) is included in Appendix B and was located near st. 16 m (Figure 9).

Unit 1 is composed of interbedded stream channel and debris-flow deposits that dip gently (typically 3°) southwest and were exposed the full length of the trench. Unit 1 in the East Trench correlates to Unit 1 in the West Trench and is lithologically very similar, but overall is better stratified, with finer-grained and better-sorted channel deposits, including thin beds of pea-sized gravel (shown stippled on Figure 9) that were very good marker horizons. One in particular, 1c on Figure 9, could be traced along most of the trench. Unit 1 is not only offset by the main fault and several secondary faults, it is also warped down to the west across a wide monocline associated with the main fault (Figure 9). As a result of the uplift, the top of Unit 1 is partially eroded east of st. 13 m.

Units 2a, 2b, and 2 (undifferentiated) are a tan sandy clayey silt that overlies Unit 1 and is only locally preserved on the downthrown side of faults between st. 13 and 24 m, and between st. 37 and 39 m (Figure 9). These units are thickest (0.6 m) adjacent to the main fault, and taper westward. The sediments are extensively bioturbated, but faint laminations are preserved in some places, particularly in Unit 2a. We interpret these deposits to be eolian and reworked (colluviated) eolian sediments.

The upper contact of Units 2 and 2b is abrupt and wavy to irregular. It includes the top of a buried soil (S_2) that also extends across the top of Unit 1 where Units 2b and 2 were not present (Figure 9). S_2 is characterized by a K horizon which is quite distinct from the A and B horizons of the modern soil (S_3 in the overlying Unit 3). Unit 2b was primarily distinguished from Unit 2a based on the top of a buried soil, S_1 (Figure 9). However, Unit 2b was also slightly coarser (sandier and with more gravel), not as well-sorted, more bioturbated and contained more intraclasts than Unit 2a. The top of S_1 is marked by a large increase in the concentration of pores, roots, and rootlets underlain by a horizon of more concentrated and prominent carbonate laminations (along the top of both Unit 2a and Unit 1, Figure 9). However, S_1 can only be distinguished from S_2 adjacent to faults on the downthrown side, where the stratigraphic sequence and soil profile are expanded. Elsewhere, where the soil profile is more condensed, overprinting by carbonate accumulation during S_2 formation has apparently obscured the top of S_1, and/or the top of S_1 has been eroded away, as likely was the case in the footwall of the main fault.

Two samples (MCET2-L5Y and MCET2-L5Z on Figure 9) were collected from a possible Av horizon at the top of Unit 2a for IRSL analysis and results for MCET2-L5Y are still pending. The IRSL age for MCET2-L5Z is 92.0 ± 7.0 ka (Table 1). This age suggests that Unit 2a in the East Trench is slightly older than Unit 2 in the West Trench and that Unit 2b in the East Trench may thus correlate with Units 4 and/or 2 in the West Trench. This interpretation would be consistent with correlation of S_1 in the East Trench to S_1 in the West Trench, and S_2 in the East Trench to S_2 and/or S_3 in the West Trench. Due to the extensive bioturbation and soil development, we did not sample Unit 2b for IRSL age analysis.

Unfortunately the critical cross-cutting relations between faults and Units 2b and 2 in the East Trench are obscured by krotovina (present on both the north and south walls). The matrix of the large krotovina near the main fault is texturally similar to Unit 2b, but the krotovina includes a concentration of cobble clasts and gravel near its base. This coarser pocket may or may not have originally been fault-scarp colluvium derived from Unit 1. Regardless, all of Unit 2a and much of Unit 2b lies stratigraphically below the upper extent of the main fault (near vertical st. +1 m on Figure 9). Based on this relation, we infer that Unit 2a and possibly much of Unit 2b is faulted. Whether Units 2a or 2b are folded is also ambiguous. Neither Units 2a or 2b appear as warped as Unit 1. Although Unit 2a appears warped, it does not extend far enough east so that this relation is definitive.

Unit 3 is a brown to gray, brown clayey gravelly sandy silt that we interpret to be slopewash colluvium. It overlies Units 1, 2b, and 2, extends the full length of the trench, and is thickest over faults (Figure 9). Unit 3 is poorly sorted and extensively bioturbated, including burrows and abundant roots, particularly over faults. Unit 3 includes the modern soil, S_3, that consists of an A/B horizon (Appendix B). S_3 is similar in degree of development to the modern soil in the West Trench (S_5), but is generally thicker. Unit 3 is neither faulted nor folded in the East Trench.

2.2.3.2 Structure

Structures exposed in the East Trench include: (1) the main fault (near st. 13 m) and associated broad monocline (between st. 11 and 22 m); (2) the zone of secondary faults between st. 7 and 11 m; (3) a small fault near st. 19 ½ m; and (4) a fault near st. 37 m (Figure 9). All faults are steeply east-dipping to subvertical. They individually show both normal and reverse slip, but overall offset fan deposits 2.5 ± 0.5 m down to the west. All faults were identified by shear fabric of gravel clasts and/or offsets of beds in Unit 1. In particular, shear fabric associated with the fault near st. 37 m was apparently obliterated by krotovina and we infer the existence of this fault based on the observed offsets of beds in Unit 1. All faults were observed on both the north and south walls of the trench, except the small fault at st. 19 ½ m, which was only observed on the south wall and died out by marker horizon 1b (Figure 9). Additionally, the geometry of the secondary faults between st. 7 and 11 m was simpler on the north wall, showing fewer splays than on the south wall.

The main fault strikes N35°W and dips 60°E. It is characterized by a 20- to 30-cm-wide silty, sandy, gravel zone with well-developed shear fabric throughout, including up to the top where it was apparently cut out by the large krotovina at st. 14 to 15 m (Figure 9). Thus, any free-face that may have been associated with the youngest faulting event on the main fault is not preserved. Surprisingly, the main fault shows reverse slip, offsetting all beds within Unit 1 by a similar amount and showing 55 ± 10 cm of discrete slip (throw) at the fault. However, the associated monoclinal warping displaces beds an additional 140 ± 15 cm (including offset on the small fault at st. 19½ m), so that the total throw measured across the faulted monocline on marker horizon 1c is 195 ± 0.25 cm down to the west. Notably, the base of the K horizon of soil S_2 appears to be offset much less across the faulted monocline, only about 55 ± 10 cm down to the west. In addition, the base of the K horizon shows a marked angular discordance to the moncline (Figure 9). Based on the cross-cutting relations, all of the deformation on the faulted monocline postdates Unit 1 and predates Unit 3. The monclinal warping appears to predate much of the soil development (i.e., carbonate accumulation of the K horizon) and perhaps some

loess deposition (Unit 2b?) as well. As previously discussed, at least some slip on the main fault likely post-dates Unit 2a and may post-date some of Unit 2b as well.

The zone of secondary faults between st. 7 and 11 m include both normal and reverse faults (Figure 9). These faults are located near the upper hinge of the monocline associated with the main fault, and likely are secondary features associated with the warping. Individual offsets are small (2 to 10 cm) and the cumulative throw across the zone (including minor warping) is 15 ± 10 cm down to the west. All of the faults appear to terminate at, or close to, the top of Unit 1 and the base of Unit 3. Additionally, no differential offsets of different beds in Unit 1 were observed. Although minor offsets of the base of the K horizon may be present across the zone of secondary faults, these would be too small to definitively identify with such a diffuse marker horizon.

Based on the geometry of the bioturbated zone in Unit 1, we infer that the fault near st. 37 m dipped steeply to the east, similar to the main fault at st. 13 m. The vertical stratigraphic separation measured on marker 1c was 40 ± 10 cm down to the west (Figure 9). No differential offsets of Unit 1 were observed and Unit 3 did not appear faulted. Similar to the main fault, extensive bioturbation obscured cross-cutting relations with Unit 2. The base of the K horizon dips down across the fault, but is very irregular and diffuse in the area, and shows little if any net offset. Additionally, the top of the S_2 soil does not appear offset and there is a considerable amount of carbonate accumulation in the krotovina. These relations suggest faulting near st. 37 m predates much of the S_2 soil formation and thus may correlate with the older warping event on the main fault.

2.2.3.3 Trench Log Reconstruction and Event Summary

Similar to the West Trench, we did a stepwise reconstruction of the East Trench log, progressively removing deformation associated with first Event W_E, and then Event V_E. Similar to the West Trench, we assumed 2-D strain along the plane of section. Due to the fewer number of units, buried soils, and faulting events, the reconstruction was much simpler. The process was also simpler because the net throw could be measured on several markers in the East Trench. Differential offsets, and crosscutting pedologic and stratigraphic relations indicate that two separate faulting/folding events occurred. The older of these events, Event V_E, predates all events in the West Trench, and may correlate with Event V_C in the Central Trench based on geomorphic relations. Based on pedologic relations, the younger event in the East Trench, Event W_E, may correlate with Events W_W, the oldest event in the West Trench. However, large uncertainties, particularly in the timing of Event W_E, result from the ambiguous relation between faults and Units 2, 2a, and 2b. A summary of the structural, stratigraphic and pedologic evidence for each event in the East Trench, the associated estimates of net vertical displacements per event, and the timing of events follows.

Event V_E – Differential offsets across any of the structures exposed in the East Trench were not observed between Unit 1 subunits, implying that all faulting postdates Unit 1. However, the throw of the base of the K horizon across the main, faulted monocline is substantially less than on Unit 1 (~55 cm versus ~ 195 cm, respectively). This coupled with the angular discordance of the K horizon to the warping of Unit 1 indicates that much, if not all, of the warping occurred in an older event, Event V_E, that postdated deposition of Unit 1 but predated much of the carbonate accumulation that formed the K horizon.

The timing of Event V_E is somewhat ambiguous due to the krotovina obscuring the key crosscutting relations near st. 13 m. However, insights from our trench log reconstruction suggest that Event V_E occurred close to, and likely shortly after, 92 ± 14 ka. Although the deformation associated with Event V_E was apparently not that of a typical normal faulting event, it appears to have been somewhat similar to Event X_W in the West Trench. It still must have created a scarp, which was likely eroded to some degree subsequent to uplift, but how much erosion occurred prior to the next event and how much scarp-derived colluvium was shed on the downdropped block is uncertain due to the large krotovina near the fault and the overprinting of pedogenic carbonate throughout Unit 2b. The pea-size and smaller gravel in Unit 2b looks similar to, and is likely reworked from, the pea-size gravel bed above marker horizon 1a (Figure 9). Therefore, we believe it is likely that at least some of the lower portion of Unit 2b represents colluvium reworked from Units 2a and the top of Unit 1 subsequent to Event V_E.

From our reconstruction, we infer that Unit 2a likely predated Event V_E. This is based on the apparent slight warping of Unit 2a, and the fact that the gravel bed above marker 1a clearly is folded and S_1 extends across both the tops of Unit 2a and the gravel bed above marker 1a (Figure 9). Thus, if Unit 2a was deposited <u>after</u> Event V_E then S_1 must have formed subsequently as well, and essentially no colluvium was shed from a scarp that was nearly a meter high. Although this is possible, it seems highly unlikely (c.f., the thickness of Unit 5a in the West Trench). Therefore, our preferred interpretation is that Event V_E occurred after Unit 2a was deposited and very shortly after S_1 formed, that is shortly after 92 ± 14 ka based on the one available IRSL age for Unit 2a. Note that this age may be revised when the additional IRSL age analysis is complete for sample MCET2-L5Y. Even if Unit 2a was deposited before Event V_E, the event still occurred around 92 ± 14 ka, but just shortly before instead of after. Event V_E clearly occurred after deposition of the uppermost fan deposits (above marker 1a), so even if Unit 2a was deposited after Event V_E it must have been shortly thereafter as the soil that formed after the fan surface stabilized appears to drape across both deposits.

There are no direct numerical age constraints on the timing of offsets on the secondary faults between st. 7 and 11 m and the fault at st. 37 m. However, based on structural arguments, apparent crosscutting relations of pedogenic carbonate, and geomorphic relations, we believe these offsets likely occurred during Event V_E. Based on their location near the hinge at the top of the monocline, we believe that the faults between st. 7 and 11 m likely formed in association with the folding during Event V_E. Based on the apparent overprinting of pedogenic carbonate across the fault at st. 37 m, slip on this fault is likely older as well. This is also supported by geomorphic relations. This fault is at the approximate location of the antithetic fault that does not appear to offset the t_4 terrace south of Mercur Creek, which is inset into and slightly younger than the af2 surface (Figure 3). This suggests that slip on this fault occurred shortly after the af2 fan surface stabilized and before the t_4 terrace was cut.

We can determine the total net throw on marker horizon 1c for Event V_E. First, we estimate the throw associated with warping on the main fault to have been 140 ± 15 cm (Section 2.2.3.2) during Event V_E. Adding the throw across the secondary faults between st. 7 and 11 m (15 ± 10 cm) and the throw across the fault at st. 37 m (40 ± 10 cm), we determine a total throw of 195 ± 35 cm down to the west for Event V_E in the East Trench. If Event V_E in the East Trench correlates with Event V_C in the Central Trench, the total vertical slip is about 3 m down to the west.

Event W_E - The evidence for this younger event includes the 55 ± 10 cm of throw of the base of the K horizon, and the additional 45 to 65 cm of throw of marker horizons 1a, 1b and 1c across the main fault at st. 13 m. Additionally, some part of the uppermost portion of Unit 2b may be colluvium shed from the small scarp created during Event W_E, but as previously discussed, the extensive overprinting of pedogenic carbonate in Unit 2b and the disturbance by bioturbation preclude determining how much of Unit 2b was deposited in association with Event W_E. It is problematic that we could not identify any additional buried soil horizons or stratigraphic contacts within Unit 2b, although our reconstruction implies they are likely there. However, the offset associated with Event W_E was relatively small, and so it seems reasonable that subsequent bioturbation and soil development have completely obscured the contact and any buried soil horizons within Unit 2b.

Due to the ambiguous crosscutting relations, the timing of Event W_E is very poorly constrained. Event W_E obviously occurred after Event V_E, and well before deposition of Unit 3 and formation of the modern soil, S_3. Indeed, the projection of the top of S_2 across the main faulted monocline does not appear offset, suggesting that Event W_E is relatively old, but unfortunately the large krotovina obscures the critical crosscutting relation right at the fault. Additionally, the fact that the base of the K horizon does appear offset implies at least some soil formation predated Event W_W. Based on these relations, if Event W_E in the East Trench correlates with any event in the West Trench, it likely is an older event such as Event W_W, Event X_W, or possibly even Event Y_W. If Event W_E correlates with Event W_W, then it occurred shortly after 75 ± 10 ka and the upper and lower portions of Unit 2b in the East Trench respectively correlate to Units 4 and 2 in the West Trench. Based on the degree of soil development of S_2, we slightly favor this possibility. Alternatively, if Event W_E in the East Trench correlates with Event X_W in the West Trench, then it occurred after 42 ± 8 ka. Finally, although it is possible that Event W_E correlates with Event Y_W, based on the soils and the implications for a very large event, this is our least-favored possibility.

As previously alluded to, the throw measured for Event W_E in the East Trench is 55 ± 10 cm. However, depending on how this event may or may not correlate with events in other trenches, the total vertical slip could be considerably more for this event. For example, if Event W_E correlates to Event W_W in the West Trench, the total vertical slip would be about 2 m.

Table 1
Radiocarbon and Luminescence Ages for Mercur Canyon Trenches

Infrared Stimulated Luminescence (IRSL) Samples:

Field Sample No.	Lab Sample No.	Location	Method[1]	Equivalent Dose (Grays)	Dose Rate (Grays/ky)	IRSL Age (ky)[2]	Comments
MCWT2-L1	UIC725	West Trench, Unit 2 (A_v horizon)	MAAD	151.90 ± 2.24	2.21 ± 0.10	68.7 ± 5.2	Predates Event W_W. Not saturated.
MCWT2-L2	UIC728	West Trench, Unit 2 (A_v horizon)	MAAD	230.01 ± 3.53	2.85 ± 0.14	80.7 ± 6.3	Predates Event W_W. Not saturated.
MCWT4-L3	UIC734	West Trench, Unit 4	MAAD	124.47 ± 0.39	3.37 ± 0.15	37.0 ± 3.0	Predates Event X_W.
MCWT4-L4	UIC743	West Trench, Unit 4	MAAD	135.32 ± 0.58	2.97 ± 0.13	46.7 ± 3.8	Predates Event X_W.
MCET2-L5Z	UIC729	East Trench, Unit 2a	MAAD	255.68 ± 2.55	2.78 ± 0.12	92.0 ± 7.0	Predates (?) Event V_E. Not saturated.
MCET2-L5Y	———	East Trench, Unit 2a	MAAD	———	———	Results Pending	

Accelerator Mass Spectrometer (AMS) Radiocarbon Samples:

Field Sample No.	Lab Sample No.	Location	Material[3]	Radiocarbon Age[4] (^{14}C yr BP)	Calendar Corrected Age[5] (cal yr BP)	Comments
MCWT6-1RC	Beta 137743	West Trench, Unit 6a (A horizon)	Charcoal	4110 ± 60	4430 to 4830	Predates Event Z_W.
MCWT7-1RC	Beta 127742	West Trench Unit 7a	Charcoal	1510 ± 60	1295 to 15303	Postdates Event Z_W.

1 MAAD: Multiple aliquot additive dose method, measuring blue emissions.

2 Errors are 1 sigma.

3 See Appendix C.

4 Conventional age with 1 sigma error (see Appendix D).

5 Calculated by Beta Analytic Inc. (Appendix D) using calibration data in *Radiocarbon* (v. 40, no. 3, 1998) and methods by Talma and Vogel (*Radiocarbon,* v.35, no. 2, p. 317-322, 1993: A Simplified Approach to Calibrating C14 Dates). Errors are 2 sigma.

3.1 EARTHQUAKE TIMING AND RECURRENCE

Figure 10 summarizes numerical age constraints for the surface-faulting events identified in the three trenches at the Mercur Canyon site. Structural, stratigraphic and pedologic evidence exposed in the trenches indicates that at least 5, to as many as 7, separate surface-faulting earthquakes occurred on the Mercur fault since the af2 fan surface formed around 92 ± 14 ka. The ages of these events not only provide insight into rates of earthquake recurrence (i.e., recurrence intervals and slip rates) on the Mercur fault, but also its seismogenic relation to other faults of the SOMF, and the segmentation of the Oquirrh-East Great Salt lake fault zone overall. Unfortunately, large uncertainties in the ages of some events (Y_W, V_C, and W_E) make correlations of some events between trenches ambiguous, resulting in some large uncertainties in parts of the composite paleoseismic record for the Mercur fault. In this section we first briefly summarize the timing of events in individual trenches (which was previously discussed in detail in Sections 2.2.1.3, 2.2.2, and 2.2.3.3) and discuss how events may or may not correlate between trenches. Finally, we present recurrence intervals and discuss their uncertainties for the composite paleoseismic record of the Mercur fault. To facilitate our discussion of the composite paleoseismic record, we follow our reverse alphabetical notation used for events in individual trenches. For example, we refer to the youngest event on the entire Mercur fault as Event Z_M.

3.1.1 Summary of Event Chronology

The West Trench exposed evidence for 4 separate surface-faulting events, Events W_W through Z_W (Figure 10). The youngest event, Event Z_W, occurred shortly after 4.6 ± 0.2 ka and well before 1.4 ± 0.1 ka. Based on geomorphic and pedologic relations, Event Z_W does not appear to correlate to any of the events exposed in the Central or East Trenches and, thus, it comprises the youngest event on the Mercur fault, Event Z_M. This age is much younger than previously suggested by either Barnhard and Dodge (1988) or Everitt and Kaliser (1980) in their trench investigations. However, neither study had the benefit of numerical age constraints. The mid-Holocene age of Event Z_M does overlap (at 2 σ error) with the age of the youngest event recently reported for a bedrock scarp of the Lakes of Kilarney fault to the north on the SOMF (Handwerger *et al.*, 1999). This is discussed further in Section 3.4.

Numerical age constraints are poor for Event Y_W in the West Trench. Based on stratigraphic and pedologic relations (i.e., the well-developed Btk horizon that formed on the associated colluvial wedge, and the apparent lack of much soil development preceding the event), we infer that Event Y_W occurred sometime between 20 and 50 ka, but after Event X_W. Although Event Y_W may or may not correlate to Event V_C and/or Event W_E, geomorphic and pedologic evidence does not favor this possibility and suggests Events V_C and W_E are older. Regardless, Event Y_W appears to represent the next youngest event on the Mercur fault. Thus, the penultimate event, Event Y_M, on the Mercur fault likely occurred sometime between 20 and 50 ka.

Event X_W in the West Trench occurred shortly after 42 ± 8 ka. This event may or may not correlate with Events V_C and/or W_E, although geomorphic and pedologic relations suggest Event X_W may be younger. If Event X_W is younger, it represents the antepenultimate event on the Mercur fault (Event X_M), which occurred shortly after 42 ± 8 ka. Alternatively, if either Event W_E or V_C are younger (but do not correlate with Event Y_W), then Event X_M may be slightly

younger than Event X_W. However, this possibility seems the least likely based on geomorphic and pedologic relations.

Event W_W in the West Trench occurred shortly after 75 ± 10 ka and well before 42 ± 8 ka. This event may correlate to Event W_E in the East Trench, and possibly to Event V_C in the Central Trench, althrough geomorphic relations do not favor the latter, which suggest that Event V_C may be older. If Event W_W does correlate to Event W_E, and Event V_C is older, then Event W_W represents the next oldest event on the Mercur fault (Event W_M), which occurred shortly after 75 ± 10 ka. Alternatively, if either Event V_C or Event W_E are actually younger than Event W_W and older than Event X_W, then Event W_M on the Mercur fault may be relatively younger than 75 ka.

The age and relation of Event V_C in the Central Trench to other events has the largest uncertainties. The 1 m of offset on the central scarp is inferred to have occurred in one event, Event V_C, that predates the t_4 terrace, and perhaps much of the soil development on the af2 surface. Based on these relations, we infer that Event V_C most likely correlates to the oldest event in the East Trench, Event V_E. Alternatively, it may be a separate event or it may correlate to Event W_E, W_W, X_W or possibly even Event Y_W.

The age of Event W_E in the East Trench is poorly constrained. However, geomorphic pedologic and stratigraphic relations suggest that this event is likely younger than the t_4 terrace south of Mercur Creek and Event V_C in the Central Trench. Based on pedologic and stratigraphic comparisons, it may correlate to Event W_W or possibly Events X_W or Y_W.

Finally, Event V_E in the East Trench occurred around (and likely shortly after) 92 ± 14 ka. Event V_E is older than any event in the West Trench and may correlate to Event V_C in the Central Trench. This correlation would boost the vertical slip for this event from about ½ m to 1 ½ m, making it more comparable in size to other events. Alternatively, it may have been a separate smaller event.

In summary, evidence from the trenches indicates 5 to 7 surface-faulting earthquakes occurred on the Mercur fault since 92 ± 14 ka. Four of these were exposed in the West Trench (Events Z_W through W_W), two were exposed in the East Trench (Events W_E and V_E), and one was inferred for the Central Trench (Event V_C). Uncertainties in the number of events results from how Events V_C and W_E may or may not correlate to older events in the West Trench (Events W_W, X_W, or even Y_W). Event V_E is older than any event exposed n the West Trench and it may correlate with Event V_C in the Central Trench. The youngest event across the entire Mercur fault (Event Z_M) occurred shortly after 4.6 ± 0.2 ka and the penultimate event (Y_M) occurred sometime between 20 and 50 ka. Additional older events occurred at: shortly after 42 ± 8 ka (Event X_W); shortly after 75 ± 10 ka (Event W_W); and, close to, and likely shortly after, 92 ± 14 ka (Event V_E). If Events V_C and W_E were separate events, these occurred sometime between 20 and 92 ± 14 ka, but more likely near the older end of the range (i.e., > 40 ka).

3.1.2 Recurrence Intervals

Due to the uncertainties in correlating events between trenches at the Mercur Canyon site, the most robust approach to determining recurrence intervals for hazard analyses is by calculating average recurrence intervals for the past 5 to 7 events on the Mercur fault. Assuming that 5 to 7 occurred between 92 ± 14 ka and 4.6 ± 0.2 ka, yields an average recurrence interval of 12,000 to 25,000 years for the Mercur fault.

For comparison, we can also calculate some individual recurrence intervals, which yield even broader ranges of estimates. Except for the interval between Events Z_W and Y_W, these estimates should all be considered maximum for the Mercur fault as they assume Events V_C and W_E are not separate events. We estimate an interval of 15,000 to 46,000 years between events Z_W and Y_W (i.e., 20 ka – 4.8 ka and 50 ka – 4.4 ka, respectively). The estimated interval between Events Y_W and X_W ranges from 0 to 30,000 years. The estimated interval between Events X_W and W_W is 33,000 ± 15,000 years, whereas the estimated interval between Events W_W and V_E ranges from 0 to 41,000 years. Thus, uncertainties for individual intervals are as large, or larger than, variations between intervals, making it difficult to quantify possible variations of recurrence rates through time. Perhaps the most insightful qualitative observation in this regard, is the apparent lack of soil development (none?) between Events X_W and Y_W, in contrast to the significant amount of soil development (a thick Btk horizon with prominent peds) that formed between Events X_W and Z_W. This comparison suggests an order of magnitude or more variation in recurrence from a few thousand years or less to tens of thousands of years or more. However, of the 5 to 7 events observed, this is the only such order of magnitude change indicated over the past ~ 100 ka.

3.2 DISPLACEMENTS AND SLIP RATES

NVTD is a measure of vertical slip across a fault zone produced by a surface-faulting earthquake (Schwartz, 1988). It consists of apparent slip minus the effects of backtilting, antithetic faulting, and other near-field deformation. Determining the net vertical tectonic displacement per event provides an estimate of individual earthquake size and allows a comparison between successive surface-faulting earthquakes on a fault zone. A scarp profile can be used to estimate net vertical tectonic displacement if the same undeformed surface can be identified on both sides of the fault zone (Bucknam and Anderson, 1979a).

We used scarp profiles (Figure 4) to estimate the NVTD of the af2 surface across each of the three fault traces at the Mercur Canyon site. We note that although the West Trench did not extend far enough west to expose a buried antithetic fault identified on a high-resolution seismic profile (A. Mattson, University of Utah, written comm., 1-9-01), our scarp profile extended tens of meters downslope of its location. Amazingly, the net throw measured on marker horizon 1c in the East Trench (2.50 ± 0.45 m) is the same as the NVTD measured on the scarp profile (2.5 m). Therefore, we believe our topographic profiles have adequately accounted for antithetic faulting and backtilting across the zones.

However, stratigraphic and pedologic relations exposed in the West Trench suggest that the NVTD measured on the profile may be a minimum estimate. In particular, the thickness of Unit 2, which clearly predates faulting and is only preserved on the downthrown side of the fault, suggests that this material may have also been present in the footwall but was entirely eroded subsequent to faulting. The variable thickness of Unit 2 makes this difficult to determine, but if this was so, we estimate as much as an additional 0.85 m of vertical slip could have occurred across the western fault. Thus, we estimate a range for the NVTD of the af2 surface across the western fault of 6.25 to 7.1 m. Including uncertainties for both the eastern and western faults, we estimate a range of 9.25 to 11.1 m of NVTD across the entire Mercur fault.

Figure 10 summarizes displacement (throw or NVTD) per event data for the Mercur Canyon site. Due to uncertainties in correlating events between trenches, it is difficult to determine

displacements for each event across the entire Mercur fault. Preferred estimates of displacements per event for the western fault vary from 1 to 2 m and generally support characteristic behavior. However, uncertainties are large (as much as ¾ m). We note that our West Trench reconstruction (Figure 7) and preferred estimates for displacements per event assumed 6.25 m of NVTD on the western fault. However, our ranges for displacements per event on the western fault (Figure 10) reflect the uncertainties of the total NVTD.

Average displacements per event can also be calculated for the Mercur Canyon site. Note that these averages are not the same as average along-strike displacements (AD) that are typically used in empirical relations to calculate paleomagnitudes. Regardless, they provide useful constraints for such estimates (see Section 3.3 for further discussion). Assuming 5 to 7 events on the Mercur fault resulted in 9.25 to 11.1 m of NVTD yields average displacements per event of 1.3 to 2.2 m. These values are much larger than expected given the length of either the Mercur fault (17 km) or the entire SOMF (25 km). Using Wells and Coppersmith's (1994) empirical relations for all fault types, the displacements imply expected surface rupture length of 31 to 64 km (depending on the empirical relation used). The implications of this for the relation of the Mercur fault to other faults of the SOMF, and the relation of the SOMF to the Oquirrh fault are discussed further in Section 3.4. The implications of the large displacements for paleomagnitude estimates are discussed in Section 3.3.

Ideally, slip rates should be calculated for complete seismic cycles (see Machette *et al.*, 1992, for discussion). We can calculate an average slip rate for the past 4 to 6 complete seismic cycles on the Mercur fault (i.e., for all but the youngest event, Z_w, which includes the open interval of the elapsed time). Subtracting 1 m for Event Z_w, yields 8.25 to 10.1 m of NVTD that occurred between 92 ± 14 ka and 4.6 ± 0.2 ka. This yields slip rates of 0.09 to 0.14 mm/yr for the past 4 to 6 complete seismic cycles on the Mercur fault. Assuming that Event W_E in the East Trench correlates with Event W_W in the west Trench but not Event V_C in the Central Trench, we can also calculate slip rates for this seismic cycle. Assuming 2.05 m of NVTD occurred over 33,000 years (the best estimate recurrence interval between Event W_W and Event X_W) yields a best estimate slip rate of 0.06 mm/yr. Including respective uncertainties (1.45 to 2.9 m and 15,000 to 51,000 years) yields a slip-rate range of 0.03 to 0.19 mm/yr. Similarly, assuming Event V_C in the Central Trench correlates to Event V_E in the East Trench, we can calculate slip rates for this seismic cycle. Assuming 2.95 ± 0.35 m of NVTD and a recurrence interval of 17,000 (-10,000, + 34,000) years yields a best estimate slip rate of 0.17 mm/yr and a range of 0.06 to 0.47 mm/yr. For comparison, we can also calculate slip rates for the past 3 complete seismic cycles on the western fault (i.e., for Events W_W, X_W, Y_W). Subtracting 1 m for Event Z_W, yields 5.25 to 6.1 m of NVTD that occurred between 75 ± 10 ka and 4.6 ± 0.2 ka. This results in slip rates of 0.07 to 0.10 mm/yr for the past 3 complete cycles on the western fault. We conclude that the uncertainties are large for slip rates of individual seismic cycles, ranging from 0.03 to 0.19 mm/yr. Data are most robust for the past 4 to 6 complete seismic cycles, which yield average rates of 0.09 to 0.14 mm/yr for the past 100 ka.

3.3 PALEOMAGNITUDE ESTIMATES

Many empirical relations have been developed to estimate paleomagnitude from various fault parameters, such as length and displacement per event (see for example, dePolo and Slemmons, 1990 for discussion). Table 2 shows paleomagnitude estimates for the Mercur and SOMF using various recent empirical relations based on surface-rupture length (L), average (AD) or

maximum (MD) along-strike displacement per event, and slip rate (SR). Paleomagnitude estimates for the SOMF vary from M_w 6.7 to 7.2. There are many issues to consider in using these paleomagnitude estimates in hazard assessments and these are discussed below.

First, readily apparent from the estimates is that paleomagnitudes based on surface-rupture length for the SOMF are lower than those based on displacements. This has been observed on many other Quaternary faults in the ISB (e.g., Mason, 1996) and, in particular, along the Oquirrh fault to the north (Olig et al., 1994; 1996). Mason (1996) attributed this disparity to investigators consistently underestimating lengths of ruptures for various reasons and possibly overestimating displacements. Thus, he argued for using an empirical relation based on both parameters (e.g., Table 3). However, Mason's (1996) relation is based on MD. This leads into a second significant issue, the difficulty in estimating MD (or even AD) for the entire, along-strike length of the SOMF from paleoseismic data for a single site. Hemphill-Haley and Weldon (1999) discussed this problem in detail and developed an approach to better estimate paleomagnitudes based on displacement data from a few sites. Unfortunately, their approach requires data from more than one site and we have only one site for the SOMF. However, based on along-strike displacement profiles for the SOMF (Olig *et al.*, 1999a), we believe the average NVTD per event estimates for Mercur Canyon (1.3 to 2.2 m) are likely less than MD but greater than AD. Accordingly, we expect that actual paleomagnitudes lie between our estimates based on MD and AD (Table 2).

For comparison, Anderson et al (1996) developed an empirical relation based on length and slip rate, and argued that faults with lower slip rates tend to fail in earthquakes with higher static stress drops, which would in turn result in larger displacements. A recent study suggests stress drops for dip-slip earthquakes are magnitude dependent (Mai and Beroza, 2000). They recommend using regression relations that are specific for fault type (i.e. normal) rather than relations based on all types of faults even though previous investigators found that they are more statistically robust (eg., Wells and Coppersmith, 1994).

Resolving these issues is beyond the scope of this study. However, in using paleomagnitude estimates to determine maximum magnitudes for the SOMF for hazard studies in the region we recommend the following: (1) not using the Mercur fault length alone, which underestimates the maximum rupture length of the SOMF; and, (2) using a combination of approaches and relations to address uncertainties. In regard to the former, the mapping, trenching, and geochronolgy data indicate that the maximum late Quaternary rupture length of the SOMF extends beyond the Mercur fault alone (discussed further in Section 3.4). Indeed, the data support possible coseismic rupture with the Oquirrh fault to the north, which would extend the maximum rupture length to 52 km. If the Oquirrh fault and SOMF form a persistent rupture segment, then paleomagnitudes based solely on length (L = 52 km) are entirely consistent with those based solely on displacements (AD = 2.4 m) (Table 2).

Table 2

Paleomagnitude Estimates for Surface-Faulting Earthquakes on the South Oquirrh Mountains Fault

Fault Parameter[1]	Moment Magnitude (M_w)		Surface-Wave Magnitude (M_s)
	Wells and Coppersmith(1994)[2]	Anderson et al. (1996)[3]	Mason (1996)[4]
L=17 km[5]	6.5		
L=25 km[6]	6.7		
L=52 km[6]	7.1		
L=17 km, SR=0.1 mm/yr[8]		6.7	
L=25 km, SR=0.1 mm/yr[8]		6.9	
L=52 km, SR=0.1 mm/yr[8]		7.3	
MD=1.3 m[9]	6.8		
MD=2.2 m[9]	6.9		
AD=1.3 m[10]	7.0		
AD=2.2 m[10]	7.2		
AD=2.4 m[11]	7.1[12]		
MD=1.3 m, L=25 km[9]			6.8
MD=2.2 m, L=25 km[9]			6.9
MD=2.6 m, L=25 km[13]			6.9
MD=4.4 m, L=25 km[13]			7.1

1 All surface rupture lengths (L) measured straight line, end to end. Slip rates (SR) are net vertical rates.

2 Relations for all type of slip: Mw=5.08+1.16*log (L)σ, σ=0.28; Mw=6.93+0.82*log (AD), σ=0.39; Mw=6.69+0.74*log (MD), σ=0.04.

3 Mw=5.12+1.16*log (L)-0.20 log (SR)

4 Ms=0.55*log (MD*L) = 5.95, σ=0.20

5 Mercur fault only (Dry Canyon to Fivemile Pass)

6 SOMF (Soldier Canyon to Fivemile Pass)

7 SOMF and Oquirrh fault (Lake Point Junction to Fivemile Pass)

8 Based on 9.75 to 10.6 m of NVTD between 85-100 ka and 4.6 ± 0.2 ka

9 Average NVTDs per event range from 1.3 to 2.2 m at the Mercur Canyon site. These estimates assume the Mercur Canyon displacements represent maximum displacements along strike (MD) of the SOMF.

10 These estimates assume the Mercur Canyon average NVTDs represent average displacements (AD) along strike of the SOMF.

11 The average of displacements for the youngest event at the Big Canyon, Pole Canyon (Olig *et al.*, 1996) and Mercur Canyon trench sites.

12 Using Hemphill-Haley and Weldon's (1999) modification of Wells and Coppersmith (1994) relation with 80% of the fault sampled resulting in a MVCDS of 0.81 so that Mw = 6.93 + 0.82 log (AD x 0.81).

13 These estimates assume the Mercur Canyon average NVTDs represent AD and that MD is two times the average after Wells and Coppersmith (1994).

3.4 IMPLICATIONS FOR FAULT SEGMENTATION AND EVOLUTION

Results from this paleoseismic investigation, coupled with results from our previous surficial studies (Olig *et al.*, 1999a, 1999b), provide a variety of insights into the late Quaternary rupture behavior of the Mercur fault and its seismogenic relation to other faults of the SOMF. These results also have implications for the overall segmentation of the Oquirrh-East Great Salt Lake fault zone (Figure 1).

There are several lines of evidence that as a whole indicate that the Mercur fault does indeed rupture coseismically with the other faults of the SOMF, although it may not always do so with every fault. Indeed, trench data, displacement patterns and map relations indicate that faulting has shifted basinward overall on both the Mercur fault and the SOMF as a whole, so that much of the Quaternary offset is partitioned onto the western (basinward) splay of the Mercur fault. In addition to this basinward evolution, the late Quaternary displacement profiles (Olig et al., 1999a), the cumulative displacement profiles (Wu and Bruhn, 1994), geometric and kinematic considerations (Wu and Bruhn, 1994), the overlap of mid-Holocene ages for the most recent event on the Mercur and Lakes of Kilarney faults (this study and Handwerger et al., 1999), and the large displacements per event on the Mercur fault all indicate that the maximum Quaternary rupture length of the SOMF extends beyond the Mercur fault alone. Indeed, the data suggest that the SOMF may extend even further to the north and rupture coseismically with the Oquirrh fault. Although the evidence is strong, it is not conclusive for persistent coseismic rupture of the two faults. This is an important issue to resolve because coseismic rupture results in larger magnitude events that result in larger ground motions in the area. Additionally, coseismic rupture raises interesting questions about the structural evolution of the Oquirrh East-Great Salt Lake fault zone in comparison to the more active Wasatch fault zone to the east.

3.4.1 Fault Segmentation

Table 3 summarizes available data on the timing of surface faulting events on the various fault sections of the Oquirrh-East Great Salt Lake fault zone. The mid-Holocene age of the youngest event on the Mercur fault overlaps (at 2 σ) with the mid-Holocene age of the youngest events on both the Lakes of Kilarney fault (Handwerger et al., 1999) and the Oquirrh fault to the north (Olig et al., 1994, 1996). Additionally, ages for the penultimate and antepenultimate events on the Mercur fault overlap with the ages of respective events on the Oquirrh fault; however, constraints are generally poor and ranges are very broad in some cases (Table 3). Although this evidence is suggestive of possible coseismic rupture of the Mercur fault with these faults to the north, by itself the evidence is by no means conclusive. In part, this is because age ranges are broad for all but the youngest event. However, even for this event the data are not conclusive of coseismic rupture. This is particularly true in light of observations from recent surface rupturing earthquakes where stress-triggering of events occurs along-strike over a period of years or decades (e.g., earthquake sequences in southern California and Turkey), time frames that cannot be resolved with present dating methods. Thus, it is possible that instead of coseismic rupture of the faults during past events, an earthquake on one fault, say the Oquirrh fault, triggered a separate event that occurred years or decades later on the Lakes of Kilarney fault, which in turn triggered an event on the Mercur fault, years to decades later.

Table 3

Ages of Youngest Surface-Faulting Along Sections of the Oquirrh-East Great Salt Lake Fault Zone[1]

	Fault	Youngest Event	Penultimate Event	Older Events?[3]
East Great Salt Lake fault	Promontory Segment	Holocene?[2]	?[3]	?[3]
	Fremont Island Segment	Holocene (3 events since 13,500 ± 500)[2]		
	Antelope Island Segment	Holocene (3 events since 13,500 ± 500)[2]		
	Oquirrh fault	4,800 to 7,900[4]	20,300 - 26,400[4]	> > 33,000[4]
South Oquirrh Mountains fault of Wu and Bruhn (1994)	Soldier Canyon fault[5]	> 15,000?[6]	?[3]	?[3]
	Lakes of Killarney fault[5]	4,360 ± 1,220[7]	?[3]	?[3]
	Mercur fault	1,300 to **4,830**[8]	20 to 50 ka[8]	shortly after 42 ± 8; shortly after 75 ± 10 ka; ca. 92 ± 14 ka[8]
	West Eagle Hill fault	> 15,000?[6,9]	?[3]	?[3]
	Topliff Hills fault	> 15,000[10] or < 15,000[11]	?[3]	?[3]
	East Tintic fault	> > 15,000 (middle to late Pleistocene)[12]	?[3]	?[3]

1 Ages in calibrated radiocarbon years before the present (cal yr BP) with 1-sigma errors, except as noted. Bold indicates closer limiting age.

2 Segmentation model and ages from Dinter and Pechmann (1999, 2000).

3 Ages for events prior to the most-recent faulting are unknown.

4 From Olig et al. (1994, 1996), ages of penultimate and antepenultimate events in ^{14}C yr BP (uncalibrated).

5 Dominantly bedrock fault.

6 From Wu and Bruhn (1994). Inferred to be slightly older than the Bonneville shoreline.

7 Determined from cosmogenic ^{14}C ages of a bedrock fault scarp south of Soldier Canyon (Handwerger *et. al.*, 1999).

8 From this study. Errors are 2-sigma. Assumes 5 events, two additional separate events may have occurred after 92 ± 14 ka but before the penultimate event.

9 Supported by Olig *et al.*, (1999a, 1999b).

10 From Barnhard and Dodge (1988).

11 From Everitt and Kaliser (1980).

12 From Bucknam and Anderson (1979b).

However, large displacements per event on the Mercur fault also indicate that ruptures may extend further north onto the Lakes of Kilarney, Soldier Canyon and possibly Oquirrh faults. As discussed in Section 3.2, the displacements per event average 1.3 to 2.2 m, much larger than expected for a 17-km-long rupture confined to the Mercur fault alone. Indeed the displacements yield expected rupture lengths of 31 to 64 km, which are more consistent with the total length of the SOMF (25 km) or coseismic rupture of the Oquirrh fault (52 km).

Coseismic rupture of the Oquirrh and Mercur faults would explain the large displacements per event on the Oquirrh fault (Olig et al., 1994, 1996). Trenches at two sites on the Oquirrh fault revealed net vertical tectonic displacements per event of 2.2 to 2.7 m, much larger than expected for a 32-km-long rupture of the Oquirrh fault alone. Combining this data with displacement data in this study results in an average vertical displacement of 2.4 m, which yields an expected surface rupture length of 67 km, using the empirical relation of Wells and Coppersmith (1994) for all fault types. Thus, the displacement per event data on both faults is much more consistent with coseismic rupture rather than independent rupture.

Finally, our previous mapping and scarp profiling study (Olig et al., 1990a) revealed along strike displacement patterns that also support linkage and possible coseismic rupture of the Mercur fault with the West Eagle Hill fault and faults to the north. In particular, net vertical tectonic displacements for all different-aged Quaternary surfaces decrease on the Mercur fault at the same along–strike position that displacements become apparent on the West Eagle Hill fault. This suggests that slip on the faults may be connected at depth and they may have experienced coseismic rupture during the Quaternary. However, a more detailed paleoseismic record of specific surface-faulting events on the West Eagle Hill fault is needed to verify if and when coseismic surface rupture may have occurred.

Additionally, displacements are expected to die out at the tips of normal faults unless slip is transferred onto other structures either along strike or on cross-structures. We note that although Quaternary displacements slowly die out at the southern end of both the Mercur and West Eagle Hill faults, the displacements at the northern end of both faults appear large and do not appear to be tapering off (Olig et al., 1999a). We infer that this may be due to transference of slip onto other faults of the SOMF that are along strike to the north. Specifically, slip on the Mercur fault may be transferred to the Lakes of Kilarney and Soldier Canyon faults, and the Lakes of Kilarney fault may also be a northward continuation of the West Eagle Hill fault. This interpretation is also supported by cumulative displacement patterns for the entire SOMF that are based on combining range crest elevations and thicknesses of basin fill inferred from gravity data (Wu and Bruhn, 1994). The cumulative displacement profile for the SOMF does not taper off at the northern end of the Mercur fault. Indeed, late Quaternary displacements (Olig et al., 1999a) and the range-crest elevations (Wu and Bruhn, 1994) do not even taper off at the northern end of the SOMF, although cumulative displacements do decrease near the salient at Stockton (Wu and Bruhn, 1994).

In summary, the overlap of ages of events (particularly the youngest), the large displacements per event, and the along-strike displacement patterns on the SOMF all indicate coseismic rupture of the Mercur fault with other faults of the SOMF (particularly the faults to the north), and suggest coseismic rupture with the Oquirrh fault. Although the data strongly favor the latter they are not conclusive. Better age constraints for the penultimate event on both faults, and earlier events on the Oquirrh fault, are needed to further test this hypothesis. Such data are worth pursuing as coseismic rupture of the SOMF and Mercur faults would result in a 52-km-long

rupture with a much larger magnitude, M_w 7.1 to 7.3, than previous estimates of M_w 6.5 based on the Mercur fault length alone. These larger events would generate much larger ground motions not only at the nearby Deseret Chemical Depot, but also in Provo and Salt Lake City. In particular, coseismic rupture with the Oquirrh fault would also bring this bigger event much closer to Salt Lake City (~ 20 km away). Results in this regard have already been incorporated into a microzonation study of Salt Lake Valley (NEHRP Award No. 98HQGR1038).

A practical question relating to coseismic rupture of the SOMF and the Oquirrh fault is why are there apparently so few scarps on alluvium preserved along the section between Dry Canyon at the northern end of the Mercur fault (Wu and Bruhn, 1994; Olig et al., 1999a) and Middle Canyon near the southern end of the Oquirrh fault (Solomon, 1993)? If the two faults persistently ruptured together throughout the late Quaternary, one would expect better preservation of scarps along the range front, particularly given the apparent large displacements per event. A possible explanation is that displacements per event decrease along this section, and/or late Quaternary slip is distributed across bedrock faults at the range-front (e.g., the mid-Holocene bedrock scarp along the northern Lakes of Kilarney fault) and within the range (e.g., the Occidental fault discussed by Solomon, 1996).

Another perplexing question relates to the salient between the Oquirrh fault and SOMF near Stockton. This valleyward projection of the Oquirrh Mountains shows many of the physical characteristics that typify salients along the better-studied Wasatch fault zone, and form persistent segment boundaries along that fault (Machette et al. 1992; Wheeler and Krystinik, 1992). These characteristics include: (1) a topographic high in the hanging wall (South Mountain and the Stockton Bar); (2) a structural high in the hanging wall (Pennsylvanian and Permian sedimentary rocks exposed on South Mountain [Moore and Sorensen, 1979]); (3) a gravity high in the hanging wall (Cook and Berg, 1961; Everitt and Kaliser, 1980); (4) decreased cumulative displacement (Wu and Bruhn, 1994); and (5) apparent decreased late Quaternary displacement (Solomon, 1993; Olig et al., 1999a). Indeed, Helm (1995) postulated that the apparent segment boundary at the Stockton salient is controlled by an older, transverse, crustal structure that also influences the location of persistent segment boundaries on the Wasatch and Stansbury faults. Thus, it seems perplexing that the Stockton salient, unlike salients along the Wasatch fault zone, does not appear to form a persistent segment boundary. If this apparent distinction is real, it may somehow be related to the basinward evolution of faulting (discussed in the following section). Regardless, additional studies are needed to verify and explain why the Stockton salient does not appear to be a persistent segment boundary between the Oquirrh fault and the SOMF.

3.4.2 Fault Evolution

The paleoseismic record from the three trenches at the Mercur Canyon site indicate that slip has been preferentially partitioned onto the western fault, shifting basinward during late Quaternary time (past ~ 100 ka). This is indicated by the greater number of surface-faulting events resulting in larger cumulative late Quaternary displacements on the western fault (Figure 10). It is also indicated by the occurrence of the two youngest events (Z_W and Y_W), likely exclusively, on the western fault.

This basinward evolution of faulting is also apparent on the SOMF as a whole. Displacement patterns on the Mercur and West Eagle Hill faults indicate that late Quaternary slip has been

preferentially partitioned basinward onto the Mercur fault and most recently at least two, and may be more, surface-faulting events occurred on the Mercur fault but did not rupture the West Eagle Hill fault. This is indicated by larger NVTD on older (af2/ap2) and intermediate-age (t3/af4/t4) alluvial surfaces along the Mercur fault (Olig et al., 1999a). For example, average along-strike displacements on intermediate-age surfaces are about 4.3 m greater on the Mercur fault. Based on the average displacement per event observed at the Mercur Canyon site, this suggests two to four additional events may have ruptured the Mercur fault and not the West Eagle Hill fault during the late Quaternary.

The preferential partitioning of Quaternary slip onto the Mercur fault over the West Eagle Hill fault is also indicated by map and geomorphic relations along the faults (Olig et al, 1999a). The very shallow bedrock shelf (<25 m depth) on the downthrown side of the West Eagle Hill fault (Olig et al, 1999a), versus the greater than 900 m of basin fill on the downthrown side of the Mercur fault (Everitt and Kaliser, 1980) suggests that the cumulative offset on the Mercur fault is at least an order of magnitude larger than the cumulative offset on the West Eagle Hill fault. Granted, the thick section of Tertiary Salt Lake Formation in the basin fill along the Mercur fault does suggest that at least some of the cumulative offset is actually pre-Quaternary. However, these Tertiary deposits are not present in the hanging wall of the West Eagle Hill fault, either because they were stripped away due to uplift on the Mercur fault, or because they were never deposited on a topographic high created by greater subsequent uplift on the Mercur fault. Regardless, the shallow bedrock shelf and the preservation of late Quaternary scarps of the Mercur fault on the downthrown side of the West Eagle Hill fault also suggests that rates of late Quaternary activity are relatively higher on the Mercur fault than on the West Eagle Hill fault; otherwise Mercur fault scarps would likely be buried by a thicker package of alluvium deposited on the downthrown side of the West Eagle Hill fault.

The basinward evolution of faulting on the SOMF has important implications for seismic hazards within Rush Valley and also elsewhere in the region. As previously discussed in section 1.2, there are several small faults within Rush Valley that comprise the St. John Station and Clover fault zones (Figure 1). Whether these very short (< 5 km) faults are capable of independently generating earthquakes or they rupture dependently on the SOMF is unclear. The basinward progression of faulting on the SOMF suggests that these faults may become more active n the future, indicating that further study of these poorly understood faults is needed. This is not only important to assessing seismic hazards at Deseret Chemical Depot and in Rush Valley, but also to better understanding seismic sources in the region. Recent subsurface studies in nearby Skull Valley (Geomatrix Consultants Inc., 1999) and East Great Salt Lake (Dinter and Pechmann, 1999, 2000) have discovered abundant evidence for active faults within basins that were previously undetected. Even though those intrabasin faults typically have relatively low slip rates (< 0.1 mm/yr), understanding their behavior is still important for hazard evaluation as development is generally concentrated in valleys, directly overlying these structures (e.g., West Valley fault zone in Salt Lake Valley).

Anderson, J.G., Wesnousky, S.G., and Stirling, M.W., 1996, Earthquake size as a function of fault slip rate: Bulletin of the Seismological Society of America, V. 86,. No. 3, p. 683-690.

Arabasz, W. J., Pechmann, J. C., and Brown, E.D., 1992, Observational seismology and the evaluation of earthquake hazards and risk in the Wasatch Front area, Utah, *in* P.L. Gori and W.W. Hays (eds.), Assessment of Regional Earthquake Hazards and Risk Along the Wasatch Front, Utah, U.S. Geological Survey Professional Paper 1500-A-J, p. D1-D36.

Atwood, W.W., 1916, The physiographic conditions at Butte, Montana, and Bingham Canyon, Utah, when the copper ores in these districts were enriched: Economic Geology, v. 11, p. 732-740.

Barnhard, T. P. and Dodge, R. L., 1988, Map of fault scarps formed on unconsolidated sediments, Tooele 1° x 2° Quadrangle, northwestern Utah, U. S. Geological Survey Miscellaneous Field Studies Map MF-1990, scale 1:250,000.

Bucknam, R. C. and Anderson, R.E., 1979a, Estimation of fault-scarp ages from a scarp-height—slope-angle relationship: Geology, v. 7, p. 11-14.

Bucknam, R. C. and Anderson, R.E., 1979b, Map of fault scarps on unconsolidated sediments, Delta 1° x 2° Quadrangle, Utah. U. S. Geological Survey Open-File Report 79-366, scale 1:250,000.

Bucknam, R. C., 1977, Map of suspected fault scarps in unconsolidated sediments, Tooele 2° sheet, Utah. U. S. Geological Survey Open-File Report 77-495, scale 1:250,000.

Cook, K.L. and Berg, J.W., 1961, Regional gravity survey along the central and southern Wasatch Front, Utah: U.S. Geological Survey Professional Paper 316-E, p. 75-89.

Currey, D.R. and Oviatt, C.G., 1985, Durations, average rates, and probable causes of Lake Bonneville expansion, still-stands, and contractions during the last deep-lake cycle, 32,00 to 10,000 yrs. Ago, *in* P.A. Kay and H. F. Diaz (eds.), Problems of and Prospects for Predicting Great Salt Lake Levels – Proceedings of a NOAA Conference held March 26-28, 1985, Salt Lake City, Center for Public Affairs and Administration, University of Utah, p. 9-24.

dePolo, C.M. and Slemmons, D.B., 1990, Estimation of earthquake size for seismic hazards: Geological Society of America Reviews in Engineering Geology, v. VIII, p. 1-27.

Dinter, D.A. and Pechmann, J.C., 1999, Sublacustrine paleoseismology: evidence for recent earthquakes on the East Great Salt Lake fault, Utah [abs]: Association of Engineering Geologists Program with Abstracts, p. 62-63.

Dinter, D.A., and Pechmann, J.C., 2000, Late Quaternary slip rates and recurrence intervals of large earthquakes on the East Great Salt Lake normal fault, Utah: Estimates from high resolution seismic reflection data: Geology Society of America Abstracts with Programs, v. 32, no. 7, p. A-506.

Everitt, B.L. and Kaliser, B.N., 1980, Geology for assessment of seismic risk in the Tooele and Rush Valleys, Tooele County, Utah Geological and Mineral Survey Special Studies 51, 33 p.

Forman, S.L., 1999, Infrared and red-stimulated luminescence dating of Quaternary sediments from Spitsbergen, Svalbard: Arctic, Antarctic and Alpine Research, v. 31, no. 1, p. 34-49.

Forman, S.L., Jackson, M.E., McCalpin, J. and Maat, P., 1988, The potential of using thermoluminescence to date buried soils developed on colluvial and fluvial sediments from Utah and Colorado, U.S.A.: Preliminary results. Quaternary Science Reviews, v 7, p. 287-293.

Forman, S.L., Nelson, A.R., and McCalpin, J.P., 1991, Thermoluminescence dating of fault-scarp-derived colluvium—deciphering the timing of paleoearthquakes on the Weber segment of the Wasatch fault zone, north-central Utah: Journal of Geophysical Research, v. 96, p. 595-606.

Forman, S.L., Pierson, J., and Lepper, L., 1999, Luminescence geochronology, *in* Noller, J.S., Sowers, J.M., and Lettis, W.R., eds., Quaternary Geochronology: Methods and Applications, American Geophysical Union, Washington, D.C., p. 157-176.

Geomatrix Consultants, Inc., 1999, Fault evaluation study and seismic hazard assessment, Private Fuel Storage Facility, Skull Valley, Utah: unpublished report prepared for Stone & Webster Engineering Corp., three volumes, variously paginated.

Gilbert, G. K., 1890, Lake Bonneville, U. S. Geological Survey Monograph 1, 438 p.

Gilluly, J., 1928, Basin-Range faulting along the Oquirrh Range, Utah: Bulletin of the Geological Society of America, v. 39, p. 1103-1130.

Gilully, J., 1932, Geology and ore deposits of the Stockton and Fairfield Quadrangles, Utah, U. S. Geological Survey Professional Paper 173, 171 p.

Handwerger, D.A., Cerling, T.E., and Bruhn, R.L., 1999, Cosmogenic ^{14}C in carbonate rocks: Geomorphology, v. 27, p. 13-24.

Hecker, S., 1993, Quaternary tectonics of Utah with emphasis on earthquake-hazard characterization, Utah Geological Survey Bulletin 127, 157 p.

Helm, J.M. 1995, Quarternary faulting in the Stansbury fault zone, Tooele County, Utah, *in* Lund, W.R. (ed.), Environmental and Engineering Geology of the Wasatch Front Region: Utah Geological Association Publication 24, p. 31-44.

Hemphill-Haley, M.A., and Weldon II, R.J., 1999, Estimating prehistoric earthquake magnitude from point measurements of surface rupture: Bulletin of the Seismological Society of America, v. 89, no. 5, p. 1264-1279.

Machette, M.N., Personius, S.F., and Nelson, A.R., 1992, Paleoseismology of the Wasatch fault zone-A summary of recent investigations, conclusions, and interpretations, *in* P. L. Gori and W. W. Hays (eds.), Assessment of Regional Earthquake Hazard and Risk Along the Wasatch Front, Utah, U. S. Geological Professional Paper 1500A, p. A1-A72.

Mai, P.M., and Beroza, G.C., 2000, Source scaling properties from finite-fault rupture models: Bulletin of the Seismological Society of America, v. 90, no. 3, p. 604-615.

Mason, D.B., 1996, Earthquake magnitude potential of the Intermountain Seismic Belt, USA, from surface-parameter scaling of Late Quaternary faults: Bulletin of the Seismological Society of America, v. 86, no. 5, p. 1487-1506.

Mattson, A., and Bruhn, R.L., 2000, Slip-rate estimates for undated fault scarps along the Wasatch fault zone and the west flank of the Oquirrh Mountains: Geological Society of America Abstracts with Programs, v. 32, no. 7, p. A-120.

Moore, W.J. and Sorensen, M.L. 1979, Geologic map of the Tooele 1° x 2° Quadrangle, Utah: U.S. Geological Survey Miscellaneous Investigation Series Map I-1132, 1:250,000 scale.

Nelson, A.R., 1992, Lithofacies analysis of colluvial sediments – An aid in interpreting the recent history of Quaternary normal faults in the Basin and Range Province, western United States: Journal of Sedimentary Petrology, v. 63, p. 607-621.

Olig, S.S., Gorton, A.E., Black, B.D., and Forman, S.L., 2000, Evidence for young, large earthquakes on the Mercur fault: Implications for segmentation and evolution of the Oquirrh-East Great Salt Lake fault zone, Wasatch Front, Utah: Geological Society of America Abstracts with Programs, v. 32, no. 7.

Olig, S.S., Gorton, A.E., and Chadwell, L., 1999a. Mapping and Quaternary fault scarp analysis of the Mercur and West Eagle Hill faults, Wasatch Front, Utah: unpublished technical report submitted to the U.S. Geologic Survey NEHRP Award No. 1434-HQ-97-GR-03154.

Olig, S.S., Gorton, A.E., and Chadwell, L.C., 1999b, Quaternary behavior along the southern Oquirrh fault zone, Utah [abs.]: Association of Engineering Geologists Program with Abstracts, p. 80.

Olig, S.S., Lund, W.R., Black, B.D., 1994, Large mid-Holocene and late Pleistocene earthquakes on the Oquirrh fault zone, Journal of Geomorphology, v. 10, p. 285-315.

Olig, S.S., Lund, W.R., Black, B. D., and Mayes, B., 1996. Paleoseismic investigation of the Oquirrh fault zone, Tooele County, Utah: Utah Geological Special Study 88, p. 18-64.

Oviatt, C. G., Currey, D.R., and Sack, D., 1992, Radiocarbon chronology of Lake Bonneville, eastern Great Basin, U.S.A. Paleogeography, Paleoclimatology, Paleoecology, v. 99, p. 225-241.

Schwartz, D.P. and Coppersmith, K.J., 1984, Fault behavior and characteristic earthquakes--examples from the Wasatch and San Andreas fault zones: Journal of Geophysical Research, v. 89, p. 5681-5698.

Schwartz, D.P., 1988, Geology and seismic hazards – Moving into the 1990s, *in* Von Thun, J.S., editor, Earthquake engineering and soil dynamics II – Recent advances in ground-motion evaluation: American Society of Civil Engineers, Proceedings, p. 1-42.

Scott, W.E., McCoy, W.D., Shroba, R.R., and Rubin, M., 1983, Reinterpretation of the exposed record of the last two cycles of Lake Bonneville, Western United States. Quaternary Research, v. 20, p. 261-285.

Smith, R. B., and Sbar, M. L., 1974, Contemporary tectonics of the interior of the western United States with the emphasis of the Intermountain Seismic Belt: Geological Society of America Bulletin, v. 85, p. 1205-1218.

Smith, R. B., and Arabasz, W. J., 1991, Seismicity of the Intermountain seismic belt in D.B. Slemmons, E.R. Engdahl, M.D. Zoback, M. L. Zoback, and D. Blackwell (eds.), Neotectonics of North America, Geological Society of North America, SMV V-1, p. 185-228.

Solomon, B. J., 1993, Quaternary geologic maps of Tooele Valley and the West Desert Hazardous Industry Area, Tooele County, Utah: Utah Geological Survey Open-File Report 296, 48 p., scale 1:24,000.

Solomon, B. J., 1996, Surficial geology of the Oquirrh fault zone, Tooele County, Utah, *in* W.R. Lund (ed.), The Oquirrh Fault Zone, Tooele County, Utah: Surficial Geology and Paleoseismicity, Utah Geological Survey Special Study 88, p. 1-17.

Solomon, B.J., Everitt, B.L., Currey, D.R., Paulick, J.S., Wu, D., Olig, S.S., and Burr, T.N., 1992, Quaternary geology and geologic hazards of Tooele and northern Rush Valleys, Utah, *in* J.R. Wilson (ed.), Field Guide to Geologic Excursions in Utah and Adjacent Areas of Nevada, Idaho, and Wyoming. Utah Geological Survey Miscellaneous Publication 92-3, p. 179-205.

Spooner, N.A., Aitken, M.J., Smith, B.W., Franks, M., and McElroy, C., 1990, Archaeological dating by infrared-stimulated luminescence using a diode array: Radiation Protection Dosimetry, v. 34, p. 82-86.

Swan, F.H., III, Schwartz, D.P., and Cluff, L.S., 1980, Recurrence of moderate to large magnitude earthquakes produced by surface faulting on the Wasatch fault zone, Utah, Bulletin of the Seismological Society of America, v. 70, p. 1431-1462.

Wells, D. L. and Coppersmith, K. J., 1994, Analysis of empirical relationships among magnitude, rupture length, rupture area, and surface displacement, Bulletin of the Seismological Society of America, v. 84, p. 974-1002.

Wheeler, R. L. and Krystinik, K. B., 1992, Persistent and nonpersistent segmentation of the Wasatch fault zone, Utah: statistical analysis for evaluation of seismic hazard: U. S. Geological Survey Professional Paper 1500-B, p. B1-B47.

Wong, I., Olig, S., Green, R., Moriwaki, Y., Abrahamson, N., Baures, D., Silva, W., Somerville P., Davidson, D., Pilz, J., and Dunne, B., 1995, Seismic hazard evaluation of the Magna tailings impoundment, Utah Geological Association Publication 24, 1995 Symposium and Field Conference on Environmental and Engineering Geology of the Wasatch Front Region, p. 95-110.

Wu, Daning, and Bruhn, R. L., 1994, Geometry and kinematics and active normal faults, South Oquirrh Mountains, Utah: Implication for fault growth, Journal of Structural Geology v. 16, p. 1061-1075.

Youngs, R. R., Swan, F.H., Power, M. S., Schwartz, D. P. and Green, R. K., 1987, Probabilistic analysis of earthquake ground shaking hazard along the Wasatch front, Utah, *in* P. L. Gori and W.W. Hays (eds.), Assessment of Regional Earthquake Hazards and Risk Along the Wasatch Front, Utah, U. S. Geological Survey Open-File Report 87-585, v. II, p. M1-M110.

Zoback, M.L., 1983, Structure and Cenozoic tectonism along the Wasatch fault zone, Utah, *in* D.M. Miller, V. R. Todd, and K.A. Howard (eds.), Tectonics and Stratigraphy of the Eastern Great Basin, Geological Society of America Memoir 157, p. 3-27

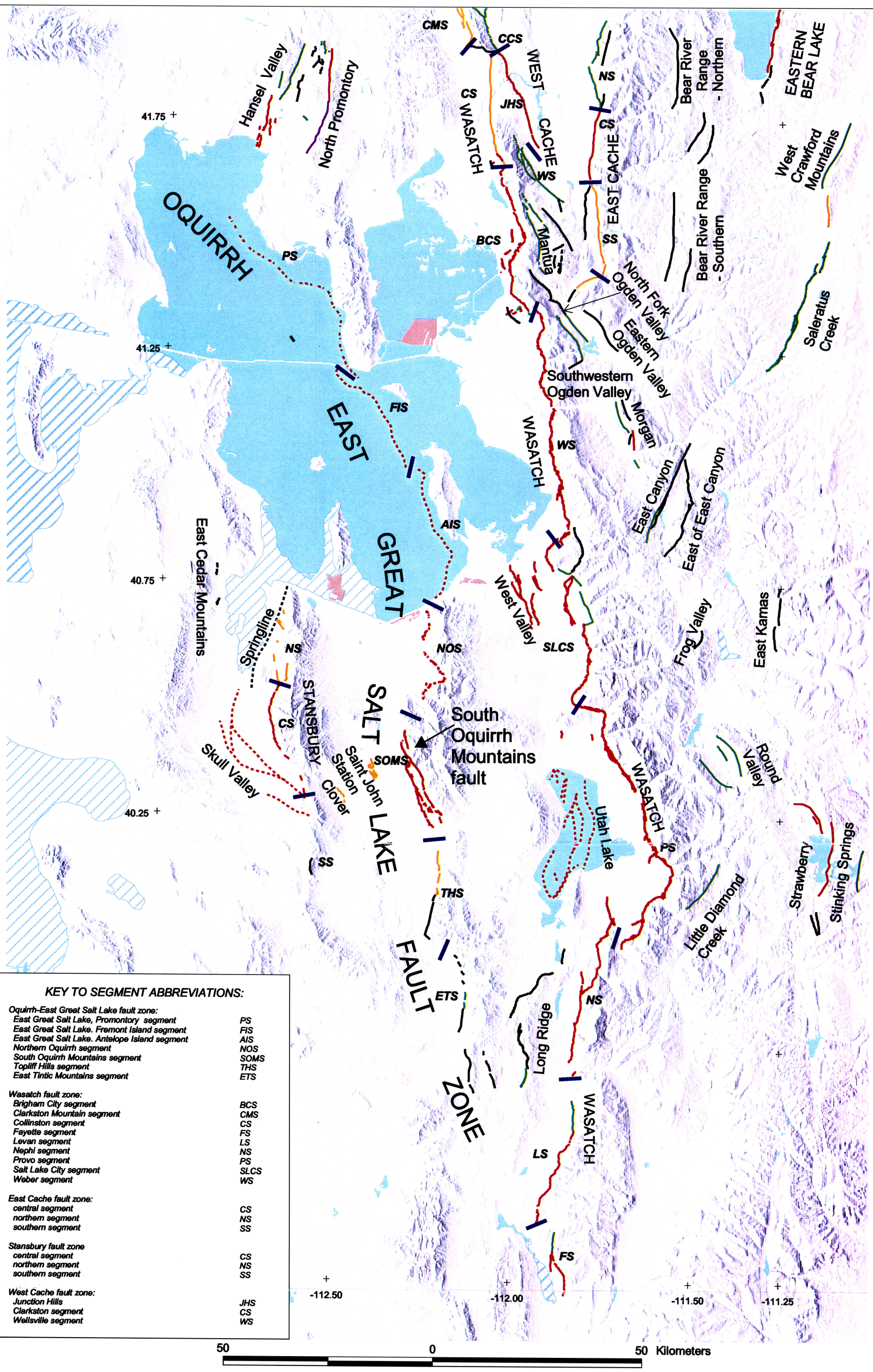

KEY TO SEGMENT ABBREVIATIONS:

Oquirrh-East Great Salt Lake fault zone:	
East Great Salt Lake, Promontory segment	*PS*
East Great Salt Lake. Fremont Island segment	*FIS*
East Great Salt Lake. Antelope Island segment	*AIS*
Northern Oquirrh segment	*NOS*
South Oquirrh Mountains segment	*SOMS*
Topliff Hills segment	*THS*
East Tintic Mountains segment	*ETS*
Wasatch fault zone:	
Brigham City segment	*BCS*
Clarkston Mountain segment	*CMS*
Collinston segment	*CS*
Fayette segment	*FS*
Levan segment	*LS*
Nephi segment	*NS*
Provo segment	*PS*
Salt Lake City segment	*SLCS*
Weber segment	*WS*
East Cache fault zone:	
central segment	*CS*
northern segment	*NS*
southern segment	*SS*
Stansbury fault zone	
central segment	*CS*
northern segment	*NS*
southern segment	*SS*
West Cache fault zone:	
Junction Hills	*JHS*
Clarkston segment	*CS*
Wellsville segment	*WS*

Legend

Fault Age

- Holocene to latest Pleistocene (red) 0 - 30,000 years ago
- Late Pleistocene (orange) 10,000 - 130,000 years ago
- Mid to Late Pleistocene (green) 10,000 - 750,000 years ago
- Early to Mid Pleistocene (purple) 130,000 - 1,650,000 years ago
- Quaternary (black) < 1,650,000 years ago

- Mapped
- Concealed
- Segment boundaries

Note: Segmented faults shown with all uppercase labels.

Base Map Data from the Utah Automated Geographic Reference Center (AGRC)

Fault Sources: Hecker, 1993; Geomatrix Consultants, 1999; Olig et al., 1999a; Coogan and King, 1999, J.C. Pechmann, UUSS, written communication, 2000, J.L. Jarva, UGS, digital communication, 2000.

Project No. 51F0SK9707.00	Mercur Fault, Utah	Map of the Oquirrh-East Great Salt Lake Fault Zone and Selected Nearby Faults	Figure 1
URS Greiner Woodward Clyde			

Version 10-24-2000

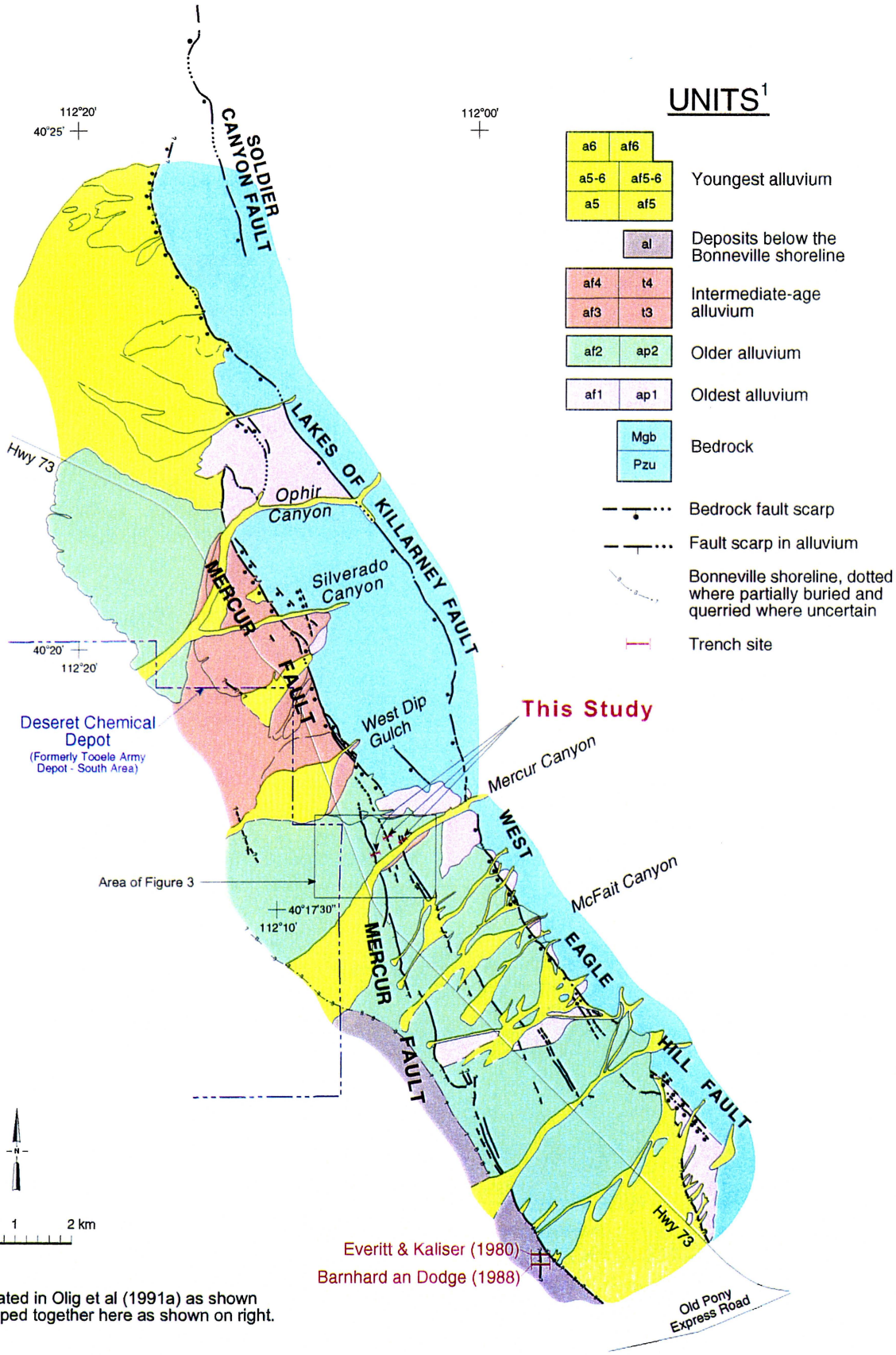

[1]Units differentiated in Olig et al (1991a) as shown on left are grouped together here as shown on right.

URS	Project No. 51-F0SK9707.00 Mercur Fault	SURFICIAL GEOLOGY AND TRENCH LOCATIONS ON THE SOUTH OQUIRRH MOUNTAINS FAULT	Figure 2

51-F0SK9707.00-00000/100300/gos

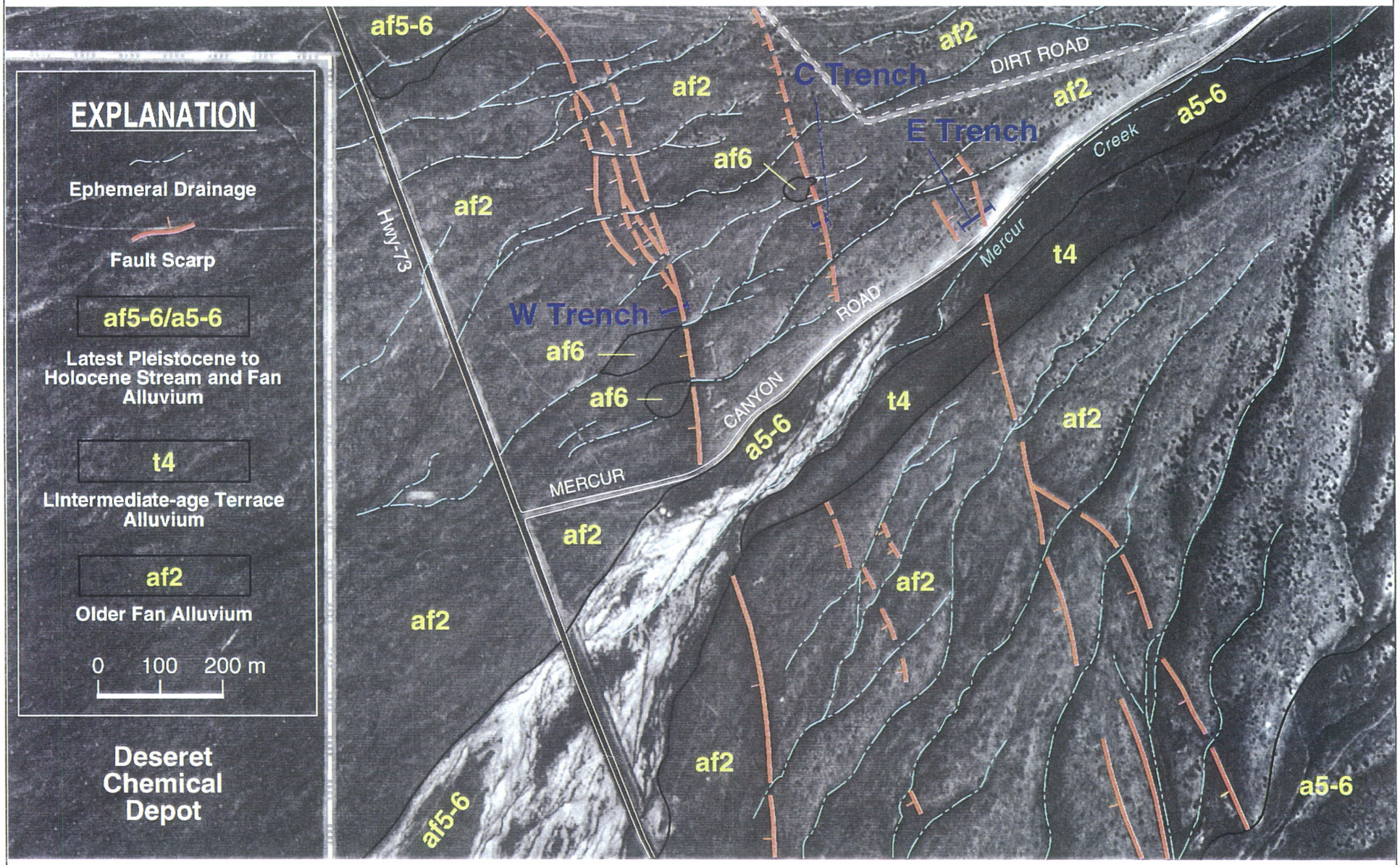

URS	Project No. 51-F0SK9707.00 Mercur Fault	AERIAL PHOTOGRAPH WITH SURFICIAL GEOLOGY OF THE MERCUR CANYON TRENCH SITE	Figure 3

51-F0SK9707.00-00000/100300/gos

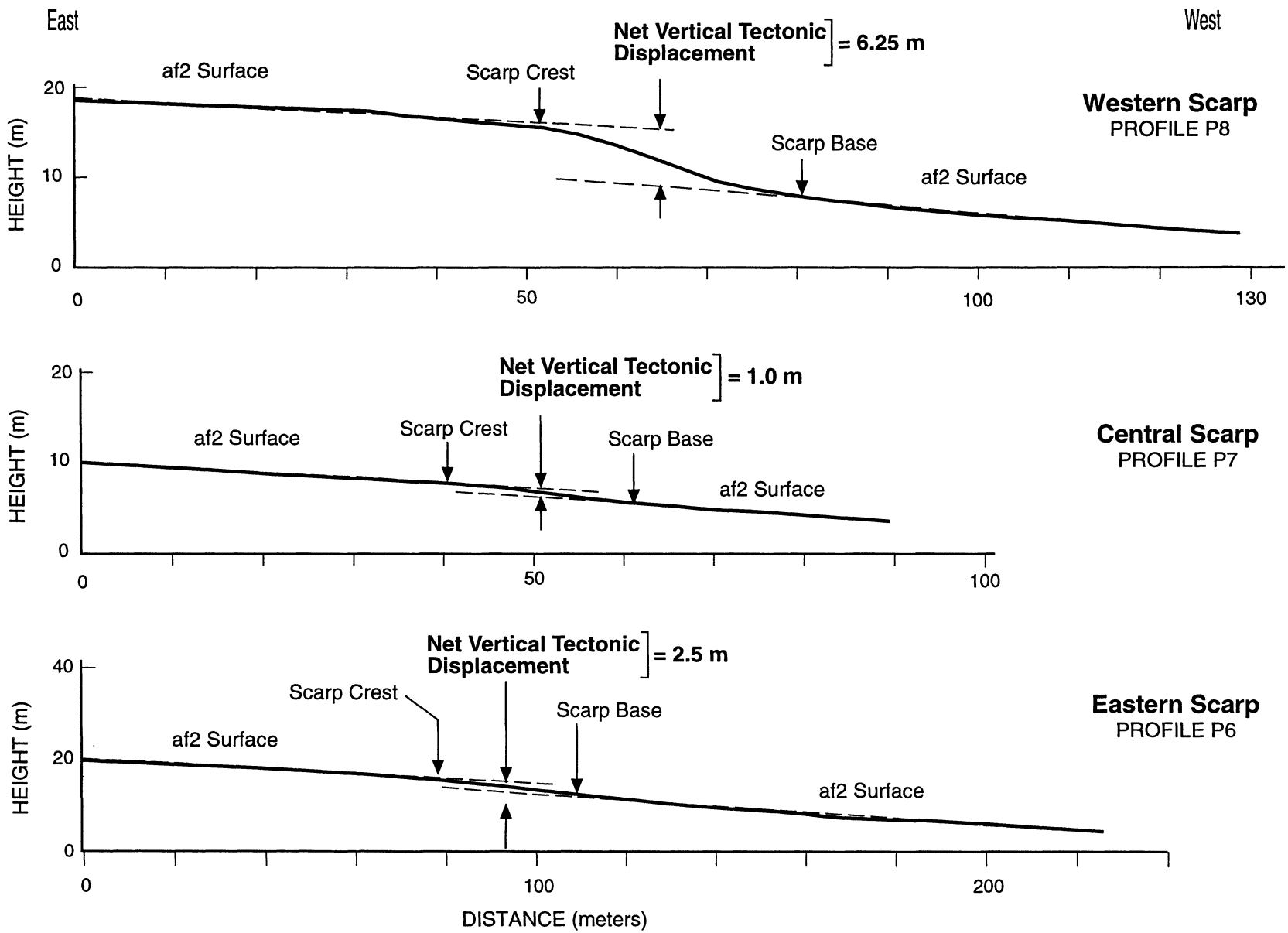

URS	Project No. 51-F0SK9707.00 Mercur Fault	TOPOGRAPHIC FAULT SCARP PROFILES FOR THE MERCUR CANYON TRENCH SITE	Figure 4

51-F0SK9707.00-00000/100300/gos

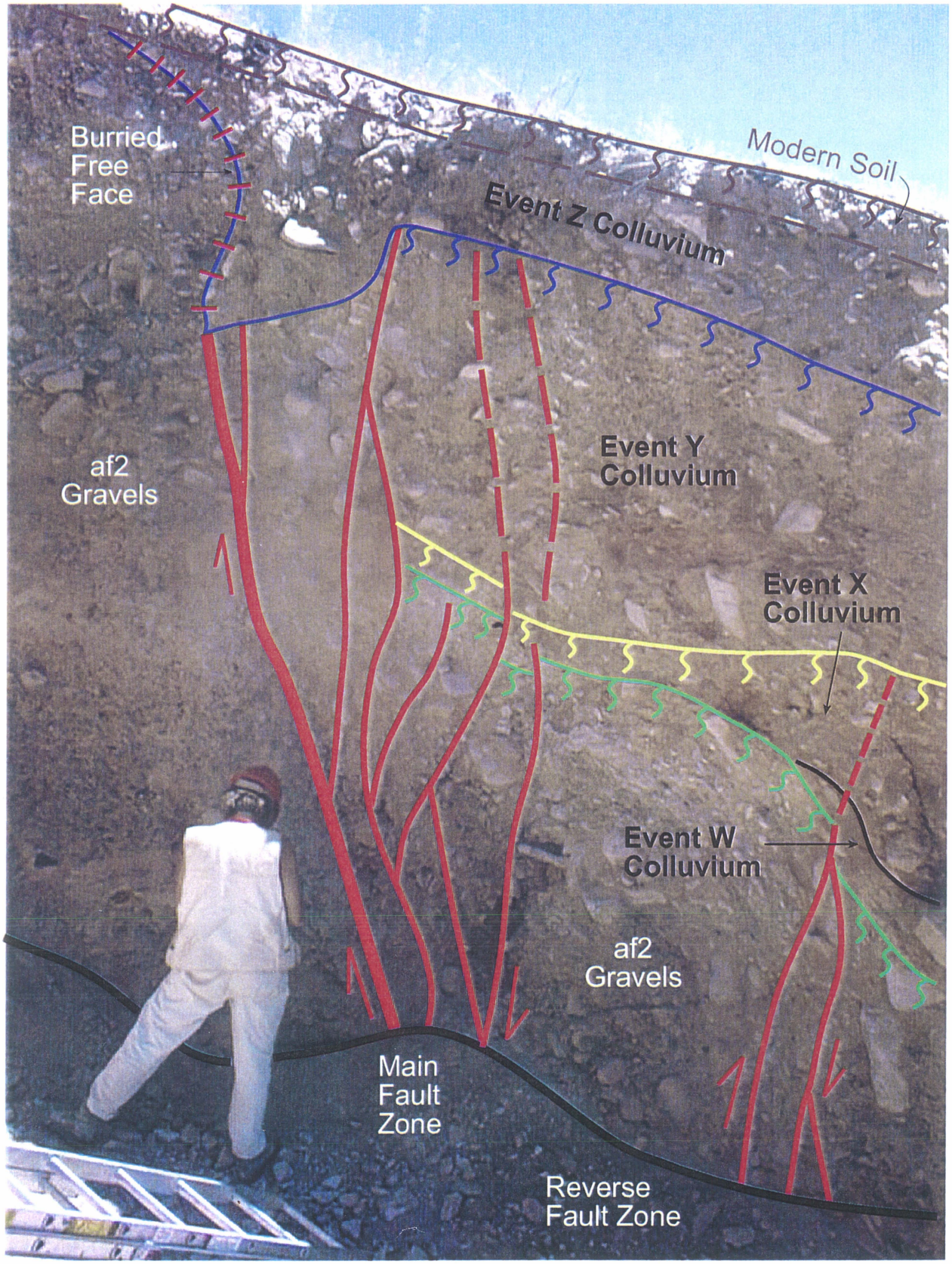

Note: See Figure 6 for detailed trench log.

URS	Project No. 51-F0SK9707.00 Mercur Fault	ANNOTATED PHOTOGRAPH OF MAIN FAULT ZONE, MERCUR CANYON WEST TRENCH, SOUTH WALL	Figure 5

51-F0SK9707.00-00000/100300/gos

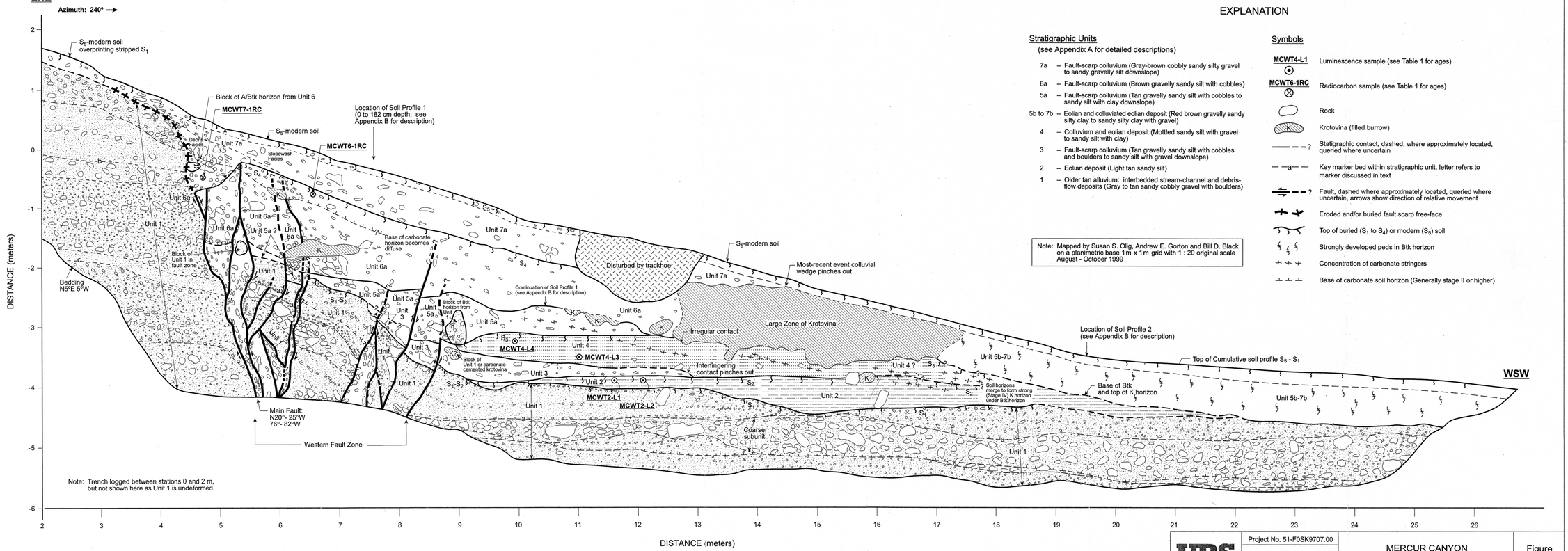

EXPLANATION

Stratigraphic Units

(see Appendix A for detailed descriptions)

- 7a – Fault-scarp colluvium (Gray-brown cobbly sandy silty gravel to sandy gravelly silt downslope)
- 6a – Fault-scarp colluvium (Brown gravelly sandy silt with cobbles)
- 5a – Fault-scarp colluvium (Tan gravelly sandy silt with cobbles to sandy silt with clay downslope)
- 5b to 7b – Eolian and colluviated eolian deposit (Red brown gravelly sandy silty clay to sandy silty clay with gravel)
- 4 – Colluvium and eolian deposit (Mottled sandy silt with gravel to sandy silt with clay)
- 3 – Fault-scarp colluvium (Tan gravelly sandy silt with cobbles and boulders to sandy silt with gravel downslope)
- 2 – Eolian deposit (Light tan sandy silt)
- 1 – Older fan alluvium: interbedded stream-channel and debris-flow deposits (Gray to tan sandy cobbly gravel with boulders)

Note: Mapped by Susan S. Olig, Andrew E. Gorton and Bill D. Black on a planimetric base 1m x 1m grid with 1 : 20 original scale August - October 1999

Symbols

- MCWT4-L1 – Luminescence sample (see Table 1 for ages)
- MCWT6-1RC – Radiocarbon sample (see Table 1 for ages)
- Rock
- Krotovina (filled burrow)
- Statigraphic contact, dashed, where approximately located, queried where uncertain
- Key marker bed within stratigraphic unit, letter refers to marker discussed in text
- Fault, dashed where approximately located, queried where uncertain, arrows show direction of relative movement
- Eroded and/or buried fault scarp free-face
- Top of buried (S_1 to S_4) or modern (S_0) soil
- Strongly developed peds in Btk horizon
- Concentration of carbonate stringers
- Base of carbonate soil horizon (Generally stage II or higher)

URS	Project No. 51-F0SK9707.00 Mercur Fault	MERCUR CANYON WEST TRENCH LOG	Figure 6

51-F0SK9707.00-00000/090900/gos

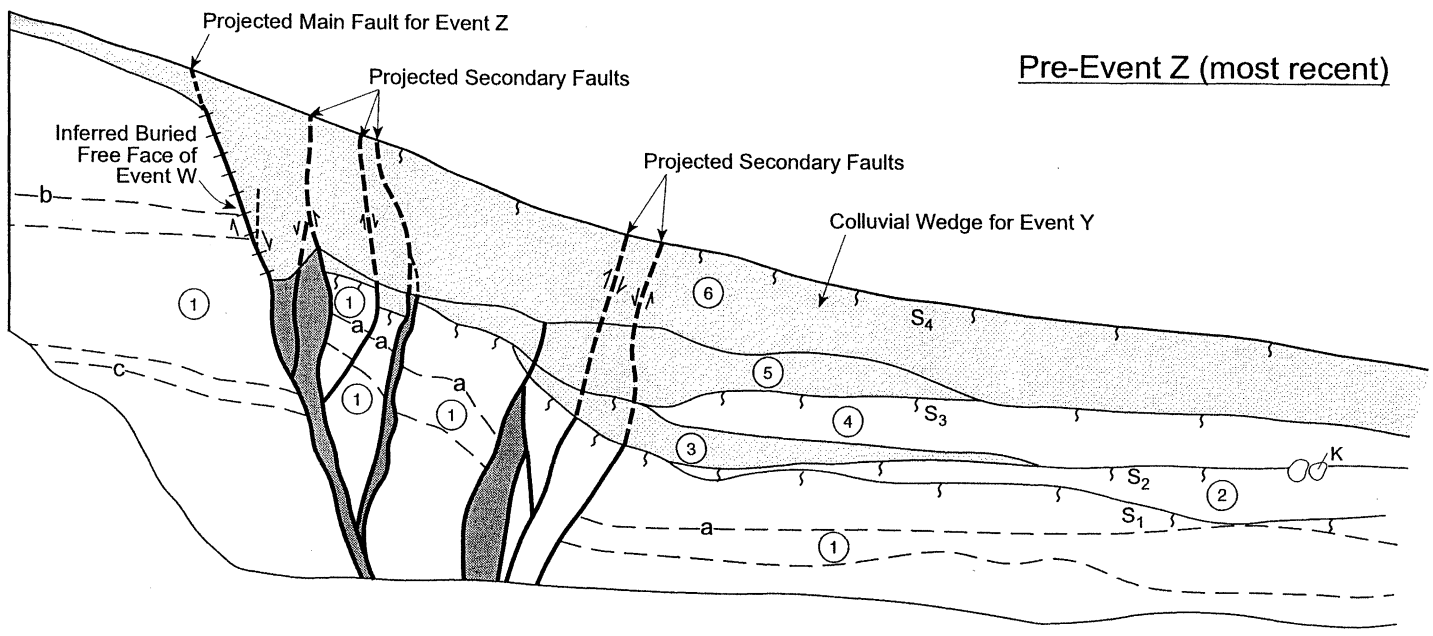

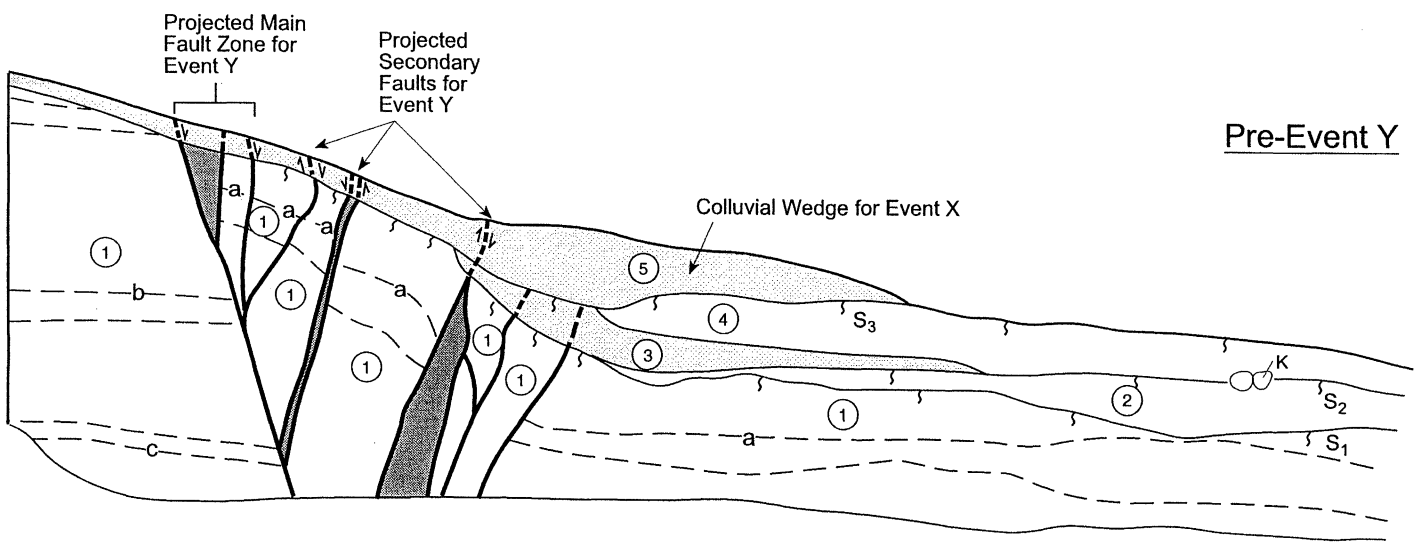

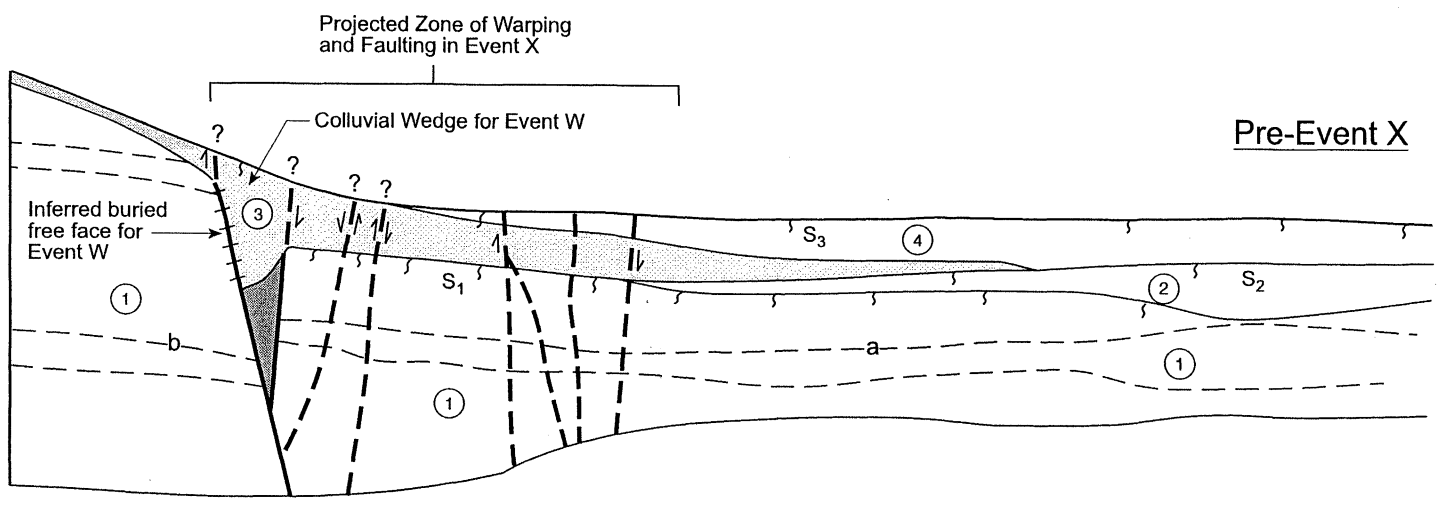

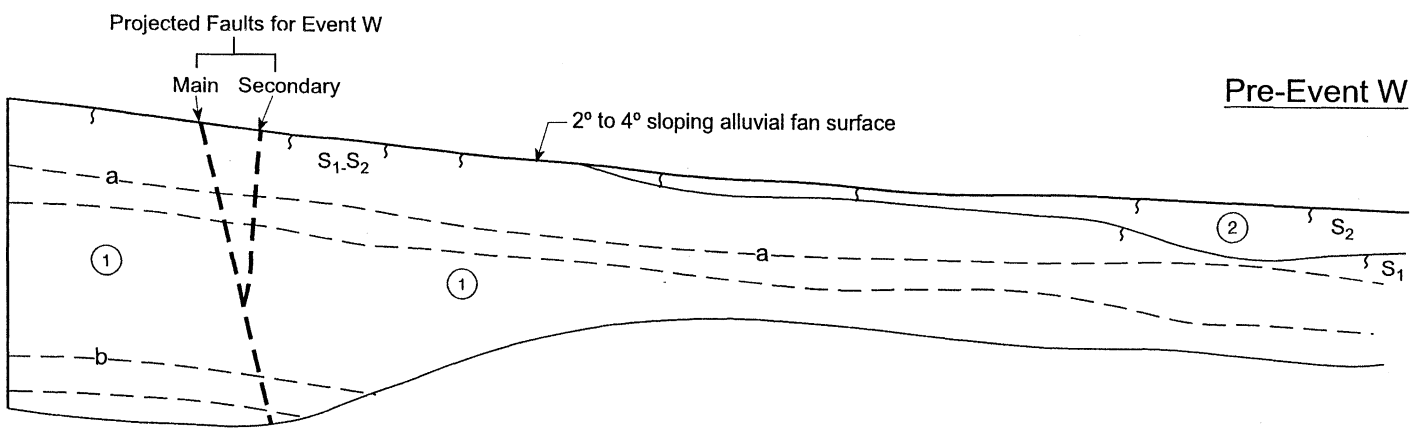

Note: See Figure 6 for actual trench log of the present, and for explanation of symbols and units (1) through (6).

1 m

1 m

Scale

URS	Project No. 51-F0SK9707.00 Mercur Fault	RECONSTRUCTION OF MERCUR CANYON WEST TRENCH LOG	Figure 7

51-F0SK9707.00-00000/100300/gos

URS	Project No. 51-F0SK9707.00 Mercur Fault	PHOTOGRAPH OF MERCUR CANYON CENTRAL TRENCH, SOUTH WALL	Figure 8

EXPLANATION

Stratigraphic Units
(see Appendix A for detailed descriptions)

3 – Slopewash colluvium (Brown to gray-brown clayey gravelly sandy silt)

2 – Colluvium and eolian deposit (Tan sandy clayey silt [subunit 2a] to light tan sandy clayey silt with gravel [subunit 2b])

1 – Older fan alluvium: interbedded stream-channel and debris-flow deposits (Gray to tan sandy cobbly gravel)

Symbols

MCET2-L5Z — Luminescence sample (see Table 1 for ages)

Rock

K — Krotovina (filled burrow)

? — Statigraphic contact, dashed, where approximately located, queried where uncertain

c — Key marker bed within stratigraphic unit, letter refers to marker discussed in text

? — Fault, dashed where approximately located, queried where uncertain, arrows show direction of relative movement

Top of buried (S_1 to S_2) or modern (S_0) soil

Base of carbonate soil horizon (Stage II or higher)

Note: Mapped by Susan S. Olig, Andrew E. Gorton and Greg N. McDonald on a planimetric base 1m x 1m grid with 1 : 20 original scale
August - October 1999

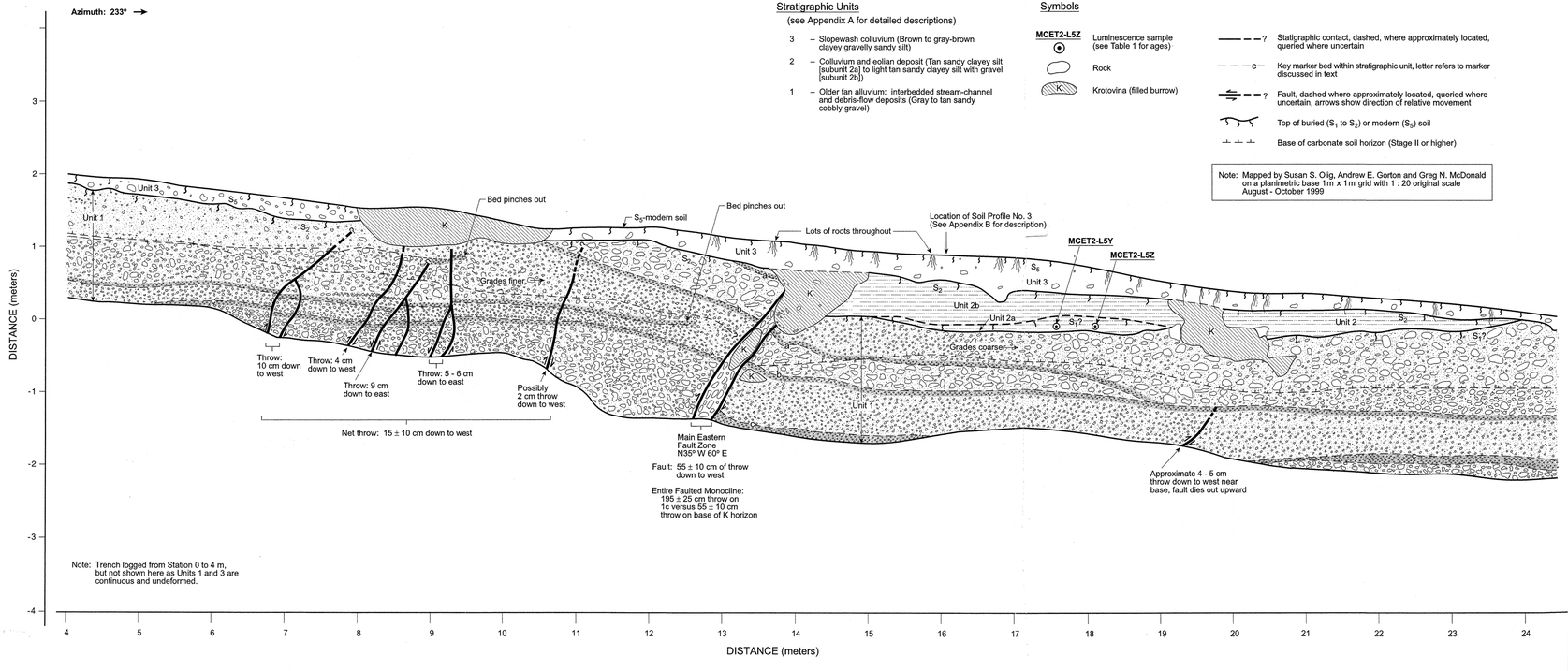

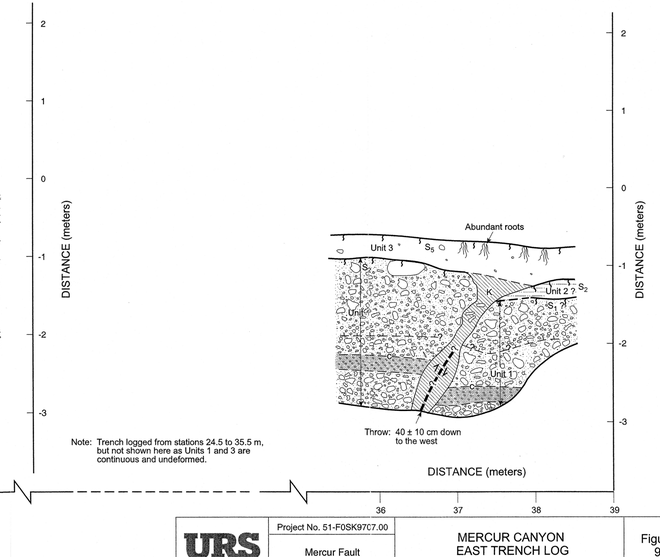

URS	Project No. 51-F0SK97C7.00 Mercur Fault	MERCUR CANYON EAST TRENCH LOG	Figure 9

51-F0SK9707.00-00000/011701/gos

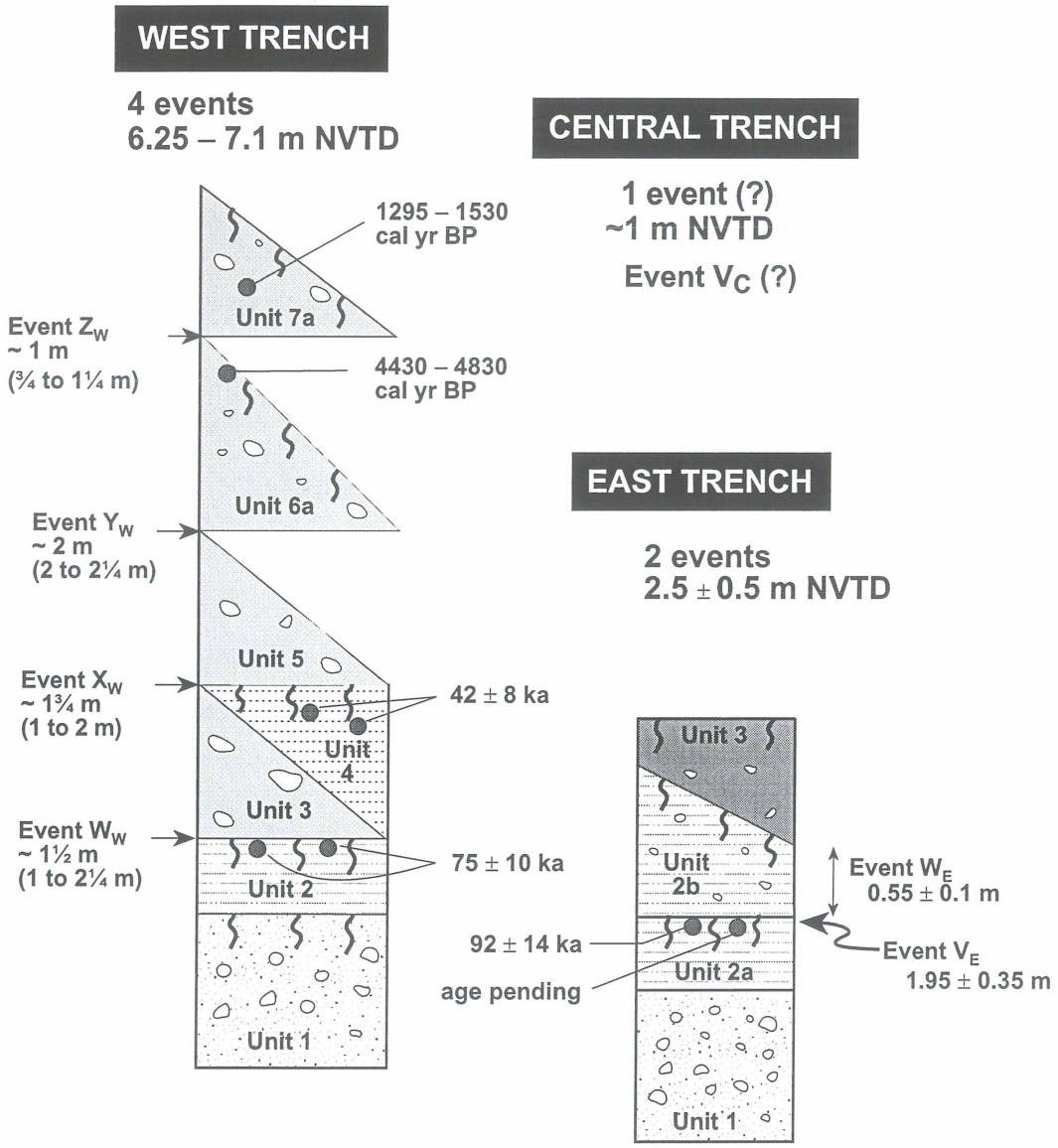

Note: Errors on ages are 2 sigma. See Table 1 for specific age data.

URS	Project No. 51-F0SK9707.00 Mercur Fault	SUMMARY DIAGRAM OF SURFACE-FAULTING EVENTS AT THE MERCUR CANYON SITE	Figure 10

51-F0SK9707.00-00000/011701/gos

Appendix A
Lithologic Unit Descriptions

UNIT DESCRIPTION

Initials: SSO + AEG

Project: NEHRP Mercur Fault

Date: 8-24-99

Location: Mercur Canyon W. Trench (Main Scarp)

Depth: 90-470cm
St. 4 m (FW)

Unit: 1

Genetic Name: Older alluvial fan sediments (af2)

		% Total	Rounding	Composition
PSA:	>30cm Boulders	5-10	sub ∡	average:
	7.5 - 30cm Cobbles	20-25	"-rd	Dominantly limestone-
0.048 - 7.5 cm	Gravel	45	"-rd	90, other-10%
0.08 - 4.8mm	Sand	15		(includes quartzite,
	Silt	10		granite & sandstone)
	Clay			(highly wthd)

Max. Size: 60 cm (HW)

Average Size: med to coarse gravel

USCS: Sandy cobbly gravel with boulders

	Dry	Wet
Color:	10 YR 6/4 Light yellowish brown	10 YR 4/4 Dark yellowish brown

Plasticity: none (except debris flows) **Dry Strength:** **Dilatency:** NA

Bedding: Dips in FW average 5° to 7° West; in HW range from 5° to 8° W outside def. zone

Sorting: well-sorted to very well-sorted **Clast** or **Matrix Supported** except interbedded debris flows

Contacts: Bottom not exposed; In HW top ... is irregular where burrowed but generally undulating (bar and swale topo.). In FW top is truncated by scarp.

Thickness: up to 5m exposed (minimum for fan)

Cementation: none (pea gravel beds) to (laminar [stage IV] K horizon in HW St. 20→W) **HCl rx:** es to ev

Carbonate: none to stage IV

Other: **Roots** **Rootlets** **Root Pores** **Organics** **Staining**
Vesicles Debris flows **Pedogenic Horizons** K **Fe Mg**

Interbedded stream channel and debris flow deposits. Dominantly braided stream (90-95%) deposits. Bedding has distinct lensing of pea gravels and coarser beds varying in thickness from 5 to ~100cm. Green - top of af2 surface
Pink - subunits
Yellow - base carbonate in FW
Black - " " " HW

UNIT DESCRIPTION

Initials: SSO + AEG

Project: NEHRP-Mercur fault

Date: 8-24-99

Location: Mercur Canyon W. Trench

Depth: St. 11 m (HW)

Unit: 2

Genetic Name: Eolian deposit on af2 fan

PSA:	% Total	Rounding	Composition
Boulders	Occ.	v rd	Average:
Cobbles	Occ.	rd	95% limestone
Gravel	5-10	sub ⅔-rd	5% other (sand-
Sand	20	"	stone, quartzite)
Silt	>70		
Clay			

Max. Size: 20 cm **Average Size:** vfs - silt

USCS: Sandy silt with gravel

	Dry	Wet
Color:	10 YR 7/4 to 6/4 mottled	10 YR 5/4
	Very pale brown to light yellowish brown	Yellowish brown

Plasticity: low to med **Dry Strength:** High **Dilatency:** slow to rapid

Bedding: Poorly bedded but some faint laminations
lots of bioturbation

Sorting: Very well sorted **Clast or Matrix Supported**

Contacts: Lower: undulating, gradational to distinct; Upper: flat to irregular (where burrowed) gradational

Thickness: Very irregular 0 to ~70 cm

Cementation: strongly (cs) **HCl rx:** ev

Carbonate: Stage II to III for most part (gets higher downslope)

Other: Roots Rootlets **Root Pores** Organics Staining
Vesicles **Pedogenic Horizons B+k** Fe Mg

Filled in low spots in bar and swale topo on af2 fan gravels. Formed top of af2 fan surface prior to 1st faulting event. Has stage II to II+ carbonate and subangular blocky peds. In W. trench only present in HW but is present to E in FW (in C + E trenches) Between Pink (pea gravels in unit 1) and Green (top B+k)

S1

UNIT DESCRIPTION

Initials: SSO + AEG

Project: NEHRP Mercur fault

Date: 8-24-99

Location: Mercur Canyon W Trench

Depth: St. 8.2 m (HW)

Unit: 3

Genetic Name: Fault scarp colluvium (1st event)

PSA:	% Total	Rounding	Composition
Boulders	0-10	subrd.	Limestone
Cobbles	0-10	sub & to rd.	
Gravel	10-15	"	
Sand	15	"	
Silt	50-75		
Clay			

Variable - fines away from fault + downslope

Max. Size: 30 cm **Average Size:** sand & silt

USCS: gravelly sandy silt w/ cobbles & boulders (near fault) to sandy silt with gravel (downslope)

Dry **Wet**

Color: 10 YR 6/4 Light yellowish brown — 10 YR 4/4 Dark yellowish brown

Plasticity: low **Dry Strength:** none to low **Dilatency:** none

Bedding: none

Sorting: very poor **Clast or Matrix Supported** (Matrix) mostly, except near fault

Contacts: upper: clear to gradual, flat to wavy (but warped)
lower: distinct to abrupt, flat (but warped)

Thickness: 0 to 60 cm (wedged shaped)

Cementation: weak **HCl rx:** es to ev

Carbonate: Stage I - II+ (carbonate flecks, nodules, stringers inc. downslope)

Other: Roots Rootlets Root Pores Organics Staining

Vesicles Pedogenic Horizons Fe Mg

Unit only locally preserved under the colluvial wedge for the 2nd event (Unit 5) and Unit 4 from st. 7½ to 12½ m. Apparently Eroded to E and pinches out to W. Fines to W and is wedge-shaped. Is deformed (folded + slightly sheared) Block of carbonate below ~ 8.75m may be block of K horizon on unit 1 or possibly carbonate-cemented krotovina.
base - green
top - black to lavender

UNIT DESCRIPTION

Initials: SSO & AEG

Project: NEHRP Mercur fault

Date: 8-24-99

Location: Mercur Canyon W Trench

Depth: st. 10m (HW)

Unit: 4

Genetic Name: Eolian deposit @ base of paleoscarp

PSA:	% Total	Rounding	Composition
Boulders	0		Limestone w/ occ.
Cobbles	occ.	rd	others (sandstone,
Gravel	5-10	subrd-rd	granitic)
Sand	15-20	"	
Silt	70-80		
Clay			

Max. Size: 15 cm Average Size: silt

USCS: Sandy silt with gravel to sandy silt with clay

	Dry mottled	Wet
Color:	10 YR 6/4 to 10 YR 4/6	10 YR 4/6
	Light yellowish brown to yellowish brown	Dark yellowish brown

Plasticity: low Dry Strength: low Dilatency: none to slow

Bedding: Poor. Homogeneous unit (even mottling appears evenly distributed)

Sorting: moderate to well Clast or Matrix Supported

Contacts: upper: gradual to abrupt, smooth to irregular (locally where burrowed)
lower: clear (over Unit 3) to gradual (over Unit 2)

Thickness: 0 to 61 cm

Cementation: weak to indurated HCl rx: es

Carbonate: (increase downslope w/inc. carbonate) Stage I (@ st. 10m) to Stage IV, increasing downslope to W

Other: Roots Rootlets Root Pores carbonate coated Organics Staining

Vesicles Pedogenic Horizons Bk → K Fe Mg

Present from st. 9m to W end of trench but merges with other units ~ st. 16 to 19m (overprinted by merging soil horizons too). Fines to W (downslope). May include colluviated loess. Has slope-// stringers of carbonate st. 11½-12½m and 16-17m. Reddening and increasing ped structure (but still weak) from st. 10 to 12½ m until overprinted by carbonate

H:\ADMIN\OLIG\UNITDEF1.SSO\1 M0715941410

Top - black to blue-black
Base - lavendar to green

UNIT DESCRIPTION

Initials: SSO & AEG

Project: NEHRP Mercur fault

Date: 8-24-99

Location: Mercur Canyon W Trench

Depth: St. 8 1/2 m (HW)

Unit: 5a

Genetic Name: "Fault scarp" colluvium (2nd event)

PSA:	% Total	Rounding	Composition
Boulders	Occ	rd	Limestone
Cobbles	5-10	subrd	occ. other (eg. blocks of unit 1)
Gravel	5-25	~~s~~ to rd	
Sand	20	↓	
Silt	55-70		
Clay			

Coarser end of range near scarp

Max. Size: 57 cm

Average Size: sand

USCS: Gravelly sandy silt with cobbles to sandy silt with clay

	Dry	Wet
Color:	10 YR 6/4 Light yellowish brown	10 YR 5/4 yellowish brown

Plasticity: Low

Dry Strength: low

Dilatency: slow to rapid

Bedding: none

Sorting: very poorly sorted

Clast to Matrix Supported

Contacts: upper: abrupt to clear, smooth to wavy; lower: abrupt to gradual smooth to wavy (heal area)

Thickness: 0 to ~85 cm (Wedge-shaped)

Cementation: none to weak

HCl rx: es to ev

Carbonate: It (coating in pores, nodules & flecks)

Other: Roots Rootlets Root Pores Organics Staining

Vesicles Pedogenic Horizons Fe Mg

Only locally present in HW from ~ st. 5 m to ~12 1/2 m. Fines to W. of st. 9 1/2 m. This unit was deposited at the base of a scarp created by folding and shearing during the 2nd event. It looks like a heterogeneous mix of Units 3 and 4 with even a block of Unit 1 thrown in (~st 9 m)

H:\ADMIN\OLIG\UNITDEF1.SSO\1

Base - black
"Free face" equivalent - red black

M0715941410

UNIT DESCRIPTION

Initials: SSO & AEG

Project: Mercur fault NEHRP **Date:** 8-24-99

Location: Mercur Canyon W Trench **Depth:** St. 7 1/2 m (HW)

Unit: 6a

Genetic Name: Fault Scarp colluvium (3rd or Penultimate event)

PSA:	% Total	Rounding	Composition
Boulders	occ to 5	∠ to subrd.	Dominantly
Cobbles	occ to 15	sub ∠ to rd	limestone
Gravel	15 to 30	↓	
Sand	15 to 20		
Silt	30-65		
Clay			

fines to W away from fault, and debris facies is coarser

Max. Size: 32 cm **Average Size:** sand to gravel

USCS: gravelly sandy elastic silt to sandy gravelly elastic silt with cobbles

	Dry (down slope)	Dry (near fault)	Wet (down slope)	Wet (near fault)
Color:	10 YR 5/4	to 10YR 6/4	10 YR 4/4	- 10YR 5/4
	Yellowish brown	Lght. yell. brn.	Dark yellowish brown	

Plasticity: medium **Dry Strength:** medium **Dilatency:** none

Bedding: none to weakly stratified (debris and slopewash facies, respectively)

Sorting: very poorly sorted to poorly sorted Clast ~~or~~ to Matrix mostly Supported

Contacts: upper: abrupt to clear, smooth except where bio-turbated (irregular occaissionally)

Thickness: 0 to ~140cm (Wedge-shaped)

Cementation: weakly **HCl rx:** es to ev

Carbonate: I to II+

Other: Roots Rootlets Root Pores carbonate coated Organics Staining Vesicles clay films Pedogenic Horizons Btk subangular blocky peds Fe Mg

Unit only locally present near main fault in HW from ~st. 475 to ~17 m*. Includes both debris facies and slopewash facies, however a large Krotovina has disturbed much of th. latter and shearing during the MRE apparently cut the heal. Thick slopewash facies (much thicker than other wedges).

H:\ADMIN\OLIG\UNITDEF1.SSO\1 M0715941410

* Merges with other units & is overprinted by soil W of st. 17m.

Yellow - base Blue - top

UNIT DESCRIPTION

Initials: SSO+AEG

Project: NEHRP Mercur fault

Date: 8-24-99

Location: Mercur Canyon W Trench

Depth: ~St. 6½ m (HW)

Unit: 7a

Genetic Name: Fault scarp colluvium (4th or most recent event)

PSA:	% Total	Rounding	Composition
Boulders	oc to 5	ang. to rd	limestone
Cobbles	10-15	↓	
Gravel	25-30		
Sand	15		
Silt	45-50		inc. 90of downslope
Clay			

Debris facies is coarser end of range

Max. Size: 40 cm

Average Size: gravel

USCS: Cobbly sandy silty gravel to sandy gravelly silt with cobbles

	Dry	Wet
Color:	10 YR 6/3 Pale brown	10 YR 5/4 yellowish brown

Plasticity: low

Dry Strength: none to low

Dilatency: rapid to slow

Bedding: none in debris facies but there is slope // fabric in slopewash facies

Sorting: very poorly sorted

Clast ~~or~~ to Matrix Supported

Contacts: upper: gradual to diffuse - merges with modern soil/slope wash

Thickness: 0 to 75 cm (long skinny wedge shape)

Cementation: none to weak

HCl rx: es

Carbonate: I+ 1 (disseminated)

Other: Roots, Rootlets, Root Pores, Organics, Staining, Vesicles, Pedogenic Horizons Bk angular blocky, Fe Mg

More organics than any other units. Coarser than underlying colluvial wedge (Unit 6) Present only locally in HW from St 1½m to ~1 ½m. Includes debris (with broad heal) and slopewash facies (upper section + downslope)

Base - blue
Free face - blue red

H:\ADMIN\OLIG\UNITDEF1.SSO\1

M0715941410

UNIT DESCRIPTION

Initials: SSO + AEG

Project: NEHRP Mercur fault

Date: 8-26-99

Location: Mercur Canyon W Trench

Depth: St 19.5m (HW)

Unit: 5b - 7b

Genetic Name: Eolian and colluviated eolian deposit

PSA:	% Total	Rounding	Composition
Boulders	0		limestone and
Cobbles	occ.	⅓ to	some minor
Gravel	10-15		sandstone
Sand	15		
Silt	70-75		
Clay			

Max. Size: 20 cm Average Size: silt

USCS: gravelly sandy silty clay to sandy silty clay with gravel

	Dry	Wet
Color:	10YR 6/4 - 5/4 Light yellowish brown to yellowish brown	10YR 5/4 to 4/4 Light to dark yellowish brown

Plasticity: med-high Dry Strength: med-high Dilatency: none

Bedding: none

Sorting: moderate to well Clast or Matrix Supported

Contacts: abrubpt to gradual, wavy to irregular

Thickness: 50-75 cm

Cementation: cw+ to cs HCl rx: es

Carbonate: Stage II+ (none in upper 20-30 cm) modern soil

Other: Roots, Rootlets, Root Pores, Organics, Staining, Vesicles, Pedogenic Horizons B+K, Fe Mg

H:\ADMIN\OLIG\UNITDEF1.SSO\1 M0715941410

UNIT DESCRIPTION

Initials: SSO & AEG

Project: NEHRP Mercur fault

Date: 8-28-99

Location: Mercur Canyon E Trench

Depth: ~1m below level line st. 16m

Unit: 1

Genetic Name: Alluvial fan deposits

PSA:	% Total	Rounding	Composition
Boulders	5	rd	Limestone (& some quartzite, granite sandstone, mudstone)
Cobbles	15-25	sub rd-rd	
Gravel	40	~-rd	
Sand	25	~-rd	
Silt	5-15		
Clay			

Max. Size: ~45cm **Average Size:** med gravel

USCS:

	Dry	Wet
Color:	10 YR 6/3 Pale brown	10 YR 5/4 Yellowish brown

Plasticity: none **Dry Strength:** loose to hard (w/ K horizon) **Dilatency:** slow to rapid

Bedding: well stratified, strong clast imbrication, lots of lensing and channeling

Sorting: well to very-well sorted **Clast or Matrix Supported** (Mostly clast, some debris flow)

Contacts: lower: not exposed; upper: abrupt to gradual, smooth to broken

Thickness: ~2.5m max. exposed in trench (but base not exposed)

Cementation: none to strong **HCl rx:** e+

Carbonate: none to stage III+ (some stage IV- near st. 38 m where laminations are starting to form)

Other: Roots Rootlets Root Pores Organics Staining

Vesicles **Pedogenic Horizons** K Fe Mg

Interbedded stream channel and debris flow deposits (dominantly former). Same unit as Unit 1 in W trench

UNIT DESCRIPTION

Initials: SSO & AEG

Project: NEHRP Mercur fault

Date: 8-28-99
Rev. 10-15-99

Location: Mercur Canyon East Trench

Depth: +15 cm (from LL)
St ~15 3/4 m

Unit: 2, 2a, 2b

Genetic Name: colluvium + Eolian deposits on af2 surface

PSA:	% Total	Rounding	Composition
Boulders	—		Limestone
Cobbles	occ	subrd-rd	
Gravel	5-10	sub ⅔-rd	
Sand	20-30		
Silt	60-75		
Clay			

Max. Size: _____ Average Size: silt to sand

USCS: Sandy clayey silt to sandy clayey silt w/ gravel

	Dry faintly mottled	Wet
Color:	10 YR 8/2 Very pale brown	10 YR 7/3 Very pale brown

Plasticity: medium Dry Strength: med to high Dilatency: rapid

Bedding: faint thin laminations where not bioturbated by roots or burrows (2a)

Sorting: moderate to well Clast or Matrix Supported

Contacts: upper: irregular to broken, abrupt; lower: smooth to wavy, clear to gradual

Thickness: 0-63 cm (wedged shaped)

Cementation: strong HCl rx: ev

Carbonate: Stage III+ (platy plugged & almost laminar)

Other: Roots, Rootlets, Root Pores, Organics, Staining, Vesicles, Lots of burrows, Pedogenic Horizons, Fe Mg

S1 ?- top of 2a; Btk K.

Only locally present in HW near st. 37 m and main fault (st. 37 → 39 m) Unit 2 & Units 2b/2a → Unit 2 (st. 14 → 24 m) but may have been present in FW @ st. 8-11 m (above secondary faults) but was burrowed. Also Many other locations throughout trench where top of Unit 1 (af2 ~~surf~~ gravels) has been almost engulfed by infiltration of fines and carbonate (including on downthrown side of small fault at st. ~37 m) This unit may correlate to Units 2 and 4 in W Trench.

UNIT DESCRIPTION

Initials: SSO + AEG

Project: NEHRP Mercur fault

Date: 8-28-99

Location: Mercur Canyon East Trench

Depth: St. 15 3/4 m

Unit: 3

Genetic Name: Modern soil

PSA:	% Total	Rounding	Composition
Boulders	occ		Limestone with
Cobbles	occ to 5	sub ∡-rd	minor other (qtzite)
Gravel	25	∡ to sub rd	
Sand	25	rd	
Silt	> 50		
Clay			

Max. Size: ~40 cm

Average Size: silt to sand

USCS: Clayey gravelly sandy silt

Color:	Dry	Wet
	10 YR 6/3 Pale brown	10 YR 5/4 Yellowish brown

Plasticity: medium

Dry Strength: loose

Dilatency: rapid

Bedding: none

Sorting: Poor

Clast or Matrix Supported

Contacts: Lower: clear to abrupt, irregular to broken (very bioturbated)

Thickness: Variable

Cementation: none

HCl rx: ef

Carbonate: variable: none to Some disseminated in matrix with nodules (Stage I-)

Other: lots Roots, Rootlets, Root Pores, Organics, Staining, Vesicles, Pedogenic Horizons A/B some, Fe Mg

Present throughout trench. Only unit clearly not faulted.

Appendix B
Soil Profile Descriptions

Table B-1. – Description of Soil Profile SP1

Form from Birkeland et al. (1991). Courtesy of D. Jorgenson (1989).

Location Mercur Canyon, West Trench, top at 7.58 m, jogged to 10.45 m[1], Ophir 7.5' Quadrangle. Page 1 of 2

Site No. SP1 **Date** 8/25/99 **Time** ~1300 **Vegetation** Cheatgrass, sage, juniper, rabbitbrush [1]

Elevation ~5550 ft **Slope** 17° **Aspect** S60°W **Geomorphic Surface** Downthrown side of western fault scarp on older alluvial fan (af2)

Parent Material(s): Colluvium, loess, and alluvial-fan gravels **Described by** SSO and AEG

Depth (cm)	Horizon	Color	Structure	Gravel %	Consistence			Texture	pH/ Eff rxn	Clay Films	Bound-aries	Notes
		wet / dry			Wet	Moist	Dry					
30	A	10YR 5/3 brown ---------- 10YR 6/3 to 6/4 pale brown to light yellowish brown	m & vf gr sg f pl 1 m pr 2 c cpr 3 vc abk sbk	0 50 <10 75 10 >75 25 40-50	so o ss ps s p vs vp	lo vf fr f vfi efi	lo so sh h vh eh	S SiCL LS SiL SL Si SCL SiC L C CL SC	ev	none	a s c w g i d b	Roots; cw; loose, slope parallel fabric; PM = Unit 7
70	Btkj	10YR 5/3 brown ---------- 10YR 6/3 to 6/4 pale brown to light yellowish brown	m vf gr sg f pl 1 m pr 2 c cpr 3 vc abk sbk	0 50 <10 75 10 >75 25 35-40	so o ss ps s p vs vp	lo vf fr f vfi efi	lo so sh h vh eh	S SiCL LS SiL SL Si SCL SiC L C CL SC	ev	v1 f pf 1 po 2 d br 3 co p cobr	a s c w g i d b	Stage I+ to II- CaCO3; cw+; slope parallel fabric; roots (less than overlying horizon); root pores; mottled; PM = Unit 7
100	2Btkb	10YR 5/4 yellowish brown ---------- dark:10YR 5/3 brown, light:10YR 7/3 very pale brown	m vf gr sg f pl 1 m pr 2 c cpr 3 vc abk sbk	0 50 <10 75 10 >75 25	so o ss ps s p vs vp	lo vf fr f vfi efi	lo so sh h vh eh	S SiCL LS SiL SL Si SCL SiC L C CL SC	ev	v1 f pf 1 po 2 d br 3 co p cobr	a s c w g i d b	cs; Stage II to III+ CaCO3; mottled; roots (but less than overlying horizon), more CaCO3 than overlying horizon; overprinted by modern soil; PM = Unit 6
155	2Btk2b	10YR 5/4 yellowish brown ---------- dark:10YR 5/4 yellowish brown, light:10YR 7/3 very pale brown	m vf gr sg f pl 1 m pr 2 c cpr 3 vc abk sbk	0 50 <10 75 10 >75 25	so o ss ps s p vs vp	lo vf fr f vfi efi	lo so sh h vh eh	S SiCL LS SiL SL Si SCL SiC L C CL SC	ev	v1 f pf 1 po 2 d br 3 co p cobr	a s c w g i d b	cw, Stage I+ to II CaCO3; mottled; less CaCO3 and less ped structure than horizon above; PM = Unit 6 slopewash
182	2Btk3b	10YR 5/4 yellowish brown ---------- 10YR 7/3 very pale brown	m vf gr sg f pl 1 m pr 2 c cpr 3 vc abk sbk	0 50 <10 75 10 >75 25	so o ss ps s p vs vp	lo vf fr f vfi efi	lo so sh h vh eh	S SiCL LS SiL SL Si SCL SiC L C CL SC	es+	v1 f pf 1 po 2 d br 3 co p cobr	a s c w g i d b	cw; Stage I+ CaCO3; slightly mottled; not as well developed as horizon above; PM = Unit 6 slopewash facies
234 [2]	3Bkb?	10YR 5/4 yellowish brown ---------- 10YR 6/4 light yellowish brown, 10YR 8/3 very pale brown mottles	m vf gr sg f pl 1 m pr 2 c cpr 3 vc abk sbk cpr thin and angular	0 50 <10 75 10 >75 25	so o ss- ps s p vs vp	lo vf fr f vfi efi	lo so sh h vh eh	S SiCL LS SiL SL Si SCL SiC L C CL SC	es	none	a s c w g i d b	Jogged to st. 10.45m. cw; platy in a vertical orientation; lots of CaCO3-coated pores; evenly mottled; Stage I to I+ CaCO3 color highly variable; PM = toe of Unit 5
271 [2]	4Bkb	10YR 5/4 yellowish brown ---------- 10YR 6/4 light yellowish brown w/ 7/3 very pale brown mottles	m vf gr sg f pl 1 m pr 2 c cpr 3 vc abk sbk	0 50 <10 75 10 >75 25	so+ o ss ps s p vs vp	lo vf fr f vfi efi	lo so sh h vh eh	S SiCL LS SiL SL Si SCL SiC L C CL SC	ev	none	a s c w g i d b	Stage I to I+ CaCO3; cw; evenly and finely mottled; PM = Unit 4

Table B-1. – (Continued)

Location Mercur Canyon, West Trench, top at 7.58 m, jogged to 10.45 m[1], Ophir 7.5' Quadrangle. Page 2 of 2

Site No. SP1 (con't) **Date** 8/25/99 **Time** ~1300 **Vegetation** Cheatgrass, sage, juniper, rabbitbrush [1]

Elevation ~5560 ft **Slope** 17° **Aspect** S60°W **Geomorphic Surface** Downthrown side of western fault scarp on older alluvial fan (af2)

Parent Material(s): Colluvium, loess, and alluvial-fan gravels **Described by** SSO and AEG

Depth (cm)	Horizon	Color	Structure	Gravel %	Consistence			Texture	pH/ Eff rxn	Clay Films	Bound-aries	Notes
		wet / dry			Wet	Moist	Dry					
300 [2]	4Bk2b	10YR 5/4 yellowish brown ---------- 10YR 6/4 light yellowish brown	m vf gr sg f pl 1 m pr 2 c cpr 3 vc abk sbk	0 50 <10 75 10 >75 25	so+ o ss ps s p vs vp	lo vf fr f vfi efi	lo so sh h vh eh	S SiCL LS SiL SL Si SCL SiC L C CL SC	ev	none	a s c w g i d b	cw, Stage I+ CaCO3; more disseminated CaCO3 than overlying horizon; not mottled; sandier than horizon above; PM = Unit 3
312 [2]	5Btkb	10YR 6/4 light yellowish brown ---------- dark:7.5YR 6/3.5 light brown, light:10YR 8/2 very pale brown	m vf gr sg f pl 1 m pr 2 c cpr 3 vc abk sbk	0 50 <10 75 10 >75 25	so o ss ps s p vs vp	lo vf fr f vfi efi	lo so sh h vh eh	S SiCL LS SiL SL Si SCL SiC L C CL SC	ev+	v1 f pf 1 po 2 d br 3 co p cobr	a s c w g i d b	cw to cs; more platy where CaCO3 is present; Stage II to II+ CaCO3, becomes Stage IV downtrench; strongly, variably, and irregularly mottled; lots of root pores/vesicles; PM = Unit 2
356 [2]	6Btkb	10YR 7/4 very pale brown ---------- dark:10YR 7/3 very pale brown, light:10YR 8/2 very pale brown	m vf gr sg f pl 1 m pr 2 c cpr 3 vc abk sbk	0 50 <10 75 10 >75 25	so o ss ps s p vs vp	lo vf fr f vfi efi	lo so sh h vh eh	S SiCL LS SiL SL Si SCL SiC L C CL SC	ev+	v1 f pf 1 po 2 d br 3 co p cobr	a s c w g i d b	Stage II CaCO3, becomes Stage IV downtrench; cw to cs; less CaCO3 and more gravel than overlying horizon; strongly, variably, and irregularly mottled; lots of root pores/vesicles; PM = Unit 1
412 [2]	6Bkb	10YR 6/4 light yellowish brown ---------- 10YR 6/4 to 7/4 light yellowish brown to very pale brown	m vf gr sg f pl 1 m pr 2 c cpr 3 vc abk sbk	0 50 <10 75 10 >75 25	so o ss- ps- s p vs vp	lo vf fr f vfi efi	lo so sh h vh eh	S SiCL LS SiL SL Si SCL SiC L C CL SC	ev	none	a s c w g i d b	Stage I to I+ CaCO3; cw; PM = Unit 1 coarse subunit
447 [2]	Parent material	10YR 5/4 to 5/6 yellowish brown ---------- 10YR 6/4 light yellowish brown	m vf gr sg f pl 1 m pr 2 c cpr 3 vc abk sbk	0 50 <10 75 10 >75 25	so o ss ps s p vs vp	lo vf fr f vfi efi	lo so sh h vh eh	S SiCL LS SiL SL Si SCL SiC L C CL SC	es-	none	not exposed	No CaCO3 Stage; no cementation; PM = Unit 1

Notes: 1) Recently burned and taken over by cheatgrass, eolian sediments visibly banked up against base of scarp formed on old fan surface.
2) This Soil Profile was split: from 0 to 182 cm below ground surface located at Station 7.58 meters, and 182 cm to bottom of trench located at Station 10.45 meters. Therefore, depths shown below 182 cm indicate true horizon thicknesses but not actual depth below the ground surface.

Table B-2. – Description of Soil Profile SP2
Form from Birkeland et al. (1991). Courtesy of D. Jorgenson (1989).

Location Mercur Canyon, West Trench, at 19.53 meter mark, Ophir 7.5' Quadrangle. Page 1 of 1

Site No. SP2 **Date** 8/26/99 **Time** 0900 **Vegetation** Cheatgrass, juniper, rabbitbrush, sage

Elevation ~5560 ft **Slope** 5° **Aspect** S60°W **Geomorphic Surface** Older alluvial fan af2 (hanging wall)

Parent Material(s): Colluvium, loess, and alluvial-fan gravels **Described by** SSO and AEG

Depth (cm)	Horizon	Color	Structure	Gravel %	Consistence			Texture	pH/ Eff rxn	Clay Films	Bound-aries	Notes
		wet / dry			Wet	Moist	Dry					
26	A/B	10YR 4/6 dark yellowish brown 10YR 5/6 yellowish brown to 7.5YR 5/6 strong brown	m vf gr sg f pl 1 m pr 2 c cpr 3 vc abk sbk	0 50 <10 75 10 >75 25	so o ss ps s p vs vp	lo vfr fr fi vfi efi	lo so sh h vh eh	S SiCL LS SiL SL Si SCL SiC L C CL SC	es	v1 f pf 1 po 2 d br 3 co p cobr	a s c w g i d b	Lots of modern roots; Stage I+ CaCO3; root pores; vesicles; cw to cs; PM = Unit 7
67	2Btk	7.5YR 4/4 brown dark:7.5YR 5/4 brown to 10YR 5/4 yellowish brown, light:7.5YR 8/1 white	m vf gr sg f pl 1 m pr 2 c cpr 3 vc abk sbk	0 50 <10 75 10 >75 25	so o ss ps s p vs vp	lo vfr fr fi vfi efi	lo so sh h vh eh	S SiCL LS SiL SL Si SCL SiC L C CL SC	ev-	v1 f pf 1 po 2 d br 3 co p cobr	a s c w g i d b	cs-; Stage I+ to II CaCO3; mottled color; root pores, vesicles especially in top 20 cm; PM = 5b-7b
97	3K	10YR 7/3 very pale brown dark:10YR 6/4 light yellowish brown, light:10YR 8/1 white; ave.: 10YR 7/3 very pale brown	m vf gr sg f pl 1 m pr 2 c cpr 3 vc abk sbk	0 50 <10 75 10 >75 25	so+ o ss ps- s p vs vp	lo vfr fr fi vfi efi	lo so sh h vh eh	S SiCL LS SiL SL Si SCL SiC L C CL SC	ev	none	a s c w g i d b	Mottled; cs; Stage III to IV CaCO3; coalescing slope parallel CaCO3 stringers; more gravel than overlying horizon; PM = Unit 2
110	4K	10YR 7/4 very pale brown dark:10YR 8/3 very pale brown, light:10YR 8/1 white; ave.: 10YR 7/3 very pale brown	m vf gr sg f pl 1 m pr 2 c cpr 3 vc abk sbk	0 50 <10 75 10 >75 25	so+ o ss ps- s p vs vp	lo vfr fr fi vfi efi	lo so sh h vh eh	S SiCL LS SiL SL Si SCL SiC L C CL SC	ev	none	a s c w g i d b	Faintly mottled; cs; Stage III to IV CaCO3; more gravel than overlying horizon; PM = Unit 1
132	4K2	10YR 6/3 pale brown 10YR 8/2 very pale brown	m vf gr sg f pl 1 m pr 2 c cpr 3 vc abk sbk	0 50 <10 75 10 >75 25	so+ o ss ps- s p vs vp	lo vfr fr fi vfi efi	lo so sh h vh eh	S SiCL LS SiL SL Si SCL SiC L C CL SC	ev	none	a s c w g i d b	cs+; Stage III to IV CaCO3; mottled; PM = Unit 1
188	4Bk	10YR 5/4 yellowish brown dark:10YR 7/3 very pale brown, light:10YR 8/2 very pale brown	m vf gr sg f pl 1 m pr 2 c cpr 3 vc abk sbk	0 50 <10 75 10 >75 25	so o ss ps s p vs vp	lo vfr fr fi vfi efi	lo so sh h vh eh	S SiCL LS SiL SL Si SCL SiC L C CL SC	ev	none	a s c w g i d b	cs; Stage II to III- CaCO3 color highly variable; PM = Unit 1 coarse subunit
207	4Bk2	10YR 6/4 light yellowish brown 10YR 7/4 very pale brown	m vf gr sg f pl 1 m pr 2 c cpr 3 vc abk sbk	0 50 <10 75 10 >75 25	so+ o ss ps s p vs vp	lo vfr fr fi vfi efi	lo so sh h vh eh	S SiCL LS SiL SL Si SCL SiC L C CL SC	ev-	none	a s c w g i d b	cw; Stage I CaCO3; PM = Unit 1
217 (base of trench)	4Ck	10YR 5/3 brown 10YR 6/3 pale brown	m vf gr sg f pl 1 m pr 2 c cpr 3 vc abk sbk	0 50 <10 75 10 >75 25	so+ o ss ps- s p vs vp	lo vfr fr fi vfi efi	lo so sh h vh eh	S SiCL LS SiL SL Si SCL SiC L C CL SC	es	none	a s c w g i d b	No cementation; Stage I- CaCO3

Table B-3. – Description of Soil Profile SP3

Form from Birkeland et al. (1991). Courtesy of D. Jorgenson (1989).

Location Mercur Canyon East Trench at 16.07 meter mark. Page 1 of 1

Site No. SP3	**Date** 8/29/99	**Time**	**Vegetation**	Blue bunchgrass, juniper, prickly pear, rabbitbrush, sage	
Elevation	**Slope** ~5° - 7° W	**Aspect**	**Geomorphic Surface**	Downthrown side of eastern fault scarp on older alluvial fan (af2)	
Parent Material(s): Colluvium, loess, and alluvial-fan gravels			**Described by**	SSO and AEG	

Depth (cm)	Horizon	Color	Structure	Gravel %	Consistence			Texture	pH	Clay Films	Bound-aries	Notes
		wet / dry			Wet	Moist	Dry					
40	A	10YR 4/4 dark yellowish brown -------- 10YR 6/4 light yellowish brown	m sg 1 2 3 vf f m c vc gr pl pr cpr abk sbk	0 50 <10 75 10 >75 25 from unit description	so ss s vs po ps p vp	lo vfr fr fi vfi efi	lo so sh h vh eh	S LS SL SCL L CL SiCL SiL Si SiC C SC	es-	none	a c g d s w i b	Lots of roots, rootlets; none to Stage I- CaCO3 disseminated; root pores; organics; extensively bioturbated; no cementation; PM = Unit 3
75	2K1b	10YR 7/4 very pale brown -------- dark:10YR 7/4 very pale brown, light:10YR 8/2 very pale brown	m sg 1 2 3 vf f m c vc gr pl pr cpr abk sbk	0 50 <10 75 10 >75 25 from unit description	so ss s vs po ps p- vp	lo vfr fr fi vfi efi	lo so sh h vh eh	S LS SL SCL L CL SiCL SiL Si SiC C SC	ev	none	a c g d s w i b	cs-; platy texture; Stage III+ CaCO3; mottled color; rootlets; root pores abundant; PM = Unit 2b
98	2K2b	dark:10YR 6/4 light yellowish brown, light:10YR 7/2 light grey -------- dark:10YR 7/3 very pale brown, light:10YR 8/1 white	m sg 1 2 3 vf f m c vc gr pl pr cpr abk sbk	0 50 <10 75 10 >75 25 from unit description	so ss+ s vs po ps p vp	lo vfr fr fi vfi efi	lo so sh h vh eh	S LS SL SCL L CL SiCL SiL Si SiC C SC	ev	v1 1 2 3 f d p pf po br co cobr	a c g d s w i b	less roots, less structure than overlying horizon; mottled color; cs+; Stage III+ CaCO3; less sand than overlying horizon; slightly more gravel than overlying horizon; PM = Unit 2b
135	3Kb	10YR 5/4 yellowish brown -------- 10YR 7/3 very pale brown	m sg 1 2 3 vf f m c vc gr pl pr cpr abk sbk	0 50 <10 75 10 >75 25 from unit description	so+ ss s vs po ps- p vp	lo vfr fr fi vfi efi	lo so sh h vh eh	S LS SL SCL L CL SiCL SiL Si SiC C SC	ev	none	a c g d s w i b	root pores; vesicles; some roots; cs; Stage III CaCO3, becomes Stage IV- downtrench; PM = Unit 2a/1
190	3Bkb	10YR 5/3 brown -------- dark:10YR 7/4 very pale brown	m sg 1 2 3 vf f m c vc gr pl pr cpr abk sbk	0 50 <10 75 10 >75 25 from unit description	so ss s vs po ps- p vp	lo vfr fr fi vfi efi	lo so sh h vh eh	S LS SL SCL L CL SiCL SiL Si SiC C SC	es+	none	a c g d s w i b	Stage I to II CaCO3; cw; some roots; PM = Unit 1
245 (base of trench)	3Ck	10YR 4/4 dark yellowish brown -------- 10YR 6/4 light yellowish brown	m sg 1 2 3 vf f m c vc gr pl pr cpr abk sbk	0 50 <10 75 10 >75 25 from unit description	so ss s vs po ps p vp	lo vfr fr fi vfi efi	lo so sh h vh eh	S LS SL SCL L CL SiCL SiL Si SiC C SC	es	none	not exposed	Stage I- CaCO3 (spotty coats on clast bottoms mainly in upper 20 cm; no cementation

Appendix C

Paleo Research Laboratories Report on Radiocarbon Sample Pretreatment

EXAMINATION OF BULK SOIL FROM A PALEOSEISMIC TRENCH ACROSS THE MERCUR FAULT, UTAH

By

Kathryn Puseman
Paleo Research Laboratories
Denver, Colorado

Paleo Research Labs Technical Report 99-85

Prepared For

URS Greiner Woodward Clyde
Oakland, California

December 1999

INTRODUCTION

Three bulk soil samples from a paleoseismic trench across the Mercur fault along the eastern margin of the Great Basin in Utah were floated to recover organic fragments suitable for radiocarbon dating. The trench transects a fault scarp on an alluvial fan surface estimated to be at least 130,000 to 150,000 years old. Botanic components and detrital charcoal were identified, and potentially radiocarbon datable material was separated.

METHODS

The bulk samples were floated using a modification of the procedures outlined by Matthews (1979). Each sample was added to approximately 3 gallons of water. The sample was stirred until a strong vortex formed, which was allowed to slow before pouring the light fraction through a 150 micron mesh sieve. Additional water was added and the process repeated until all visible macrofloral material was removed from the sample (a minimum of 5 times). The material which remained in the bottom (heavy fraction) was poured through a 0.5 mm mesh screen. The floated portions were allowed to dry.

The light fractions were weighed, then passed through a series of graduated screens (US Standard Sieves with 4 mm, 2 mm, 1 mm, 0.5 mm and 0.25 mm openings to separate charcoal debris and to initially sort the remains. The contents of each screen were then examined. Charcoal pieces larger than 1 mm in diameter were broken to expose a fresh cross-section and examined under a binocular microscope at a magnification of 70x. The remaining light fraction in the 4 mm, 2 mm, 1 mm, 0.5 mm, and 0.25 mm sieves was scanned under a binocular stereo microscope at a magnification of 10x, with some identifications requiring magnifications of up to 70x. The material which passed through the 0.25 mm screen was not examined. The coarse or heavy fractions also were screened and examined for the presence of botanic remains. Remains from both the light and heavy fractions were recorded as charred and/or uncharred, whole and/or fragments. Individual detrital charcoal/wood samples also were broken to expose a fresh cross-section and examined under a binocular microscope at a magnification of 70x.

Macrofloral remains were identified using manuals (Core et al. 1976; Martin and Barkley 1973; Panshin and Zeeuw 1980; Schopmeyer 1974) and by comparison with modern and archaeological references. The term "seed" is used to represent seeds, achenes, caryopses, and other disseminules. Because charcoal and possibly other botanic remains were to be sent for radiocarbon dating, clean laboratory conditions were used during flotation and identification to avoid contamination. All instruments were washed between samples, and samples were protected from contact with modern charcoal.

DISCUSSION

The Mercur fault is located along the eastern edge of the Great Basin in Utah at an elevation of 5570 feet. Local vegetation in this area includes juniper (*Juniperus*), sagebrush (*Artemisia*), rabbitbrush (*Chrysothamnus*), prickly pear cactus (*Opuntia*), Indian ricegrass (*Oryzopsis*), and cheatgrass (*Bromus*).

Three bulk soil samples were recovered from a paleoseismic trench across the fault. The samples were collected from the same soil horizon in the upper section of fault-scarp derived colluvium on the downthrown side of the fault. Sample MCWT6-1RC represents the insitu A-horizon buried by fault-scarp derived colluvium from the youngest faulting event at a depth of 65 cm (Table 1). This sample contained pieces of charred unidentified twig fragments that may be submitted for AMS radiocarbon dating (Tables 2 and 3). The minimum weight requirement of charcoal for AMS radiocarbon dating reported by Beta Analytic, Inc. is 5 mg or 0.005 g. A total of 0.006 g of charred twig fragments were recovered in sample MCWT6-1RC. These twig fragments were too small for identification. No other charred remains were present in the sample. Uncharred rootlets represent modern plants at the site. Non-floral remains include a few uncharred insect chitin fragments, an abundance of rock/gravel, and snail shell.

Sample MCWT7-1RC contained very small pieces of unidentified diffuse porous charcoal (0.005 g) that meet the minimum weight requirement for AMS radiocarbon dating. Uncharred seeds and rootlets represent components of the modern, local vegetation. Several uncharred insect chitin fragments indicate some disturbance from insect activity in this area. The sample also contained a few uncharred bone fragments, an abundance of rock/gravel, and snail shell fragments.

Sample MCWT7-2RC represents the A-horizon preserved on a toppled soil block at a depth of 85 cm. Charcoal in this sample was very small, and insufficient charcoal was present for AMS radiocarbon dating. Uncharred seeds and rootlets represent modern plants in the area. Non-floral remains include a few uncharred bone fragments, several uncharred insect chitin fragments, an abundance of rock/gravel, and snail shell.

SUMMARY AND CONCLUSIONS

Flotation of bulk samples from a paleoseismic trench across the Mercur fault in Utah resulted in recovery of charcoal that may be submitted for radiocarbon dating. Samples MCWT6-1RC and MCWT7-1RC yielded small amounts of charcoal that meet the minimum weight requirement for AMS radiocarbon dating. Uncharred seeds and insect chitin fragments indicate some introduction of modern material into the soil through bioturbation in this area.

TABLE 1
PROVENIENCE DATA FOR SAMPLES FROM THE MERCUR FAULT, UTAH

Sample No.	Depth	Provenience/ Description
MCWT6-1RC	65 cm	Bulk soil from insitu A-horizon buried by fault-scarp derived colluvium from youngest faulting event
MCWT7-1RC		Bulk soil from A-horizon in fault-scarp derived colluvium on the downthrown side of the fault
MCWT7-2RC	85 cm	Bulk soil from A-horizon preserved on a toppled soil block

TABLE 2

MACROFLORAL REMAINS FROM THE MERCUR FAULT, UTAH

Sample No.	Identification	Part	Charred W	Charred F	Uncharred W	Uncharred F	Weights/ Comments
MCWT6-1RC	Liters Floated						1.15 L
	Light Fraction Weight						2.64 g
	FLORAL REMAINS:						
	Rootlets					X	Numerous
	CHARCOAL/WOOD:						
	Unidentified twig	Charcoal		X			0.006 g
	NON-FLORAL REMAINS:						
	Insect	Chitin				7	
	Rock/Gravel					X	Abundant
	Snail shell				7	4	
MCWT7-1RC	Liters Floated						2.70 L
	Light Fraction Weight						17.95 g
	FLORAL REMAINS:						
	Amaranthus	Seed			3	1	
	Atriplex	Fruit				23	
	Atriplex	Seed			7		
	Sphaeralcea	Seed			3		
	Rootlets					X	Numerous
	CHARCOAL/WOOD:						
	Unidentified diffuse porous	Charcoal		X			0.005 g
	NON-FLORAL REMAINS:						
	Bone					X	Few
	Insect	Chitin				129	
	Rock/Gravel					X	Abundant
	Snail shell				X	X	0.042 g

TABLE 2

MACROFLORAL REMAINS FROM THE MERCUR FAULT, UTAH (continued)

Sample No.	Identification	Part	Charred W	Charred F	Uncharred W	Uncharred F	Weights/ Comments
MCWT7-2RC	Liters Floated						1.35 L
	Light Fraction Weight						16.68 g
	FLORAL REMAINS:						
	Atriplex	Fruit				6	
	Caryophyllaceae	Seed				1	
	Opuntia	Seed				8	
	Sphaeralcea	Seed			2		
	Rootlets					X	Numerous
	CHARCOAL/WOOD:						
	Unidentifiable - small	Charcoal		X			<0.001 g
	NON-FLORAL REMAINS:						
	Bone					X	Few
	Insect	Chitin				102	
	Rock/Gravel					X	Abundant
	Snail shell				10	18	0.024 g

W = Whole

F = Fragment

X = Presence noted in sample

g = grams

* = Estimated frequency

TABLE 3

INDEX OF MACROFLORAL REMAINS RECOVERED FROM THE MERCUR FAULT, UTAH

Scientific Name	Common Name
FLORAL REMAINS:	
Amaranthus	Pigweed, amaranth
Atriplex	Saltbush, orache
Caryophyllaceae	Pink family
Opuntia	Prickly pear
Sphaeralcea	Globemallow
CHARCOAL/WOOD:	
Asteraceae	Sunflower family

REFERENCES CITED

Core, H. A., W. A. Cote, and A. C. Day

1976 Wood Structure and Identification. Syracuse University Press, Syracuse, New York.

Martin, Alexander C. and William D. Barkley

1973 Seed Identification Manual. University of California Press, Berkeley.

Matthews, Meredith H.

1979 Soil Sample Analysis of 5MT2148; Dominguez Ruin, Dolores, Colorado. Appendix B IN The Dominguez Ruin: A McElmo Phase Pueblo in Southwestern Colorado by Alan D. Reed. Bureau of Land Management Cultural Resource Series No. 7, Denver, Colorado.

Panshin, A. J. and Carl de Zeeuw

1980 Textbook of Wood Technology. McGraw-Hill Book Co., New York.

Schopmeyer, C. S.

1974 Seeds of Woody Plants in the Unites States. Agricultural Handbook No. 450. U. S. Department of Agriculture, Forest Service, Washington, D.C.

Appendix D

Beta Analytic Inc. Report On Radiocarbon Dating Analyses

BETA

Consistent Accuracy
Delivered On Time.

Beta Analytic Inc.
4985 SW 74 Court
Miami, Florida 33155 USA
Tel: 305 667 5167
Fax: 305 663 0964
beta@radiocarbon.com
www.radiocarbon.com

DR. MURRY TAMERS
MR. DARDEN HOOD
Co-directors

Mr. Ronald Hatfield
Laboratory Manager

Mr. Christopher Patrick
Ms. Teresa Zilko-Miller
Associate Managers

January 26, 2000

Ms. Susan Olig
URS Greiner Woodward Clyde
500 12th St., Suite 200
Oakland, CA 94607-4014

Dear Ms. Olig:

Please find enclosed the radiocarbon dating result for two charcoal samples (MCWT7-1RC and MCWT6-1RC) which were received on December 16. They were very small, requiring us to convert the sample carbon to graphite and then to count the radiocarbon atomically using an accelerator mass spectrometer (AMS). They provided plenty of carbon for reliable measurements and all analytical steps went normally. The quoted errors represent 1 sigma statistics. Since these errors cannot include uncertainties outside of those which can be quantified during measurement, it is best to consider them as minimum quotes.

Printouts of the calendar calibrations are enclosed (also available in digital format via email). The two sigma results are as follows;

Beta-137742: Cal AD 420 to 655 (Cal BP 1530 to 1295)
Beta-137743: Cal BC 2880 to 2480 (Cal BP 4830 to 4430)

Our calendar calibrations are now calculated back to about 19,000 years using the newest calibration data as published in *Radiocarbon,* Vol. 40, No. 3, 1998 using the cubic spline fit mathematics as published by Talma and Vogel, *Radiocarbon*, Vol. 35, No. 2, pg 317-322, 1993: A Simplified Approach to Calibrating C14 Dates. Results are reported both as cal BC and cal BP. In this new version, we use the same smoothing mathematics as in our previous calibrations, except for dates which are older than about 10,000 BP (land) and 8200 BP (marine). The correlation data is imprecise beyond this region and we use the error limits on a spline fit beyond that range. Since the calibration database may change in the future (especially for the older samples) it is important to quote the original BP dates and the calibration references in your publications.

Our invoice is enclosed. Please, forward it to the appropriate office or send VISA charge authorization. Thank you. As always, if you have any questions or would like to discuss the results, don't hesitate to contact me.

Sincerely,

Darden Hood

BETA

BETA ANALYTIC INC.

DR. M.A. TAMERS and MR. D.G. HOOD

UNIVERSITY BRANCH
4985 S.W. 74 COURT
MIAMI, FLORIDA, USA 33155
PH: 305/667-5167 FAX: 305/663-0964
E-MAIL: beta@radiocarbon.com

REPORT OF RADIOCARBON DATING ANALYSES

Ms. Susan Olig — Report Date: January 26, 2000

URS Greiner Woodward Clyde — Material Received: December 16, 1999

Sample Data	Measured Radiocarbon Age	$^{13}C / ^{12}C$ Ratio	Conventional Radiocarbon Age (*)
Beta-137742	1370 +/- 60 BP	-16.4 o/oo	1510 +/- 60 BP
SAMPLE #: MCWT7-1RC ANALYSIS: Standard-AMS MATERIAL/PRETREATMENT:(charred material): acid/alkali/acid			
Beta-137743	3920 +/- 60 BP	-13.7 o/oo	4110 +/- 60 BP
SAMPLE #: MCWT6-1RC ANALYSIS: Standard-AMS MATERIAL/PRETREATMENT:(charred material): acid/alkali/acid			

NOTE: It is important to read the calendar calibration information and to use the calendar calibrated results (reported separately) when interpreting these results in AD/BC terms.

Dates are reported as RCYBP (radiocarbon years before present, "present" = 1950A.D.). By International convention, the modern reference standard was 95% of the C14 content of the National Bureau of Standards' Oxalic Acid & calculated using the Libby C14 half life (5568 years). Quoted errors represent 1 standard deviation statistics (68% probability) & are based on combined measurements of the sample, background, and modern reference standards.

Measured C13/C12 ratios were calculated relative to the PDB-1 international standard and the RCYBP ages were normalized to -25 per mil. If the ratio and age are accompanied by an (*), then the C13/C12 value was estimated, based on values typical of the material type. The quoted results are NOT calibrated to calendar years. Calibration to calendar years should be calculated using the Conventional C14 age.

CALIBRATION OF RADIOCARBON AGE TO CALENDAR YEARS

(Variables: C13/C12=-16.4:lab. mult=1)

Laboratory number:	**Beta-137742**
Conventional radiocarbon age:	**1510±60 BP**
2 Sigma calibrated result: (95% probability)	**Cal AD 420 to 655 (Cal BP 1530 to 1295)**

Intercept data

Intercept of radiocarbon age with calibration curve:	Cal AD 560 (Cal BP 1390)
1 Sigma calibrated results: (68% probability)	Cal AD 465 to 480 (Cal BP 1485 to 1470) and Cal AD 520 to 625 (Cal BP 1430 to 1325)

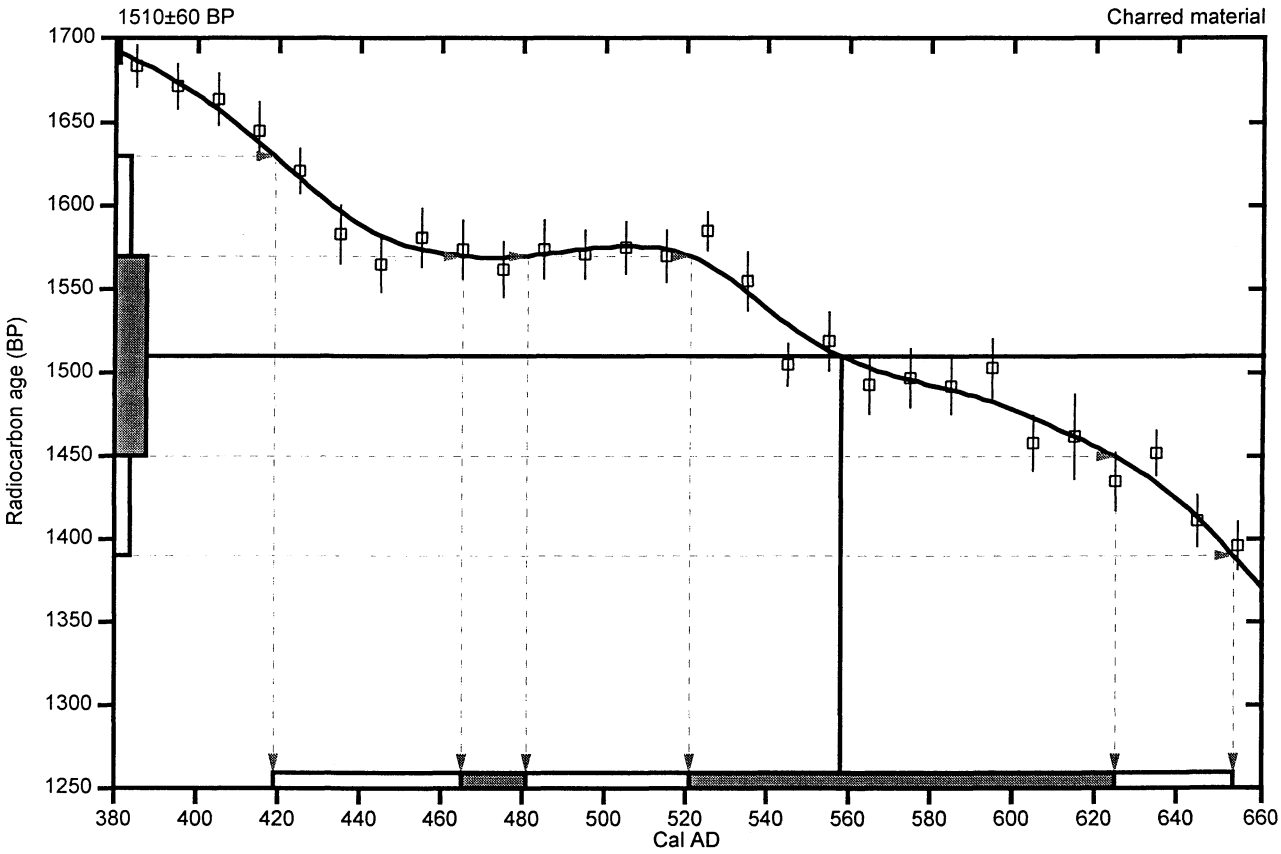

References:

Database used

INTCAL98

Calibration Database

Editorial Comment

Stuiver, M., van der Plicht, H., 1998, Radiocarbon 40(3), pxii-xiii

INTCAL98 Radiocarbon Age Calibration

Stuiver, M., et. al., 1998, Radiocarbon 40(3), p1041-1083

Mathematics

A Simplified Approach to Calibrating C14 Dates

Talma, A. S., Vogel, J. C., 1993, Radiocarbon 35(2), p317-322

Beta Analytic Radiocarbon Dating Laboratory

4985 S.W. 74th Court, Miami, Florida 33155 • Tel: (305)667-5167 • Fax: (305)663-0964 • E-mail: beta@radiocarbon.com

CALIBRATION OF RADIOCARBON AGE TO CALENDAR YEARS

(Variables: C13/C12=-13.7:lab. mult=1)

Laboratory number:	**Beta-137743**
Conventional radiocarbon age:	**4110±60 BP**
2 Sigma calibrated result: (95% probability)	**Cal BC 2880 to 2480 (Cal BP 4830 to 4430)**

Intercept data

Intercept of radiocarbon age with calibration curve:	Cal BC 2630 (Cal BP 4580)
1 Sigma calibrated results: (68% probability)	Cal BC 2865 to 2800 (Cal BP 4815 to 4750) and Cal BC 2760 to 2575 (Cal BP 4710 to 4525)

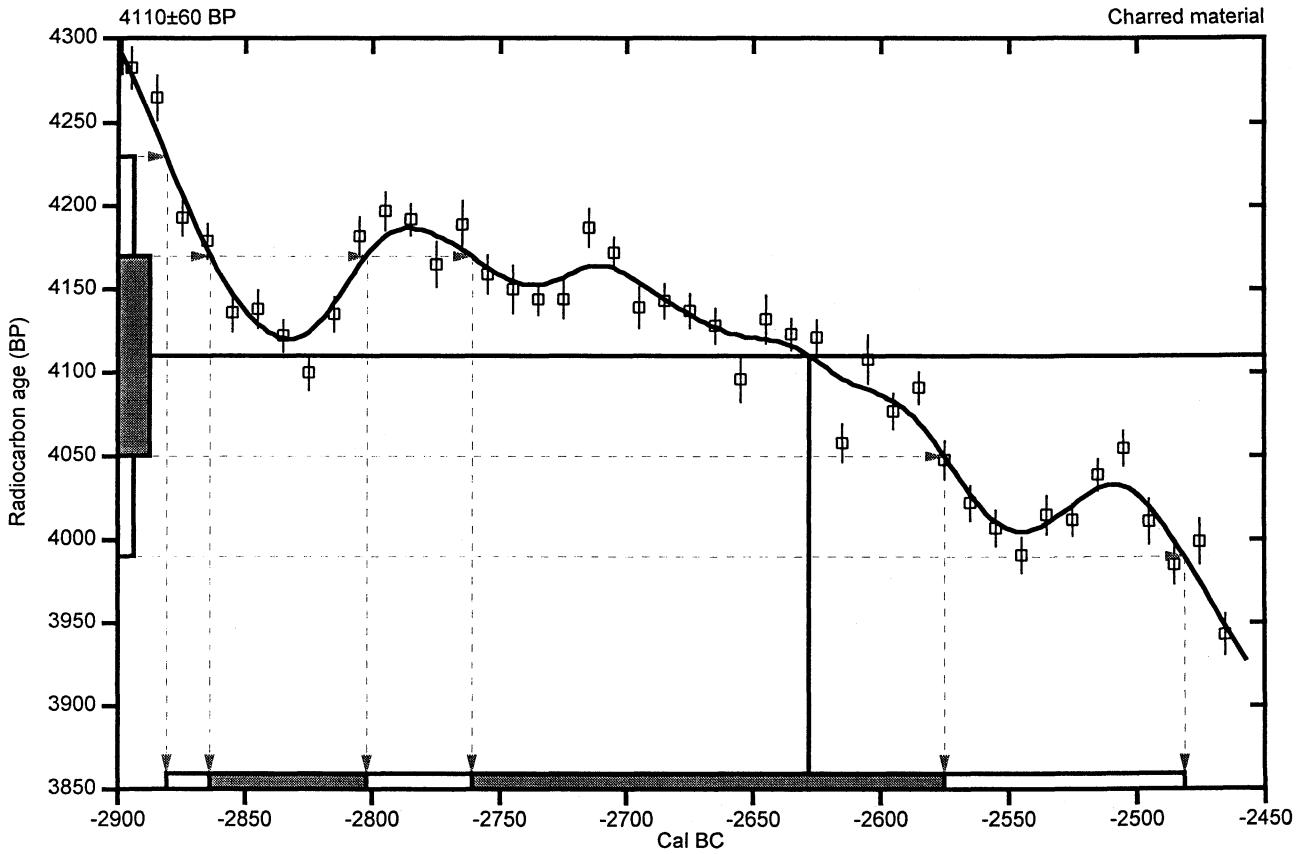

References:

Database used
INTCAL98
Calibration Database
Editorial Comment
Stuiver, M., van der Plicht, H., 1998, Radiocarbon 40(3), pxii-xiii
INTCAL98 Radiocarbon Age Calibration
Stuiver, M., et. al., 1998, Radiocarbon 40(3), p1041-1083
Mathematics
A Simplified Approach to Calibrating C14 Dates
Talma, A. S., Vogel, J. C., 1993, Radiocarbon 35(2), p317-322

Beta Analytic Radiocarbon Dating Laboratory

4985 S.W. 74th Court, Miami, Florida 33155 • Tel: (305)667-5167 • Fax: (305)663-0964 • E-mail: beta@radiocarbon.com

Appendix E
Associated Publications

EVIDENCE FOR YOUNG, LARGE EARTHQUAKES ON THE MERCUR FAULT: IMPLICATIONS FOR SEGMENTATION AND EVOLUTION OF THE OQUIRRH-EAST GREAT SALT LAKE FAULT ZONE, WASATCH FRONT, UTAH

OLIG, S. S., URS Corp., 500 12th St., Ste. 200, Oakland, CA 94607, susan_olig@urscorp.com; **GORTON, A. E.**, TNRCC, Box 13087, MC 124, Austin, TX 78711; **BLACK, B. D.**, Utah Geological Survey, 1594 W. N. Temple, Salt Lake City, UT 84114; **FORMAN, S.L.**, Univ. of Illinois of Chicago, Dept. of Geological Sciences, MC 186, 845 Taylor St., Chicago, IL 60607

Mapping, scarp profiling, trenching and geochronology of the southern Oquirrh Mountains fault (SOMF) provide insights into late Quaternary paleoseismicity, indicating a basinward migration of faulting and possible coseismic rupture with the Oquirrh fault to the north. Both the SOMF and the Oquirrh fault are part of the Oquirrh-East Great Salt Lake fault zone, a north-striking, west-dipping, range-bounding, 205-km-long normal fault that lies 22 to 55 km west of the Wasatch fault in the eastern Basin and Range. Trenches across three traces of the Mercur fault, part of the SOMF, reveal paleoseismic evidence for 5 to 7 surface-faulting earthquakes that occurred since 92 ± 7 ka (1-sigma errors). Four of these events occurred on the westernmost (basinward) trace since 75 ± 5 ka, including the youngest event that occurred shortly after 4110 ± 60 ^{14}C yr BP and before 1510 ± 60 ^{14}C yr BP. This is much younger than previous published estimates, but is consistent with unpublished mid-Holocene cosmogenic ages for a northern bedrock scarp of the SOMF. Displacements per event average 1.4 to 2.1 m, much larger than expected for a 25-km long rupture (total SOMF length). Net vertical tectonic displacements of 9.75 to 10.4 m yield an average slip rate for the Mercur fault of about 0.1 mm/yr for the past 92 ka, which is similar to slip rates for the Oquirrh fault. Overall, the overlapping ages for the youngest event, the large displacements per event for both faults, the similar late Quaternary slip rates, and along-strike displacement patterns for the SOMF all suggest coseismic rupture of the SOMF and Oquirrh fault. Paleomagnitude estimates for such a 52-km long rupture range from M_w 7.0 to 7.2, having important implications for seismic hazards in nearby Salt Lake City and the Deseret Chemical Depot where chemical weapons are stored and destroyed.

Published in Geological Society of America Abstracts with Programs, v. 32, no. 7, 2000.